

UNIVERSITY OF OKLAHOMA

GRADUATE COLLEGE

TARGETING FUSION PROTEINS CONTAINING L-METHIONINASE TO CANCER
CELLS

A DISSERTATION

SUBMITTED TO THE GRADUATE FACULTY

in partial fulfillment of the requirements for the

Degree of

DOCTOR OF PHILOSOPHY

By

NAVEEN REDDY PALWAI

Norman, Oklahoma

2007

UMI Number: 3291933



UMI Microform 3291933


Copyright 2008 by ProQuest Information and Learning Company.
All rights reserved. This microform edition is protected against
unauthorized copying under Title 17, United States Code.

ProQuest Information and Learning Company
300 North Zeeb Road
P.O. Box 1346
Ann Arbor, MI 48106-1346

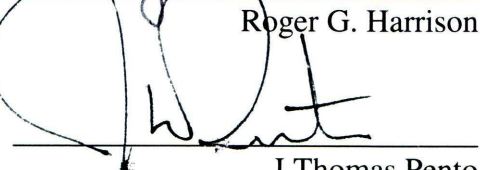
TARGETING FUSION PROTEINS CONTAINING L-METHIONINASE TO CANCER
CELLS

A DISSERTATION APPROVED FOR THE
SCHOOL OF CHEMICAL, BIOLOGICAL AND MATERIALS ENGINEERING

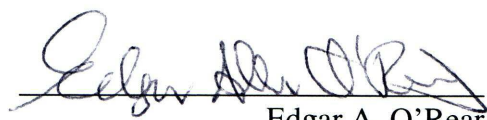
BY,




Roger G. Harrison




J. Thomas Pento



Edgar A. O'Rear



Matthias U. Nollert



Paul F. Cook

© Copyright by NAVEEN REDDY PALWAI 2007
All Rights Reserved.

ACKNOWLEDGEMENTS

I am deeply indebted to my advisor Dr. Roger G. Harrison for his continued guidance and encouragement throughout the duration of my Ph.D. Throughout my thesis-writing period, he provided encouragement, sound advice, good teaching, good company, and lots of good ideas. I would have been lost without him. My advisory committee members Dr. J. Thomas Pento, Dr. Edgar O'Rear, Dr. Vassillios Sikavitsas, Dr. Matthias Nollert and Dr. Paul Cook had been a great guidance and help during my research. I thank them for letting me use their labs when the need arose.

I would like to thank Dr. Pento's lab postdoc Dr. Xiao-Ping Zang who have been a constant source of knowledge, research papers, funny anecdotes, and fruitful discussions in research. Durga Sarvepalli and Jose Alvarez Barreto though not students of our group have been most helpful, be it with instrument training or brainstorming.

I would like to thank other staff members of the School of Chemical, Biological and Materials Engineering for the help received towards my Ph. D and also made my stay at University of Oklahoma fondly memorable.

Lastly, and most importantly, I thank my parents (Janardhan Palwai & Jayapradha Palwai) and my brothers (Shravan Palwai & Praveen Palwai). They bore me, raised me, supported me, taught me, and loved me. To them, I dedicate this dissertation.

TABLE OF CONTENTS

ACKNOWLEDGEMENTS	iv
LIST OF FIGURES	vii
LIST OF TABLES	x
1. INTRODUCTION	1
Methionine Dependency in Cancer Cells.....	4
Methioninase as Anticancer Agent.....	6
Urokinase Plasminogen Activator Receptor as a Target on Cancer Cells.....	12
Epidermal Growth Factor Receptor as Target on Cancer Cells.....	16
Phosphatidylserine (PS) as Target on Tumor Vasculature Endothelium.....	18
Experimental Hypothesis and Experimental Design.....	20
2. MATERIALS	25
Plasmids and Bacterial Strains.....	25
Media for E.coli Cell Cultures.....	25
Enzymes.....	28
DNA Synthesis, Purification, and Analysis.....	28
SDS-PAGE and Immunoblotting.....	28
Protein Purification.....	29
Media for Cancer Cell Cultures.....	29
Cell Binding Assay for ATF-methioninase.....	29
Binding Assay for L-Methioninase-Annexin.....	30
3. METHODS	31
Primer Design for PCR.....	31
Construction of Fusion Genes.....	32
ATF-Methioninase and L-Methioninase Genes.....	32
TGF-Methioninase Fusion Gene.....	35
Annexin V Gene.....	38
Site-directed Mutagenesis.....	38
Sequencing Methods.....	41
Protein Expression.....	42
Freeze Drying / Lyophilization.....	46
Methioninase Activity Assay.....	46
SDS-PAGE, Western blotting, and Protein Assays.....	46
Amino-terminal Sequencing.....	47
Culture Wounding Assay.....	47
Mouse Xenograft Assay.....	48
Measurement Using the Colorimetric Substrate, Chlorophenol Red β -D-Galactopyranoside (CPRG)	49
Binding of Methioninase-Annexin V on Plastic-immobilized Phosphatidylserine.....	49
Binding of Methioninase-Annexin V on Externally Positioned PS on the Surface of Cells.....	50
4. RESULTS AND DISCUSSION	52
Construction of Fusion Genes.....	52
Construction of the ATF-Methioninase Fusion Gene and the L-Methioninase Gene.....	52
Construction of TGF-Methioninase Fusion Gene.....	54
Construction of the L-Methioninase-Annexin Gene.....	55
Site Directed Mutagenesis of pET- 30 Ek/LIC/ATF-METH.....	56
Protein Expression and Purification.....	56

Dimer Formation of ATF-Methioninase and L-Methioninase.....	65
Freezing and Freeze Drying.....	66
Inhibitory effects of ATF-methioninase on Cancer Cells <i>In Vitro</i>	68
Daily Administration of ATF-Methioninase.....	75
Effect of TGF-methioninase on MCF-7 Cancer Cells.....	77
Specific Binding of ATF-methioninase to MCF-7 Cells.....	79
Mouse Xenograft Assay.....	81
Binding of Methioninase-Annexin V to Plastic-immobilized Phosphatidylserine.....	84
Binding of Methioninase-Annexin V on Externally Positioned PS on the Surface of MCF-7 Breast Cancer Cells.....	85
5. CONCLUSIONS.....	89
BIBLIOGRAPHY.....	91
APPENDIX A.....	101
Primers for PCR of Carrier and Target Genes.....	101
Sequencing Results for the ATF/Methioninase Fusion Gene.....	103
Sequencing Results for the TGF/Methioninase Fusion Gene.....	104
Sequencing Results for the Methioninase Gene.....	105
Sequencing Results for the Methioninase-annexin V Fusion Gene.....	106
APPENDIX B.....	108
QIAquick PCR Purification Kit Protocol.....	108
QIAquick Gel Extraction Kit Protocol.....	109
Agarose Gel Electrophoresis.....	111
Site Directed Mutagenesis by Stratagene.....	112
Transformation of XL1-Blue Supercompetent Cells.....	114
Transformation protocol (For BL21 (DE3) cells).....	114
Bio-Rad's Protein Assay.....	116
Activity Assay (Methioninase Enzyme).....	117
SDS-PAGE Analysis of Proteins.....	119
Western Blot.....	120
Protocol for Fusion Protein Injection in Nude Mice.....	121
CPRG Assay From Stratagene.....	122
Binding of Methioninase-Annexin V on Externally Positioned PS on the Surface of Cells.....	123
Binding of Methioninase-Annexin V on Plastic-immobilized Phosphatidylserine.....	125

LIST OF FIGURES

Figure 1.1. Age-adjusted cancer death rates, for males (Top) and for females (bottom), U.S. 1930-2002 (Source: ACS, Cancer Statistics 2006)	2
Figure 1.2. Structures of homocysteine and methionine	5
Figure 1.3. Reaction catalyzed by methioninase	5
Figure 1.4. Homotetramer structure of L-methioninase (Top Panel). Each color represents each monomer of L-methioninase [30].	8
Figure 1.5. Structure of L-methioninase, The N-terminal domain is held in blue, the PLP-binding domain in yellow and the C-terminal domain in red. PLP and PLP-binding Lys211 are shown in a ball and stick representation [30].....	9
Figure 1.6. The uPA/uPAR system. The pro-uPA binds to uPAR, which is converted to active uPA after cleavage by plasmin. Active uPA is responsible for converting plasminogen to plasmin, which is responsible for degradation of extracellular matrix [59].....	13
Figure 1.7. Amino acid sequence of pro-urokinase (Pro-uPA). Cleavage by plasmin protease is indicated by arrow. Dashes represents the position of disulfide bonds [65].	15
Figure 1.8. Epidermal growth factor receptor [79]. Binding of EGF or TGF- α to EGFR autophosphorylates the cytoplasmic domain of EGFR and triggers signal for proliferation.	17
Figure 1.9. General structure of the fusion proteins (not to scale) constructed for this study. ATF is the N-terminal 1-49 amino acids of the urokinase A chain. TGF- α is the transforming growth factor- α	21
Figure 2.1. The pET-30 Ek/LIC vector. General features of the pET-30 Ek/LIC vector (Novagen catalog, 2006).....	26
Figure 2.2. The pET-44 Ek/LIC vector. General features of the pET-30 Ek/LIC vector (Novagen catalog, 2006).....	27
Figure 3.1. Construction of pET-30 Ek/LIC/ATF-METH expression vector. First, the gene for ATF-methioninase was amplified by PCR from parental plasmid that inserts 5' and 3' LIC ends. Next, the gene was digested with T4 DNA polymerase to create sticky ends and annealed to linear pET-30 Ek/LIC vector. Finally, annealed product is transformed in NovaBlue cells.....	33
Figure 3.2. Construction of pET-30 Ek/LIC/METHANX expression vector. First, the genes for L-methioninase and annexin V were amplified by PCR from parental plasmids that inserts 5' LIC, 3' LIC end and BamHI sites. Next, the gene was digested with with BamHI restriction enzyme and ligated together. The ligated methioninase-annexin gene was treated with T4 DNA polymerase and annealed to linear pET-30 Ek/LIC vector. Finally, annealed product is transformed in NovaBlue cells.	36
Figure 3.3. Construction of pET-44 Ek/LIC/TGFMETH expression vector. First, the genes for L-methioninase and TGF were amplified by PCR from parental plasmids that inserts 5' LIC, 3' LIC end	

and BamHI sites. Next, the gene was digested with with BamHI restriction enzyme and ligated together. Ligated TGF-METH gene was treated with T4 DNA polymerase and annealed to linear pET-44 Ek/LIC vector. Finally, annealed product is transformed in NovaBlue cells.....37

Figure 3.4. Construction of pET-30 Ek/LIC/ANX expression vector. First, the gene for annexin V was amplified by PCR from parental plasmid that inserts 5' and 3' LIC ends. Next, the gene was digested with T4 DNA polymerase to create sticky ends and annealed to linear pET-30 Ek/LIC vector. Finally, annealed product is transformed in NovaBlue cells.....39

Figure 3.5. Site directed mutagenesis of pET-30 Ek/LIC/ATF-METH plasmid. First, PCR was performed using pET-30 Ek/LIC/ATF-METH as plasmid and mutagenic primers (Y114F, indicated by X). Next, original plasmid was digested by using DpnI enzyme, and finally the mutated plasmid is transformed in XL1-Blue super competent cells.40

Figure 3.6. Scheme for the purification of fusion proteins using immobilized metal affinity chromatography.44

Figure 4.1. (A) Agarose gel image of PCR products. *Lane 1*, ATF-methioninase (1452 bp) fusion gene, and *Lane 2*, L-methioninase gene (1284 bp). **(B)** Agarose gel image of PCR products. *Lane 1*, different ligated products formed after ligation reaction of L-methioninase and TGF. TGF-METH is indicated by arrow. *Lane2*, L-methioninase (1284 bp); *Lane3*, TGF (214 bp), and **(C)** Agarose gel image of PCR products. *Lane1*, Annexin V, *Lane2*, L-methioninase; and *Lane 3*, different ligated products formed after ligation reaction of L-methioninase (1284 bp) and annexin V (1013 bp). *Lane M*, the 1 kb DNA ladder (0.5 kb, 1 kb, 1.5 kb, 2.0 kb, 3 kb, 4 kb).53

Figure 4.2. SDS-PAGE analysis with Coomassie blue staining of the expression and purification of the ATF-methioninase fusion protein (position indicated by the arrow). The fusion protein was expressed from plasmid pET-30/Ek/LIC/ATF-Meth in *E. coli* BL21(DE3) cells at 30 °C (*lane 1* whole cells, *lane 2* soluble lysate, *lane 3* eluted fraction from first metal affinity chromatography, *lane 4* eluted fraction after cleavage with HRV 3C protease, *lane 5* pooled fractions from second metal affinity chromatography, *M* marker proteins with molecular masses indicated on the left in kiloDaltons).58

Figure 4.3. SDS-PAGE analysis with Coomassie blue staining of the expression and purification of the L-methioninase protein (position indicated by the arrow). The fusion protein was expressed from plasmid pET-30/Ek/LIC/METH in *E. coli* BL21(DE3) cells at 30 °C (*lane 1* soluble lysate, *lane 2* eluted fraction from first metal affinity chromatography, *lane 3* eluted fraction after cleavage with HRV 3C protease, *lane 4* pooled fractions from second metal affinity chromatography, *M* marker proteins with molecular masses indicated on the left in kiloDaltons).....60

Figure 4.4. SDS-PAGE analysis with Coomassie blue staining of the expression and purification of the TGF-methioninase fusion protein (position indicated by the arrow). The fusion protein was expressed from plasmid pET-44/Ek/LIC/TGF-METH in *E. coli* BL21(DE3) cells at 30 °C (*lane 1* soluble lysate, *lane 2* eluted fraction from first metal affinity chromatography, *lane 3* eluted fraction after cleavage with HRV 3C protease, *lane 4* pooled fractions from second metal affinity chromatography, *lane 5* eluted fraction from second metal affinity chromatography, *M* marker proteins with molecular masses indicated on the left in kiloDaltons).....61

Figure 4.5. SDS-PAGE analysis with Coomassie blue staining of three of the purified proteins. *Lane 1* annexin V, *lane 2* L-methioninase, *lane 3* methioninase-annexin V, *M* marker proteins with molecular masses indicated on the left in kiloDaltons.64

Figure 4.6. Western blot analysis of ATF-methioninase and L-methioninase proteins. *Lane 1*, ATF-methioninases; *lane 2*, L-methioninase.....64

- Figure 4.7.** Effect of different unit operations on specific activity of ATF-methioninase. MAC 1: First Metal Affinity Chromatography, MAC 2: Second Metal Affinity Chromatography. Each bar corresponds to the specific activity of the fusion at different purification stage and also freezing.....67
- Figure 4.8.** Effect of buffers on MCF-7 breast cancer cell migration and proliferation. *Control*, cells treated with RPMI media alone; *Buffer 1*, cells treated with RPMI media and buffer containing 20 mM sodium phosphate, 0.02 mM pyridoxal phosphate 1 mM EDTA, 1 mM PMSF, and 1 % ethanol; *Buffer 2*, Cells treated with RPMI media and buffer containing 20 mM sodium phosphate, 0.02 mM pyridoxal phosphate and 0.02 % BME.69
- Figure 4.9.** Dose-response effect of fusion protein on MCF-7 breast cancer cell migration and proliferation. ATF- methioninase (FP); mutated ATF-methioninase (M-FP); L-methioninase (L-M) were administered immediately following culture wounding. Each bar in the top panel represents the maximum distance traveled by cells in the wounded area (mean \pm SEM from 10 to 12 microscope fields). Each bar in the bottom panel represents number of viable cells in the wounded area (mean \pm SEM from 10 to 12 microscope fields).....70
- Figure 4.10.** Dose-response effect of fusion protein on SK-LU-1 lung cancer cells on proliferation and migration. ATF-methioninase (FP); mutated ATF-methioninase (M-FP); L-methioninase (L-M) were administered immediately following culture wounding. Each bar in the top panel represents the number of cells that migrated into the wounded area (mean \pm SEM from 10 to 12 microscope fields). Each bar in the bottom pannel represents number of viable cells in the wounded area (mean \pm SEM from 10 to 12 microscope fields).....71
- Figure 4.11.** Dose-response effect of fusion protein on PC-3 prostate cancer cells on proliferation and migration. ATF-methioninase (FP); mutated ATF-methioninase (M-FP); L-methioninase (L-M) were administered immediately following culture wounding. Each bar in the top panel represents the number of cells that migrated into the wounded area (mean \pm SEM from 10 to 12 microscope fields). Each bar in the bottom pannel represents number of viable cells in the wounded area (mean \pm SEM from 10 to 12 microscope fields).....73
- Figure 4.12.** Effect of daily administration of ATF-methioninase fusion protein (FP) to the MCF-7 cancer cells.....76
- Figure 4.13.** Effect of TGF-methioninase fusion protein on MCF-7 breast cancer cell proliferation and migration. Each bar in the top panel represents the maximum distance traveled by cells in the wounded area (mean \pm SEM from 10 to 12 microscope fields). Each bar in the bottom panel represents number of viable cells in the wounded area (mean \pm SEM from 10 to 12 microscope fields).78
- Figure 4.14.** Photomicrographs (40X) of MCF-7 cells treated for 18 hours with either: vehicle control (C); ATF-methioninase fusion protein (FP); mutated ATF-methioninase (M-FP); L-methioninase (L-M); or fusion protein + urokinase (UK+FP). All treatments were for 18 hours at a concentration of 10-6 M. The red/brown color represents positive staining of the L-methioninase-specific primary antibody.80
- Figure 4.17.** Binding of methioninase-annexin V to phosphatidylserine adsorbed to plastic. Blank for assay: +1° Ab, +2° Ab. Control for assay (▲): L-methioninase, +1° Ab, +2° Ab. (each A₄₅₀ measured in triplicate).....86
- Figure 4.18.** Binding of methioninase-annexin V to phosphatidyl serine exposed on MCF-7 breast cancer cells. Blank for assay: +1° Ab, +2° Ab. Control for assay (▲): L-methioninase, +1° Ab, +2° Ab. (each A₄₅₀ measured in triplicate).....87

LIST OF TABLES

Table 1.1. Molecular weight and number of amino acid residues of fusion proteins.	22
Table 3.1. Reaction composition for PCR.	34
Table 3.2. Cycling parameters for PCR.	34
Table 4.1. Average yield and specific activity of purified fusion proteins.	63

ABSTRACT

It has been shown that methionine depletion inhibits tumor cell growth and reduces tumor cell survival. The main purpose of this project is to examine three fusion proteins for targeting human cancer cells selectively and inhibiting the migration and proliferation of the cancer cells. The fusion proteins studied are ATF-methioninase (amino-terminal fragment of urokinase, amino acids 1-49, linked to the amino terminus of L-methioninase from *Pseudomonas putida*), TGF-methioninase (human transforming growth factor- α linked to L-methioninase), and methioninase-annexin V (L-methioninase linked to the amino terminus of human annexin V). The three fusion proteins were expressed as soluble proteins and purified to near homogeneity. Flash freezing and followed by lyophilization was found to be most effective way to store fusion protein samples.

The influence of the fusion protein on the growth and motility of human breast cancer cells, SK-LU-1 human lung cancer cells, and PC-3 human prostate cancer cells was examined using a culture wounding assay. ATF-methioninase inhibited the proliferation and migration of all cancer cell lines. For MCF-7 breast cancer cells, the inhibition by ATF-methioninase was much greater than for either free L-methioninase or mutated ATF-methioninase (mutated to give inactive enzyme). TGF-methioninase inhibited the proliferation and migration in MCF-7 and PC-3 cancer cells. However, the inhibition was significantly greater for ATF-methioninase compared to TGF-methioninase, especially at treatment days 2 and 3.

ATF-methioninase binding to MCF-7 cells was measured by immunocytochemical localization. MCF-7 tumor xenograft growth was measured in nude

mice for the mice treated with ATF-methioninase and L-methioninase. Treatment of s.c. implanted MCF-7 breast cancer cells mouse xenografts with ATF-methioninase gave significantly more tumor regression when compared to mouse xenografts treated with L-methioninase alone or with the vehicle control.

The methioninase-annexin V fusion protein bound specifically to phosphatidylserine (PS) immobilized on plastic plates, as well as on the surface of MCF-7 cancer cells in which PS was induced to be on the surface by the addition of hydrogen peroxide.

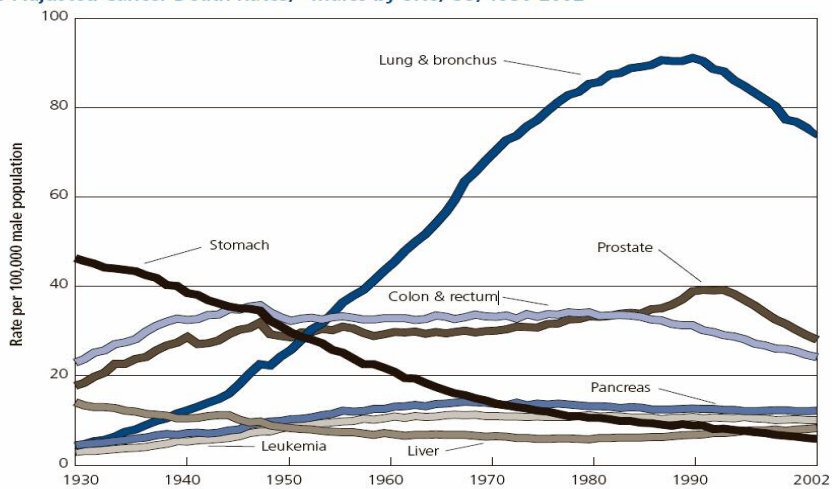
1. INTRODUCTION

Cancer is the one of the leading causes of mortality in United States of America. The rates of cancer began to fall in the U.S.A., about 13 years ago (**Figure 1.1**), but cancers still account for major percentage of total deaths in this country. In 2006, estimated cancer related deaths are 560,000 according to the American Cancer Society (ACS). Based on the estimated number of new cases of cancers for the year 2006, the top five types of cancer are as follows: prostate, breast, lung, colon, and urinary bladder.

A most feared and dangerous aspect of cancer is metastasis, where cells break away from the primary tumor site, invade local tissues and vessels, and establish new cancer colonies at distant sites. Key steps in the metastatic cascade include cell proliferation, regulated expression of extra-cellular matrix degrading enzymes, active movement through tissues, invasion through basement membranes into blood or lymph vessels, dissemination to distant locations, and invasion and movement into a target organ, where the cancer cells once again proliferate to form a secondary tumor [1, 2]. The formation of new blood vessels, angiogenesis, is a requirement for the growth of primary tumors and secondary tumors. The primary tumors itself are not lethal, but it is the metastatic spread of tumor cells to other sites, especially brain, that is lethal. Unfortunately, many tumors, like breast tumors are detected that may have already metastasized to new sites.

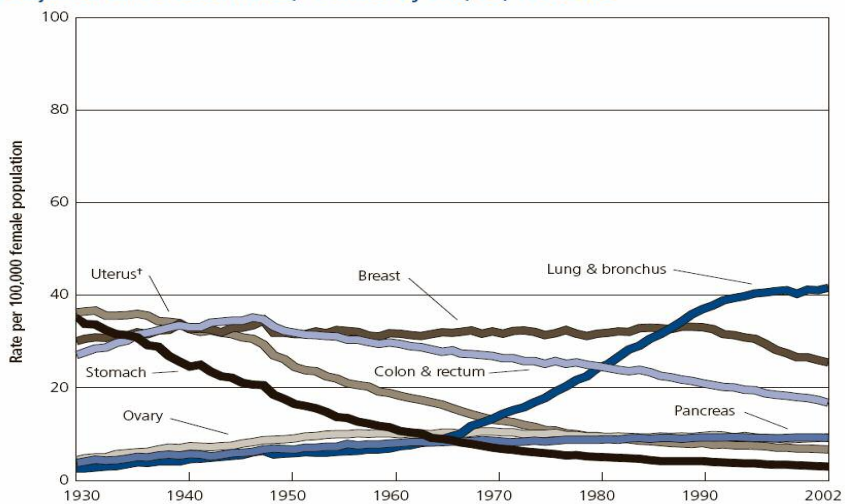
Curing cancer requires eliminating all cancer cells. Chemotherapy, radiotherapy, gene therapy, and surgery are some of the treatments for cancer [3]. Most treatment methods cannot prevent the spread of cancer in the body by metastases, which lead to numerous tumors around the body. Chemotherapy has been used widely to treat the

Age-Adjusted Cancer Death Rates,* Males by Site, US, 1930-2002



*Per 100,000, age-adjusted to the 2000 US standard population.
Note: Due to changes in ICD coding, numerator information has changed over time. Rates for cancer of the liver, lung and bronchus, and colon and rectum are affected by these coding changes.
Source: US Mortality Public Use Data Tapes 1960 to 2002, US Mortality Volumes 1930 to 1959, National Center for Health Statistics, Centers for Disease Control and Prevention, 2005.
 American Cancer Society, Surveillance Research, 2006

Age-Adjusted Cancer Death Rates,* Females by Site, US, 1930-2002



*Per 100,000, age-adjusted to the 2000 US standard population. †Uterus cancer death rates are for uterine cervix and uterine corpus combined.
Note: Due to changes in ICD coding, numerator information has changed over time. Rates for cancer of the lung and bronchus, colon and rectum, and ovary are affected by these coding changes.
Source: US Mortality Public Use Data Tapes 1960 to 2002, US Mortality Volumes 1930 to 1959, National Center for Health Statistics, Centers for Disease Control and Prevention, 2005.
 American Cancer Society, Surveillance Research, 2006

Figure 1.1. Age-adjusted cancer death rates, for males (Top) and for females (bottom), U.S. 1930-2002 (Source: ACS, Cancer Statistics 2006)

disseminated cancers, but the risk factor for damaging other normal tissues is high. Surgical removal of cancer tissue has been effective in breast and prostate cancers but has failed in curing widely disseminated cancers. In gene therapy, delivery of a gene is achieved by polymer capsules, liposomes, viruses, microinjections and electroporation [4-7]. Delivery systems of viral origin, such as adenoviruses and retroviruses, are widely used for gene therapy because of their high transfection efficiency. However, viral vectors have various disadvantages, which include toxicity and high levels of immunogenicity that restrict the repeated use of these delivery systems.

Since most of these therapies are not cancer specific, the ultimate goal of cancer therapy is to develop agents that will selectively destroy cancer cells, sparing the normal tissues of the patient. The major goal of this work is to develop a therapeutic anticancer agent which targets specifically to cancer cells and to test the effectiveness to kill the cancer cells or prevent them from growing.

The following section is an overview of the dependency of cancer cells on methionine and is followed by a description of the anticancer effects by L-methioninase from *Pseudomonas putida*. Then a review is given of three targets on the surface of cancer cells: urokinase receptor, epidermal growth factor receptor, and phosphatidyl serine. Finally, the experimental hypothesis and experimental design are discussed for three fusion proteins designed to bind to these three targets.

Methionine Dependency in Cancer Cells

Methionine is an essential nonpolar amino acid. It has many major functions: 1) the methionine derivative S-adenosyl methionine (SAM) serves as a methyl donor [8-10]; 2) it is required for the formation of polyamines, which have specific roles in embryonic development, cell cycle, cancer, neurochemistry as well as pulmonary and immune system functions; [11] 3) it plays a role in cysteine, carnitine and taurine synthesis; 4) it is incorporated into the N-terminal position of all proteins in eukaryotes, although it is usually removed after post translation modifications; 5) it is a precursor of glutathione, an antioxidant, that protects cells from toxins such as free radicals [12].

Over the decades, many metabolic anomalies are commonly found in solid tumors. Among the metabolic abnormalities recurrently found in cancers, methionine dependency and alterations of methionine metabolism have been found in many, if not in all, types of human tumors [13-20]. Methionine dependence is defined as the inability or reduced ability of cancer cells when compared with normal cells to proliferate when amino acid methionine is replaced by its immediate precursor homocysteine. Homocysteine is a non-standard amino acid that has the same structure as methionine except that it lacks a methyl group (**Figure 1.2**). All normal cells like fibroblasts, kidney, liver, and epithelial cells have been shown to be methionine independent [13, 15, 16]. Numerous tumor cell lines like breast, lung, colon, kidney, bladder, melanoma, and glioblastoma have been shown to be methionine dependent [15, 21, 22].

The biochemical basis of methionine dependence in tumor cells has not been fully elucidated. One hypothesis is that it is due to the reduced or no synthesis of methionine in cancer cells due to a deficiency of enzymes responsible for the synthesis of methionine,

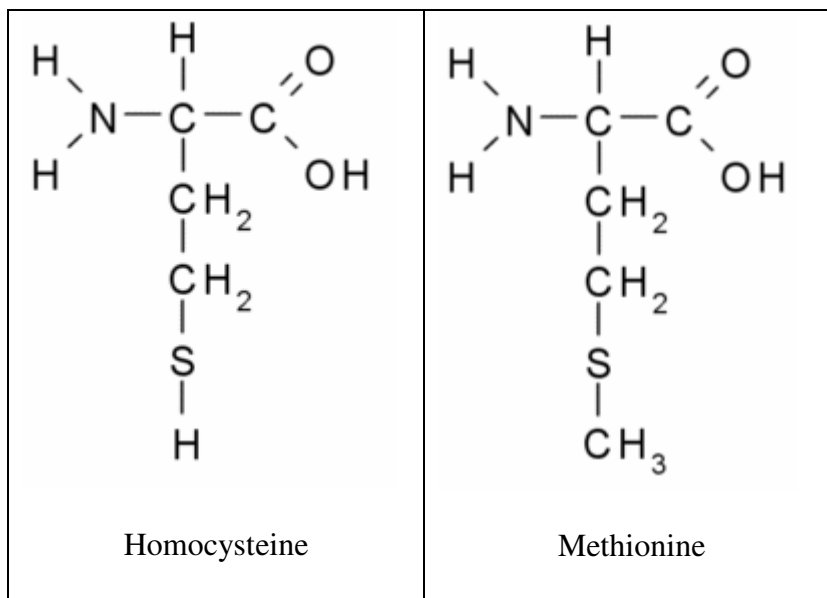


Figure 1.2. Structures of homocysteine and methionine

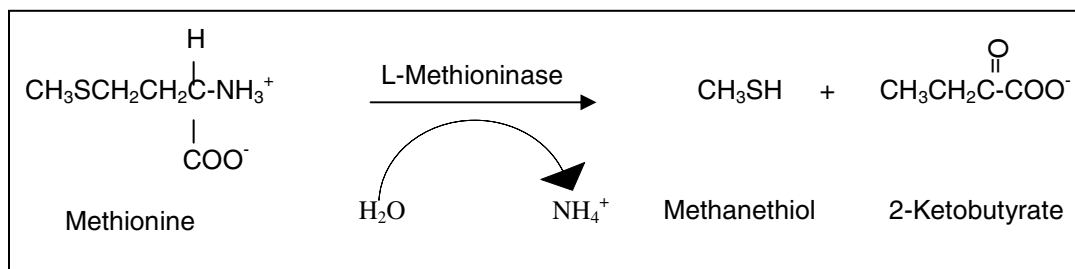


Figure 1.3. Reaction catalyzed by methioninase

methionine synthase or betaine homocysteine methyltransferase. Either of these enzymes can catalyze the methylation of homocysteine to form methionine in normal cells. Methionine synthase occurs in all mammalian tissues, while the betaine enzyme is mainly present in the liver [23]. It was shown that methionine-dependent tumor cell lines have low amounts or low activity of methionine synthase [24, 25]. Another reason for methionine dependency could be due to higher transmethylation reaction rates by methionine dependent tumor cells when compared to normal cells. Methionine plays an important role in the synthesis of methyl donor S-adenosylmethionine (SAM) which is a cofactor for transmethylation reactions. SAM donates a methyl group to form S-adenosylhomocysteine, and also SAM plays a pivotal role as a methyl donor in a myriad of biological and biochemical events [10]. Elevated transmethylation reaction rates suggest that tumor cells depend on exogenous methionine for the survival and proliferation [20]. Finally this methionine dependency could be due to non-conservation of methionine in cells which is achieved by methylthioadenosine phosphorylase, which functions solely in polyamine pathway of cells by removing methylthioadenosine product from both spermidine synthase and spermine synthase [23].

Methioninase as Anticancer Agent

L-Methioninase is a pyridoxal 5'-phosphate (PLP) enzyme that catalyses α , γ – elimination and γ -replacement of L-methionine and its S-substituted derivatives as shown in **Figure 1.3**. This enzyme was found in the extracts of a soil bacterium, *Clostridium* sp, *Pseudomonas* sp, rumen bacteria, and *Aeromonas* sp. The enzyme was initially isolated from *Clostridium sporogenes* [26]; later it was isolated from *Pseudomonas putida* [27]. The L-methioninase gene, from *Pseudomonas putida*, was cloned in *Escherichia coli* and

milligram quantities were isolated [28]. L-methioninase from *Pseudomonas putida* is known to exist as homotetramer form (**Figure 1.4**), and its quaternary structure is observed in the crystal structure (**Figure 1.4**) [29, 30]. Each monomer consists of 398 amino acids and contains a PLP molecule as cofactor, which is covalently linked to Lys 211. Each monomer consists of three domains with an N-terminal domain (residues 1-63) comprising of an α -helix and loop of 46 residues, a PLP binding domain (residues 64-262) comprising of seven parallel β -strands, and the C-terminal domain (residues 263-398) comprising of five anti parallel β -strands [29, 30] as shown in **Figure 1.5**. Cys116 of L-methioninase is a nucleophilic residue and is expected to play a key role in enzymatic reactions. It was also shown that when Tyr114 of L-methioninase is mutated to Phe114, then the enzymatic activity of L-methioninase decreased by 910 fold [31], suggesting that Tyr114 plays a critical role in the catalytic mechanism.

Various studies of using L-methioninase for treatment of animal and human subjects have been carried out. In two studies, i.v. infusion of L-methioninase for 24 hours to nine patients with advanced lung, breast or kidney cancer, or lymphoma in a phase I clinical trial resulted in serum methionine being reduced to very low levels, with no adverse effects observed [19]. L-Methioninase enzyme treatment in combination with chemotherapeutic agents such as cisplatin, 5-fluorouracil, and 1,3-bis(2-chloroethyl)-1-nitrosourea have shown efficacy and synergy, in mouse models of colon cancer, lung cancer, and brain cancer [32-35]. L-Methioninase treatment in combination with the addition of the L-methioninase gene using a retroviral vector showed a synergistic effect

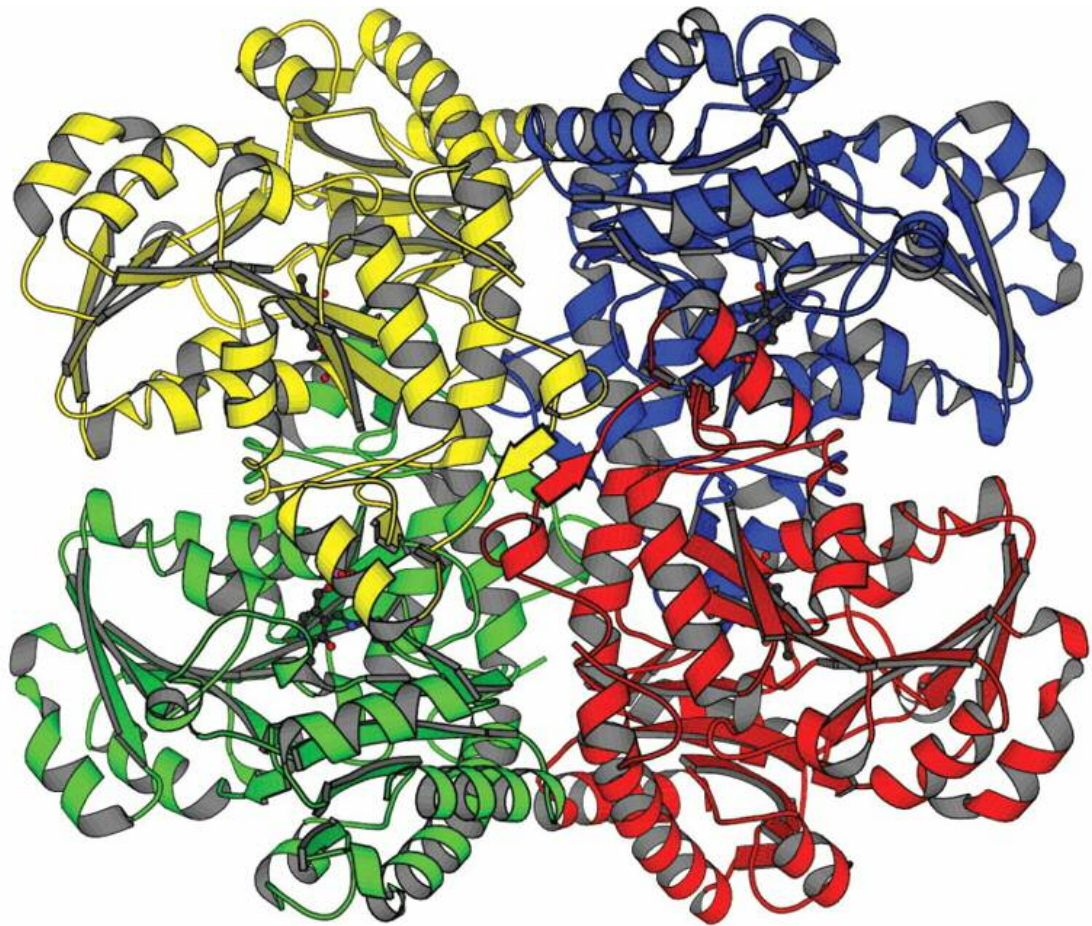


Figure 1.4. Homotetramer structure of L-methioninase. Each color represents each monomer of L-methioninase [30].

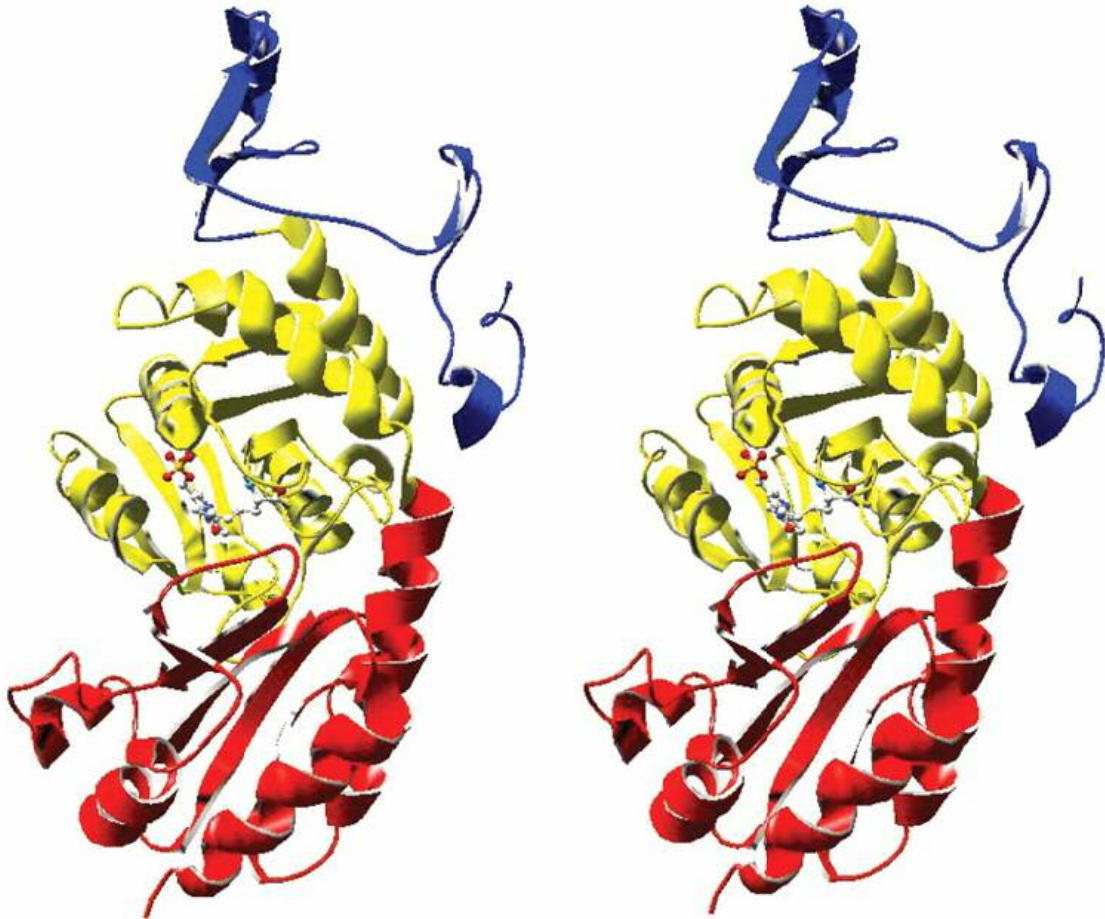


Figure 1.5. Structure of L-methioninase, The N-terminal domain is held in blue, the PLP-binding domain in yellow and the C-terminal domain in red. PLP and PLP-binding Lys211 are shown in a ball and stick representation [30].

on human ovarian cancer cells and human fibro sarcoma cells [36]. L-methioninase has been successfully conjugated to polyethylene glycol (PEG), resulting in a significant increase in the serum half-life and a large reduction in immunogenicity in rats and primates [18, 37-39].

To summarize, due to the antitumor efficacy of L-methioninase *in vitro* and *in vivo* in human tumors xenografted in nude mice and also in humans, L-methioninase has shown promise as an anticancer agent. By targeting the L-methioninase to cancer cells, the efficacy of cancer treatment should be improved by reducing the dose level and immune response. The dose can be reduced because the L-methioninase will accumulate on the cancer cell surface, where it will degrade methionine coming in contact with the cell surface. This will require less enzyme than for non-targeted enzyme, which must always be in the fluid surrounding the cells in order to be effective. The immune response can possibly be reduced because this treatment is designed to localize L-methioninase in the tumor, rather than it being delivered to the entire body.

Selectivity to cancer cells is achieved usually by fusing or attaching the anticancer agent to a ligand or molecule, which can target specifically to cancer cells. This selectivity is achieved by three ways. The first way is to use an antibody which can specifically target the antigenic moieties that are not detectable or minimally present on cells in normal cells but present in greater quantities on cancer cells. So far only few antigens have been really specific to cancers cells (tumor specific antigens (TSA)). Antibodies against TSAs like clone-specific idiotypic immunoglobulin on the surface of the malignant B cells and clone-specific T-cell antigen-receptor protein on malignant T cells are used mainly in this kind of treatment [40-42]. The second way of selectivity is

based on recognition of cell surface-associated molecules that are overexpressed and abundant on cancer cells. These surface-associated molecules include lectins, growth factors (epidermal growth factor, insulin like growth factor), cytokines, hormones, and low-density lipoproteins [43-45]. The third way of targeting cells is by targeting endothelial cells of the vasculature of the tumor. Vascular endothelial cells in tumors differ from normal cells in their metabolic pathways, gene expression, and immunological and biochemical characteristics [46-48]. The ligand-based vascular targeting agents include fusion proteins (e.g., vascular endothelial growth factor linked to gelonin), immunotoxins (e.g., monoclonal antibodies to endoglin linked to ricin, antibodies linked to cytokines or coagulant proteins), and liposomally encapsulated drugs.

In this project, the second and third ways were used to target L-methioninase (anticancer agent) to cancer cells by fusing with the peptides or protein which would target to overexpressed receptors on cancer cells and endothelial cells of the tumor vasculature. The amino terminal fragment (ATF) of urokinase and transforming growth factor- α (TGF- α) were used to target the urokinase plasminogen activator receptors and the epidermal growth factor receptors of cancer cells. Annexin V was used to target tumor vasculature endothelial cells. The rationale for selecting these peptides or proteins is explained in the following sections.

Urokinase Plasminogen Activator Receptor as a Target on Cancer Cells

The serine protease urokinase-type plasminogen activator system plays an important role in the mediation of extracellular proteolytic degradation activity. This system consists of the serine protease urokinase (uPA), urokinase plasminogen activator receptor (uPAR), plasminogen activator inhibitors (PAIs), and the proenzyme plasminogen. uPA is the two chain molecule which is formed after cleavage of single chain pro-uPA by plasmin. The system gets activated by uPA bound to uPAR by converting plasminogen to plasmin and initiating the signaling cascades (**Figure 1.6**). This signaling cascade is only initiated in cell types like leukocytes, smooth muscle cells, and endothelial cells which have a role of inflammation, angiogenesis and wound repair.

The uPAR consists of three domains and it is attached to outer cell membrane by a glycosyl phosphatidylinositol (GPI). It is a 50-60 kDa glycoprotein, with protein contributing to 31.5 kDa of the mass. It has three domains (D1, D2, and D3). The N-terminus of the uPAR is the primary site for the binding of amino terminal fragment (ATF) of uPA, but all the three domains are important for high affinity binding of uPA to uPAR. The three domains form a concave shape having a cone-shaped cavity at center. Most normal cells have little or no detectable uPAR, with some exceptions [49]. uPAR is expressed in hematopoietic cells, such as monocytes, eosinophils, neutrophilic granulocytes, skin mast cells, dendritic cells, and T-lymphocytes. It is found expressed in non-hematopoietic cells, such as endothelial cells, hepatocytes, fibroblasts, keratinocytes, smooth muscle cells, and placental trophoblasts [49]. uPAR is overexpressed in variety of cancer tissues, like breast, colon, kidney, liver, lung, oral mucosa, and ovary [50-58].

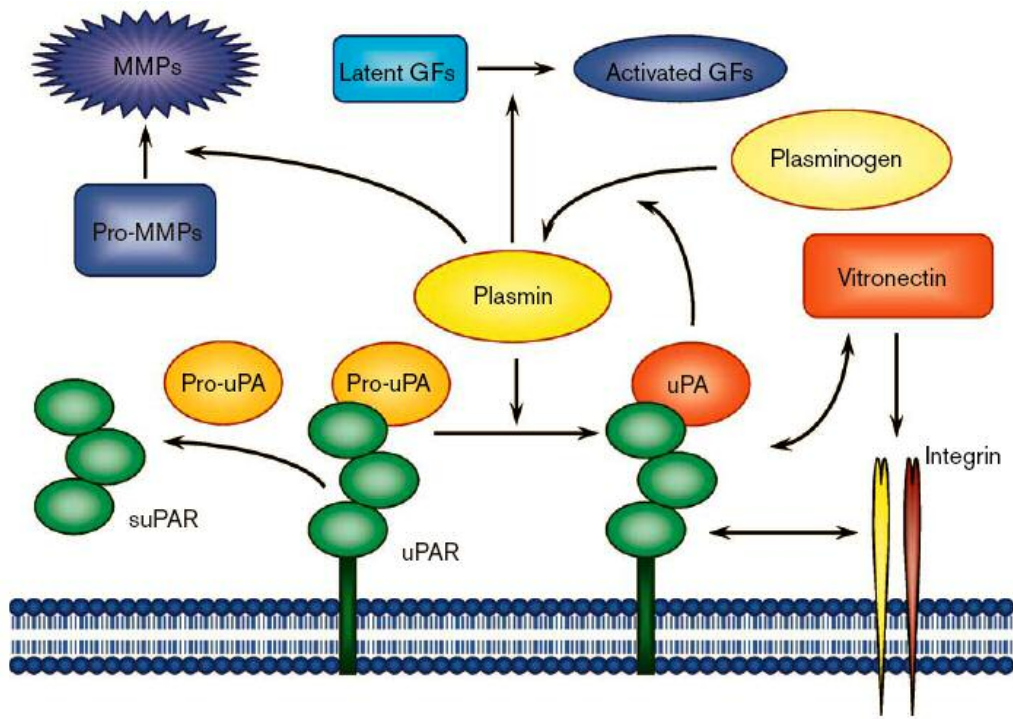


Figure 1.6. The uPA/uPAR system. The pro-uPA binds to uPAR, which is converted to active uPA after cleavage by plasmin. Active uPA is responsible for converting plasminogen to plasmin, which is responsible for degradation of extracellular matrix [59].

Pro-uPA has 411 amino acids (**Figure 1.7**). The amino terminal fragment (ATF) consists of 135 amino acids, containing a growth factor (GF) domain (10-40 amino acids) joined by a triple disulfide kringle domain (90 amino acids) [60, 61]. The C-terminal 253 amino acids comprise the serine protease domain. Pro-uPA is cleaved to give an active protein (uPA) by plasmin at Lys158, leaving A and B chains joined via disulfide linkages as shown in **Figure 1.7**. Residues 12-32 in the GF domain of chain A of uPA play a key role in binding to its receptor uPAR, and the GF domain shares sequence homology of the GF domain with epidermal growth factor (EGF) [60, 61]. The catalytic portion of uPA is necessary for the internalization of the uPA and signaling cascade [62]. It has also been shown that blocking the cell surface activity of uPA with an inactive uPA causes a reduction in metastasis by cancer cells [63].

PAI-1 is the major inhibitor of urokinase activity in plasma and in most tissues. Binding of the PAI-1 to pro-uPA forms an inactive, reversible complex which is a stable noncovalently-linked intermediate [49]. Binding of PAI-1 to pro-uPA is controlled by the amount of plasminogen, which inhibits the reaction, as well as on the concentration of vitronectin. PAI-1 possesses a vitronectin binding site and competes with uPAR for vitronectin binding [49, 64].

The ATF of uPA is an excellent choice to fuse it with L-methioninase for three reasons: (1) It will bind to a receptor that is overexpressed on many types of cancer cells. (2) It will not be internalized and will thus keep L-methioninase at the cell surface to prevent methionine from entering the cell. (3) It will prevent uPAR from binding to uPA and thus reduce metastasis and migration through tissue. Using this approach, a

synergistic inhibition of cancer cell migration and proliferation should be able to be achieved from the inactivation of the urokinase receptor as well as from the methioninase activity on cancer cells.

Epidermal Growth Factor Receptor as Target on Cancer Cells

EGFR is a 170 kDa single linear transmembrane glycoprotein consisting of a ligand binding extracellular domain (cysteine rich domains) and a cytoplasmic domain encoding tyrosine kinase, where these domains are linked through a hydrophobic membrane anchor sequence. Binding of a stimulatory ligand (like EGF or transforming growth factor- α , TGF- α) to the extracellular domain results in receptor dimerization and autophosphorylation of EGFR, which initiates the intracellular transduction [66] (**Figure 1.8**). Autophosphorylated EGFR also activates the proteins required for endocytosis and finally leads to internalization of EGFR [67-69]. It has been suggested that overexpression of the EGF receptor in tumor cells provides a mechanism for autocrine growth stimulation leading to uncontrolled growth and cellular transformation, although oncogenic transformation through the EGF receptor only occurs in the presence of excess ligand [70]. The exact role of the EGF receptor in metastasis is not known, but it has been observed that more malignant tumors express higher amounts of cell surface EGF receptors [71]. EGFR is overexpressed in head and neck squamous cell cancer and cervical, renal cell, lung, prostate, bladder, colorectal, pancreatic, breast cancer, melanoma, glioblastoma, and meningioma [72-77]. This receptor has been targeted by a fusion protein consisting of the TGF- α binding peptide linked to *Pseudomonas* exotoxin with its binding domain removed [78]. The problem with this approach is that normal cells with the receptors bound by the fusion protein are also killed, resulting in potentially

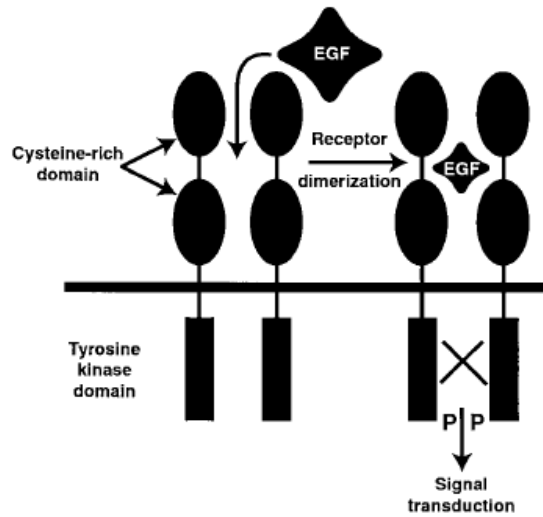


Figure 1.8. Epidermal growth factor receptor [79]. Binding of EGF or TGF- α to EGFR autophosphorylates the cytoplasmic domain of EGFR and triggers signal for proliferation.

severe side effects. TGF- α is a 51 amino acid peptide with a molecular weight of 6 kDa, which binds to EGFR with the same affinity as EGF for mammalian cells and is chosen as a targeting peptide in the fusion protein (TGF-methioninase). Comparison of targeting TGF-methioninase and ATF-methioninase to cancer cells will enable a determination of the importance of internalization by the targeted receptor to the effectiveness of treatment.

Phosphatidylserine (PS) as Target on Tumor Vasculature Endothelium

In mammalian cells, the phosphatidylserine (PS) content is higher in the plasma membrane than other organelles. When normal cells are under no stress, PS is exclusively located on the cytoplasmic side of the plasma membrane [80, 81]. Once cells are activated by certain stimuli, PS is rapidly externalized on the cell surface, followed by various physiological extracellular events. This asymmetry of PS is controlled by the ATP-dependent enzyme aminophospholipid translocase, which transports the PS to the cytoplasm and Ca²⁺ dependent enzyme scramblase, which in turn transports PS from the cytoplasm to the external surface of the cell [82, 83]. Loss of PS asymmetry is observed under different pathologic and physiologic conditions, including apoptosis, cell aging, intercellular fusion of myoblasts and trophoblasts, cell migration, activation of platelets, and cell degranulation [84-88]. Spontaneous PS exposure has been observed also in malignant cells in the absence of exogenous activators or cell injury [82, 83]. Exposure of PS is also observed in vascular endothelial cells and could be due to hypoxia/reoxygenation, acidity, thrombin, inflammatory cytokines, and reactive oxygen species in stress conditions which may generate Ca²⁺ fluxes in the tumor vascular endothelium that activate scramblase or inhibit aminophospholipid translocase [89, 90].

It has been previously shown that anionic phospholipids become exposed on the vascular endothelium of blood vessels in mice bearing various types of solid tumors [89, 90]. This was demonstrated by generating a rat immunoglobulin M monoclonal antibody, 9D2, directed against anionic phospholipids and administering it *i.v.* to the mice. Due to abundant availability of PS on tumor endothelial cells and its absence in normal endothelium cells, it has been studied as a target for cancer therapy.

Annexin V is a 36 kDa protein which binds specifically to PS in the presence of calcium. Annexin V has been crystallized and shown to have a single subunit structure with four tandem repeats [91]. It has also been shown that annexin V binds to the tumor vascular endothelium but not the normal vascular endothelium [89].

In this project, a fusion protein is designed to target L-methioninase to the tumor vasculature by fusing annexin V to the C-terminus of L-methioninase. The reasons why this design is advantageous are as follows: (1) The fusion protein can be administered *i.v.*, which is much easier than administering L-methioninase directly to the cancer cells. (2) The fusion protein will bind to the surface of the tumor vasculature and prevent methionine in the bloodstream from reaching the tumor. The dosages required should be low since the fusion protein will be binding only to the tumor vasculature.

Experimental Hypothesis and Experimental Design

Based on this literature review, the hypotheses of this study are: (1) ATF-methioninase, TGF-methioninase, and methioninase-annexin V fusion proteins will be expressed in *E. coli* in soluble and active form, (2) these fusion proteins will bind selectively to cancer cells, (3) ATF-methioninase, TGF-methioninase, and methioninase-annexin V proteins would selectively kill the cancers or cause cell growth to be inhibited both *in vitro* and *in vivo*. These hypotheses were tested using the following experimental design:

1. *Construction and expression of fusion protein genes.* Three fusion protein genes will be constructed by using the polymerase chain reaction. These genes will be cloned and expressed recombinantly in *E. coli*. The general structure of fusion proteins are shown in the **Figure 1.9**. The number of amino acid residues and molecular weights of all the fusion proteins are shown in **Table 1.1**. All the fusion proteins have a flexible linker (Gly-Ser-Gly-Ser-Gly-Ser), where the two proteins are fused without disturbing their function and are not susceptible to degradation by host proteases [92]. The ATF and TGF- α are placed at the N-terminus of the fusion protein so that the binding domains of either ATF or TGF- α are not disturbed. Annexin V was placed at C-terminus since the binding domain of annexin V is located at the C-terminus. ATF-methioninase was already expressed and purified in this lab previously [93]. So ATF-methioninase, TGF-methioninase, and methioninase-annexin fusion proteins are expected to form soluble proteins because each fusion contains a large known soluble protein, L-methioninase. The solubility of these proteins will be analyzed by the Bradford assay for total protein

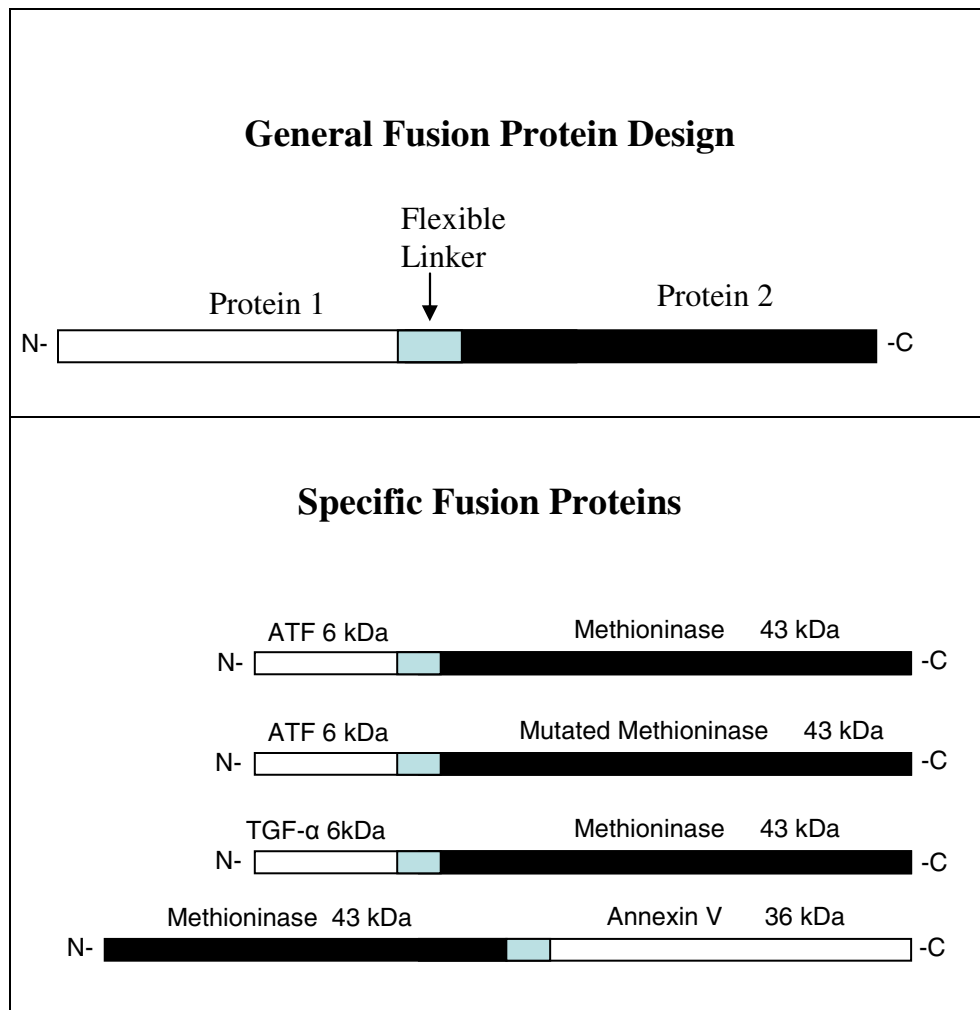


Figure 1.9. General structure of the fusion proteins (not to scale) constructed for this study. ATF is the N-terminal 1-49 amino acids of the urokinase A chain. TGF- α is the transforming growth factor- α .

Protein	Residues	Molecular Weight (KDa)
ATF-methioninase	452	48.5
Mutated ATF-methioninase	452	48.5
TGF-methioninase	454	48.6
Methioninase-annexin V	719	78.5

Table 1.1. Molecular weight and number of amino acid residues of fusion proteins.

and sodium dodecyl sulfate polyacrylamide electrophoresis (SDS-PAGE) to separate the proteins.

Amino acids 1-49 of the ATF are used since this region includes residues 12-32 that have been shown to be critical for binding to the urokinase receptor [60]. The kringle domain of urokinase A chain is excluded because this domain has been shown to bind heparin, which could bind polyanionic molecules such as proteoglycans and aid in the invasion of tissue [94]. This is the main reason to choose ATF with 1-49 amino acids over ATF with 1-135 amino acids.

2. *Examination and determination of anticancer effects of ATF-methioninase and TGF-methioninase on cancer cells.* Anticancer effects of these fusion proteins will be studied using the cell culture wounding model [93]. It is anticipated that targeting TGF-methioninase to its internalizing receptor EGFR will be less inhibitory to cancer cells than targeting ATF-methioninase to its non-internalizing receptor uPAR

3. *Examination of binding of ATF-methioninase to MCF-7 breast cancer cells.* Previously it has been shown that ATF-methioninase binds specifically to MCF-7 breast cancer cells [93]. In this present study, the specific binding of ATF-methioninase fusion protein to cancer cells will be demonstrated by immunocytochemical localization. It is expected that ATF-methioninase will bind selectively to cancer cells and that L-methioninase will not bind.

4. *Effect of targeted L-methioninase on the growth of MCF-7 breast cancer cells in nude mice.* The nude mouse xenograft model will be used to determine the influence of the ATF-methioninase upon the growth of breast cancer cells *in vivo*. It is expected that

the ATF-methioninase will not be cytotoxic to the nude mice and inhibition of tumor growth will be more effective than L-methioninase treatment alone.

5. *Determination of the binding of the methioninase-annexin fusion protein to PS.*

This is done using plastic-immobilized PS and using MCF-7 breast cancer cells, in which PS is induced to be on the cell surface by the addition of hydrogen peroxide. It is expected that binding will increase as the concentration of methioninase-annexin increases and that binding of an L-methioninase control will be minimal.

Part of the work presented following this section was published or was in press prior to the publication of this dissertation [95-97].

2. MATERIALS

Plasmids and Bacterial Strains

Plasmid pKK223-3 containing the ATF-methioninase fusion gene (pKK223-3/ATF-METH) was synthesized previously in this lab [93]. Plasmid containing TGF- α was kindly provided by Dr. Ira Pastan of the National Cancer Institute (pVC387/TGF), and plasmid containing the annexin V-soluble tissue factor fusion gene (pET-22b(+)/STFANX) was kindly provided by Dr. Stuart Lind of OU Health Sciences Center. Linear vector pET-30 Ek/LIC (Novagen, Madison, WI) was used for ATF-methioninase, L-methioninase, methioninase-annexin V, and annexin V gene constructions. A map of this plasmid showing its general features is shown in **Figure 2.1**. Linear vector pET-44 Ek/LIC (Novagen) was used for TGF- α -methioninase fusion gene construction. A map of this plasmid showing its general features is shown in **Figure 2.2**. *E. coli* NovaBlue singles were used for plasmid amplification. *E. coli* BL21(DE3) was used as the protein expression host. *E. coli* XL1-Blue was used as host for site-directed mutagenesis.

Media for E.coli Cell Cultures

Yeast extract and tryptone for LB media and all other media additives were purchased from Sigma (St Louis, MO).

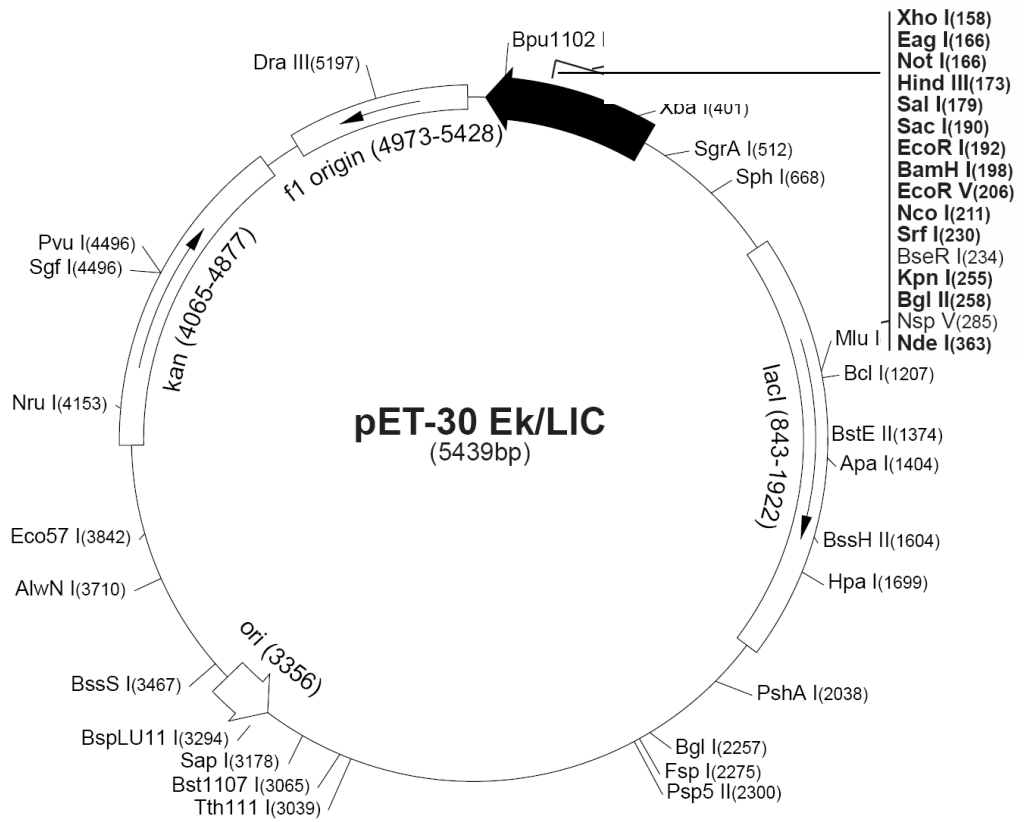
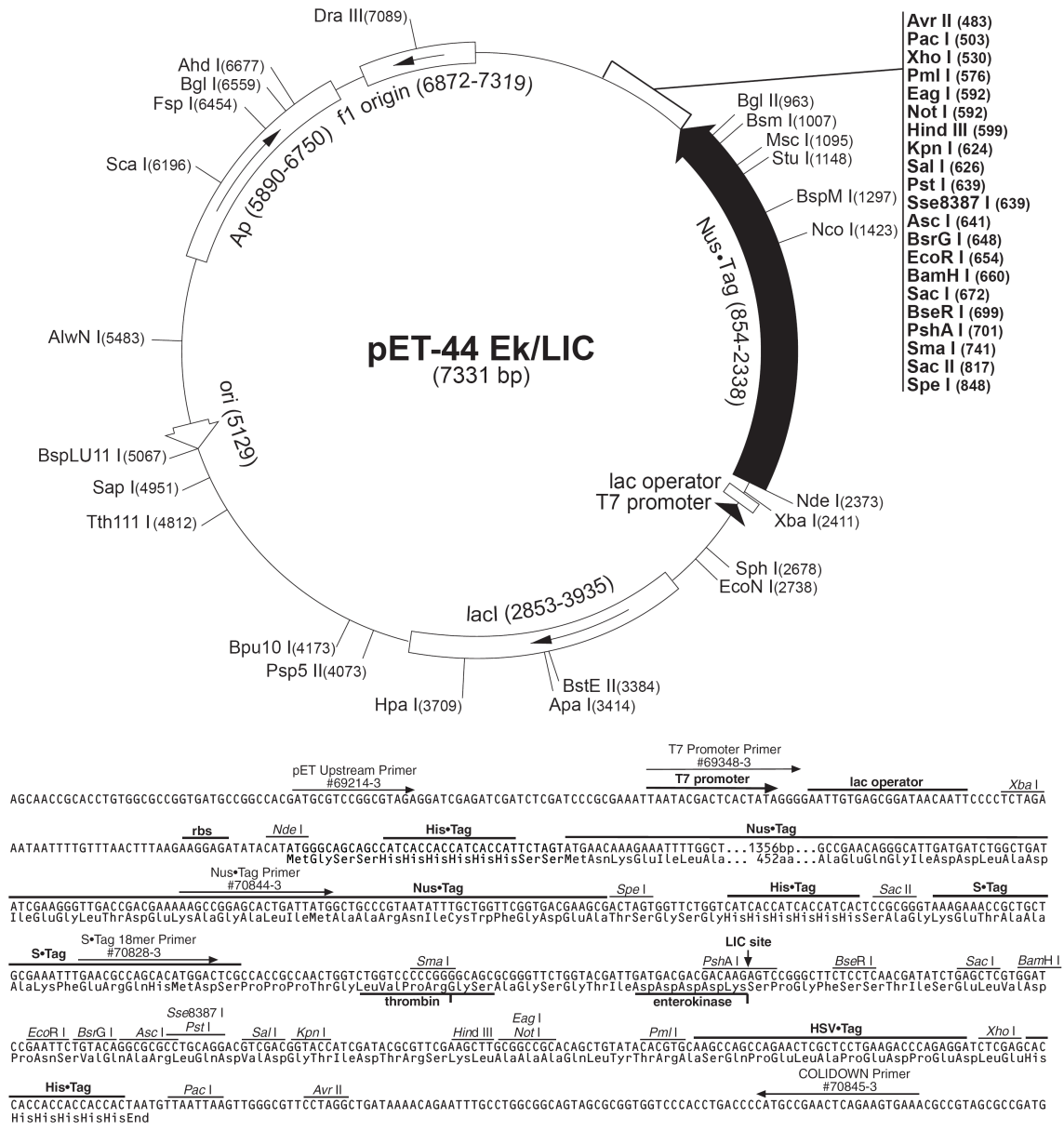


Figure 2.1.The pET-30 Ek/LIC vector. General features of the pET-30 Ek/LIC vector (Novagen catalog, 2006).



pET-44 Ek/LIC cloning/expression region

Figure 2.2. The pET-44 Ek/LIC vector. General features of the pET-30 Ek/LIC vector (Novagen catalog, 2006).

Enzymes

Expand[™] PCR reagents were purchased from Boehringer Mannheim Corp. (Indianapolis, IN). T4 DNA ligase and restriction enzyme BamHI were purchased from New England BioLabs (Beverly, MA). T4 DNA polymerase and HRV 3C protease were purchased from Novagen. DpnI enzyme and PfuTurbo DNA polymerase for site-directed mutagenesis were purchased from Stratagene (La Jolla, CA).

DNA Synthesis, Purification, and Analysis

Primers for the PCR amplification of the gene fragments were synthesized by the Molecular Biology Resource Facility at University of Oklahoma Health Sciences Center (Oklahoma City, OK). All the primers were desalted, analyzed and not purified. The Qiaquick PCR purification kit, Qiaquick agarose gel purification kit, and Qiaquick plasmid purification kit were purchased from Qiagen (Valencia, CA). SeaKem® LE agarose was purchased from Cambrex Bio Science Rockland, Inc.(Rockland, ME). The 1kb DNA ladder and λ DNA-BstEII digest ladder were purchased from New England Biolabs. The sequencing of all the genes was performed by the Oklahoma Medical Research Foundation (OMRF) DNA sequencing facility using primers that we specified.

SDS-PAGE and Immunoblotting

The PROTEAN[™] large format and small format electrophoresis cells (Bio-Rad, Hercules, CA) were used for protein analysis by SDS-PAGE. All the reagents used for making SDS-PAGE gels were purchased from Bio-Rad. Rabbit anti-L-methioninase monoclonal primary antibody was produced in purified form and obtained from Sigma Genosys (St. Louis, MO). Goat anti-rabbit IgG secondary antibody with horseradish

peroxidase (HRP) conjugated was purchased from Sigma. Nitrocellulose membranes, NitroBind were purchased from Micron Separations Inc. (Westborough, MA).

Protein Purification

HisTrap chromatography columns (5 ml) were purchased from GE Health Bio-Sciences Corp. (Piscataway, NJ). Flow adapters were purchased from Bio-Rad. For detection of proteins at 280 nm, an ISCO UA-5 chart recorder and absorbance/fluorescence detector with a type-10 optical unit (Isco, Lincoln, NE) were used. A Gilson MiniPuls 3 peristaltic pump (Gilson Medical Electronics Inc., Middletown, WI) was used for chromatography during protein purification. Centriprep centrifugal filters were from Millipore (Billerica, MA).

Media for Cancer Cell Cultures

MCF-7 human breast cancer cells were obtained from the Michigan Cancer Foundation (Detroit, Michigan). RPMI 1640 media (without phenol red), 2 mM L-glutamine, gentamicin, penicillin, streptomycin, and estradiol were all purchased from Sigma. Bovine calf serum was purchased from Hyclone (Logan, UT). Dulbecco's Modified Eagle Medium (DMEM) was purchased from Gibco Life technologies (Grand Island, NY). Matrigel was obtained from BD Biosciences (Franklin Lakes, NJ).

Cell Binding Assay for ATF-methioninase

Rabbit anti-L-methioninase monoclonal primary antibody was produced in purified form by Sigma Genosys (St. Louis, MO). Goat anti-rabbit IgG secondary antibody with HRP conjugated was purchased from Sigma. Hemotoxylin was purchased from Vector Laboratories (Burlingame, CA).

Binding Assay for L-Methioninase-Annexin

Phosphatidylserine, O-phenylenediamine (OPD), and phosphate citrate buffer were purchased from Sigma, and polypropylene plates were purchased from Corning Inc. (Acton, MA). MCF-7 cells were cultured in Dulbecco's Modified Eagle Medium (DMEM) (Gibco Life technologies) supplemented with fetal calf serum (heat inactivated) (Atlanta Biologicals, Norcross, GA), 86 mg/mL penicillin, and 86 mg/mL streptomycin (Invitrogen, Carlsbad, CA). Accutase was purchased from Innovative Cell Technologies, Inc. (San Diego, CA). Rabbit anti-L-methioninase monoclonal primary antibody was produced in purified form and obtained from Sigma Genosys. Goat anti-rabbit IgG secondary antibody with HRP conjugated was purchased from Sigma.

3. METHODS

Primer Design for PCR

Primers were designed to have a sequence that is a reverse complement of a region of template or target DNA and also have incorporated sequences (such as ligation independent cloning sites, HRV 3C protease site, and other restriction enzyme sites). Following is an example of a set of a primers used to amplify the fusion gene containing 49 amino acids of urokinase and L-methioninase (complete list of all primer sequences is shown in Appendix A).

Sequence of the 5' primer for amplifying the urokinase gene:

5' - LIC site HRV 3C Protease site
GAC / GAC / GAC / AAG / ATG / CTT / GAA / GTC / CTC / TTT / CAG / GGA /
CCC / AGC / AAT / GAA / CTT / CAT / CAA / GTT / CC – 3'
Complementary to urokinase 5' end

It should be noted that the gene encoding the LIC site and the gene encoding HRV 3C protease site were introduced on all fusion genes (primers for respective fusion genes are listed in Appendix A). The sequence for the 3' PCR primer is

5' – LIC site Complementary to methioninase
GAG / GAG / AAG / CCC / GGT / TAT / CAT / GCA / CAC / GCC / TCC / AAT /
 3'end
GCC / AAC / TCG – 3'

The melting temperature (T_m) of primers and the propensity to form dimers with itself or other primers in the reaction were calculated by using a program provided by the website <http://www.basic.northwestern.edu/biotools/oligocalc.html>. The design of primers was

based on these criteria: 1) length of primers were above 17 bases, 2) G + C composition was more than 50-60 %, 3) 3' end of primer was G or C, or CG or GC, 4) T_m of primers was between 55-80 °C, and 5) ability of primer to form secondary structure was minimized. All the primers were obtained from Molecular Biology Resource Facility at the University of Oklahoma Health Sciences Center and were in the desalted state.

Construction of Fusion Genes

ATF-Methioninase and L-Methioninase Genes

A general outline of the ligation independent cloning (LIC) scheme for ATF-methioninase (pET-30 Ek/LIC/ATF-METH) and L-methioninase (pET-30 Ek/LIC/METH) is shown in **Figure 3.1**. The DNA sequences encoding the ATF-methioninase fusion protein and L-methioninase from pKK223-3/ATF-METH [93] were amplified by the polymerase chain reaction using the Expand High Fidelity PCR system (Boehringer Mannheim, Indianapolis, IN). The optimal PCR reaction compositions and thermal cycling parameters are shown in **Table 3.1** and **Table 3.2**. Similar reaction conditions were used since all the genes were of similar size. Each gene after PCR reaction was purified by the Qiaquick PCR purification protocol (See Appendix B). Purified gene was treated with T4 DNA polymerase to create LIC sticky ends on the gene, and this treated gene was annealed to the pET-30 Ek/LIC linear vector. Annealed product (1 µl) was used for transformation into NovaBlue cells. Complete protocol for ligation independent cloning from Novagen is given in Appendix B. Plasmids containing the gene inserts were extracted using Qiaquick purification protocol and then transformed into *E. coli* BL21 (DE3), which was used as protein expression host.

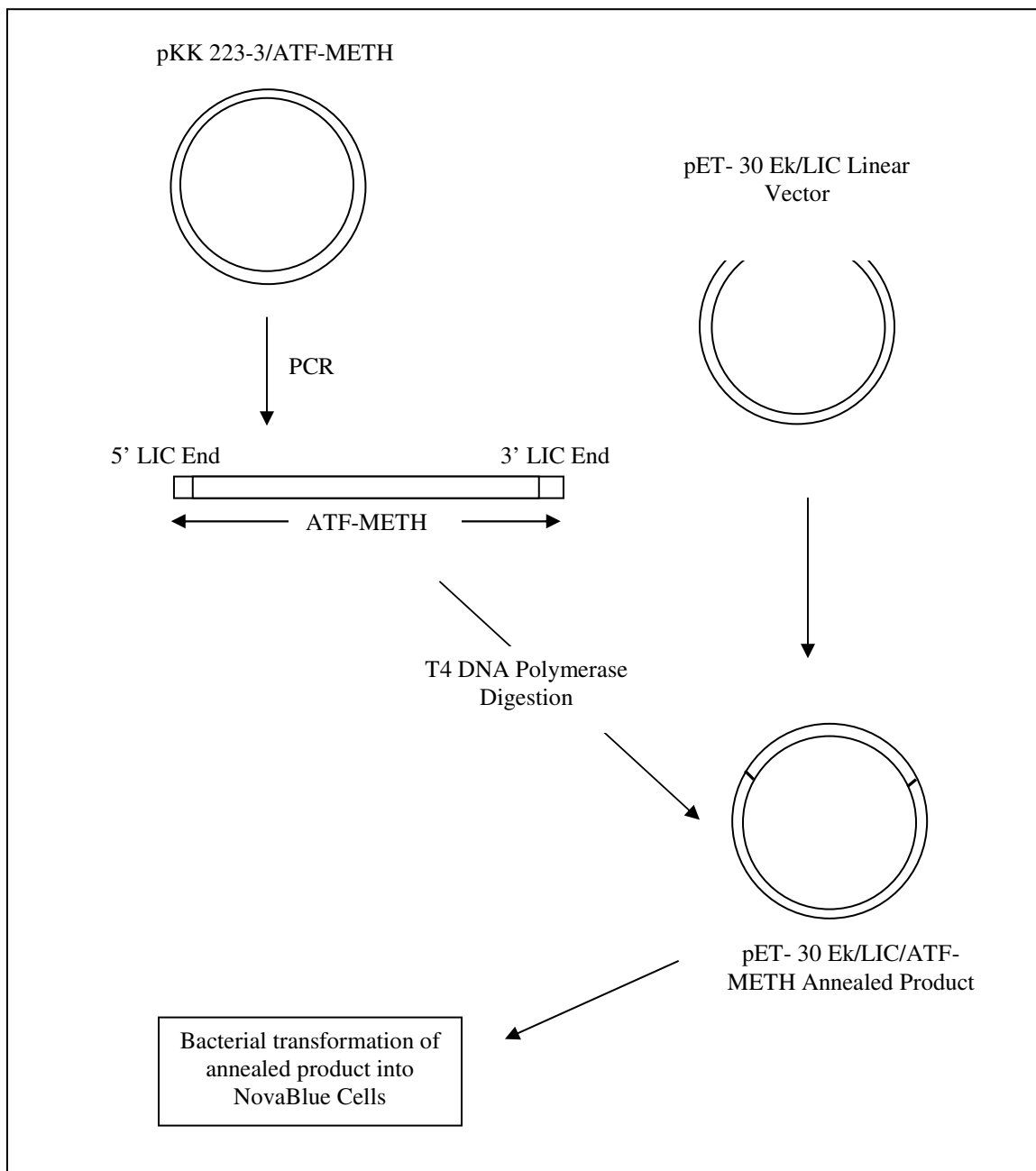


Figure 3.1. Construction of pET-30 Ek/LIC/ATF-METH expression vector. First, the gene for ATF-methioninase was amplified by PCR from parental plasmid that inserts 5' and 3' LIC ends. Next, the gene was digested with T4 DNA polymerase to create sticky ends and annealed to linear pET-30 Ek/LIC vector. Finally, annealed product is transformed in NovaBlue cells.

Component	Volume (μ l)	Stock solution concentration/amount	Final concentration/amount
Buffer	10	10 X	1 X
MgCl ₂	6	25 mM	1.5 mM
dNTP mix	2	10 mM	200 mM (each dNTP)
5' Primer	2	15 μ M	300 nM
3' Primer	2	15 μ M	300 nM
Template	0.5	~ 40 ng/ μ l	~ 20 ng
Polymerase	1	-	3.5 U
dH ₂ O	76	-	-

Table 3.1. Reaction composition for PCR.

No. of Cycles	Time	Temperature °C
1	2 min	94
29	45 s	94
	45 s	55
	2 min	72
1	5 min	72
1	∞	4

Table 3.2. Cycling parameters for PCR.

L-Methioninase-Annexin V Fusion Gene

A general outline of the ligation independent cloning scheme for L-methioninase-annexin (pET-30 Ek/LIC/METHANX) is show in **Figure 3.2**. The DNA sequences of L-methioninase and annexin V were amplified using pKK223-3/ATF-METH and pET-22b(+)/STFANX (obtained from Stuart Lind at the OU Health Sciences Center) as templates respectively by PCR. Primers were designed to incorporate an LIC sticky end at the N-terminus and a BamHI restriction enzyme site at the C-terminus end of the L-methioninase gene. Similarly primers were designed to incorporate a BamHI site at the N-terminus and a LIC sticky end at the C-terminus of the annexin V gene. Purified PCR products of L-methioninase and annexin V were treated separately with the BamHI restriction enzyme in recommended buffer solution. The products from restriction enzyme digestions were purified using Qiaquick PCR purification kit. Purified products were ligated together using T4 DNA ligase. This reaction was carried out for 16 h at 4 °C according to ligase manufacturer recommendations. Ligated product was run on an agarose gel. The appropriate fragments were cut and agarose gel-purified by the Qiaquick gel purification kit (see Appendix B). The purified L-methioninase-annexin V gene was treated with T4 DNA polymerase and annealed to pET-30 Ek/LIC vector as discussed previously in this section.

TGF-Methioninase Fusion Gene

A general outline of the ligation independent cloning scheme for TGF-methioninase (pET-44 Ek/LIC/TGF-METH) is show in **Figure 3.3**. The DNA sequences of L-methioninase and TGF were amplified using pKK223-3/ATF-METH and pVC387/TGF as templates respectively by PCR. PCR gene fragments were agarose gel-

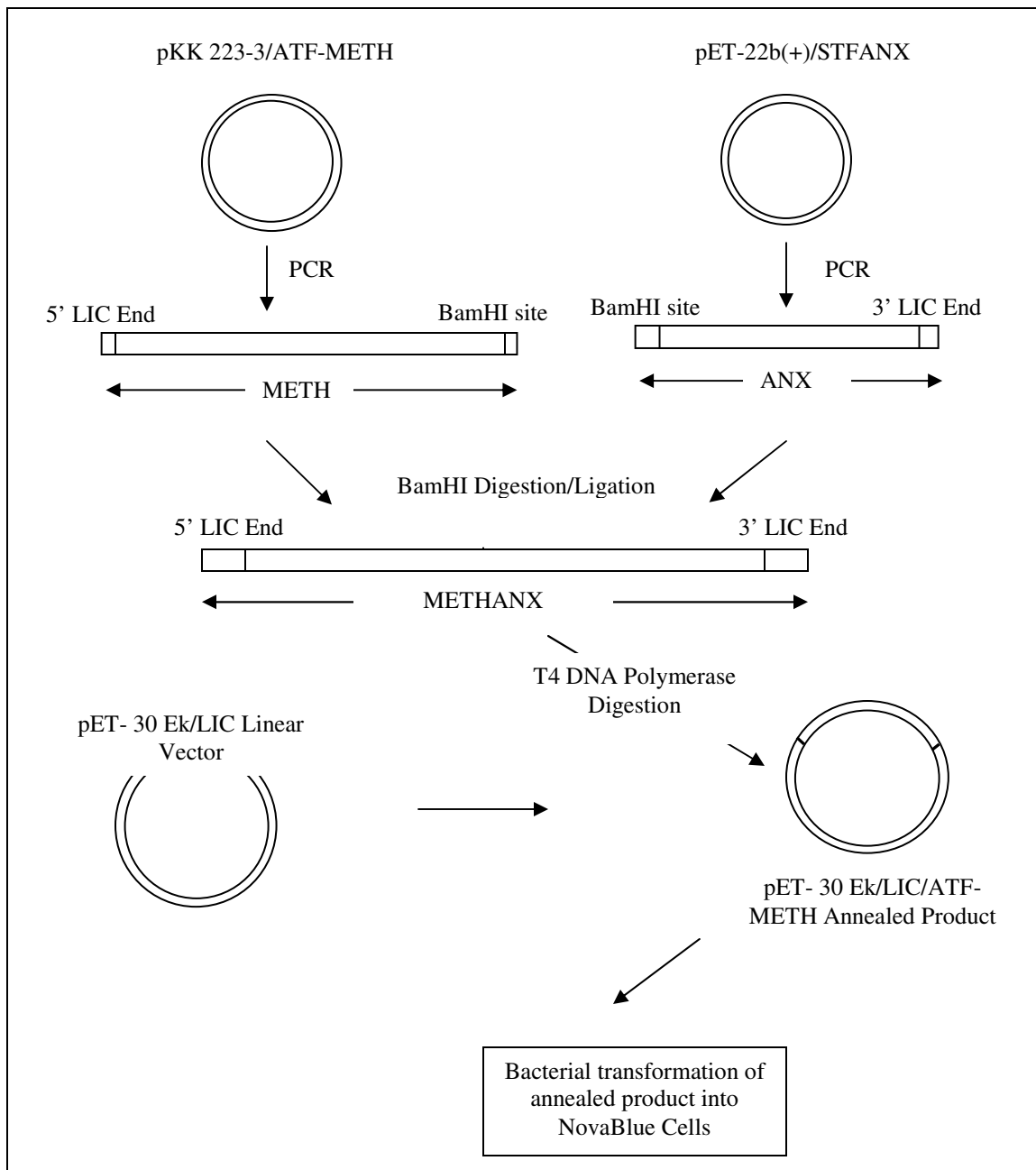


Figure 3.2. Construction of pET-30 Ek/LIC/METHANX expression vector. First, the genes for L-methioninase and annexin V were amplified by PCR from parental plasmids that inserts 5' LIC, 3' LIC end and BamHI sites. Next, the gene was digested with with BamHI restriction enzyme and ligated together. The ligated methioninase-annexin gene was treated with T4 DNA polymerase and annealed to linear pET-30 Ek/LIC vector. Finally, annealed product is transformed in NovaBlue cells.

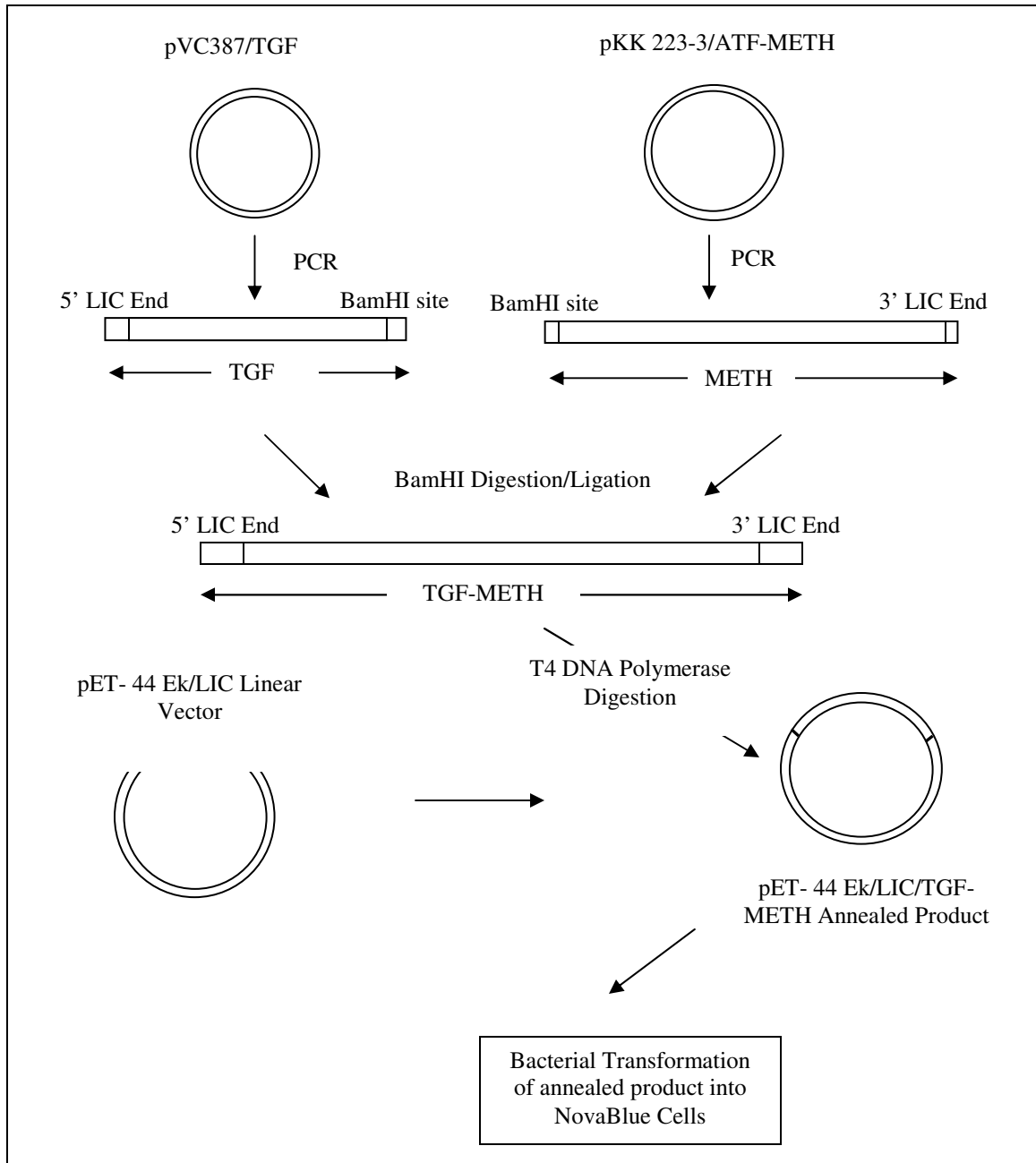


Figure 3.3. Construction of pET-44 Ek/LIC/TGFMETH expression vector. First, the genes for L-methioninase and TGF were amplified by PCR from parental plasmids that inserts 5' LIC, 3' LIC end and BamHI sites. Next, the gene was digested with with BamHI restriction enzyme and ligated together. Ligated TGF-METH gene was treated with T4 DNA polymerase and annealed to linear pET-44 Ek/LIC vector. Finally, annealed product is transformed in NovaBlue cells.

purified prior to restriction enzyme digestion according to the Qiagen protocol. After digestion of these gene fragments with BamHI enzyme, they were purified using Qiaquick PCR purification protocol (See Appendix B). The two fragments were ligated using T4 DNA ligase. Ligated product was purified according to the Qiaquick agarose gel purification protocol. The ligated product was annealed to the pET-44 Ek/LIC linear vector and transformed into NovaBlue cells according to the Novagen protocol. Plasmids containing the gene inserts were extracted using Qiaquick purification protocol and then transformed into *E. coli* BL21 (DE3), which was used as protein expression host.

Annexin V Gene

A general outline of the ligation independent cloning scheme for annexin V (pET-30 Ek/LIC/ANX) is show in **Figure 3.4**. The DNA sequence of annexin V was amplified using pET- 22b(+)/STFANX as template by PCR. The annexin V gene after PCR reaction was purified by the Qiaquick PCR purification protocol (See Appendix B). Purified gene was treated with T4 DNA polymerase to create LIC sticky ends on the gene, and this treated gene was annealed to the pET-30 Ek/LIC linear vector. Annealed product (1 µl) was used for transformation into NovaBlue cells. Plasmids containing the gene inserts were extracted using the Qiaquick purification protocol and then transformed into *E. coli* BL21 (DE3), which was used as protein expression host.

Site-directed Mutagenesis

A general outline of the site-directed mutagenesis procedure is shown in **Figure 3.5**. Plasmid containing the ATF-methioninase fusion protein gene (pET-Ek/LIC/ATF-METH) was mutated by site-directed mutagenesis using PCR. Both of the mutagenic

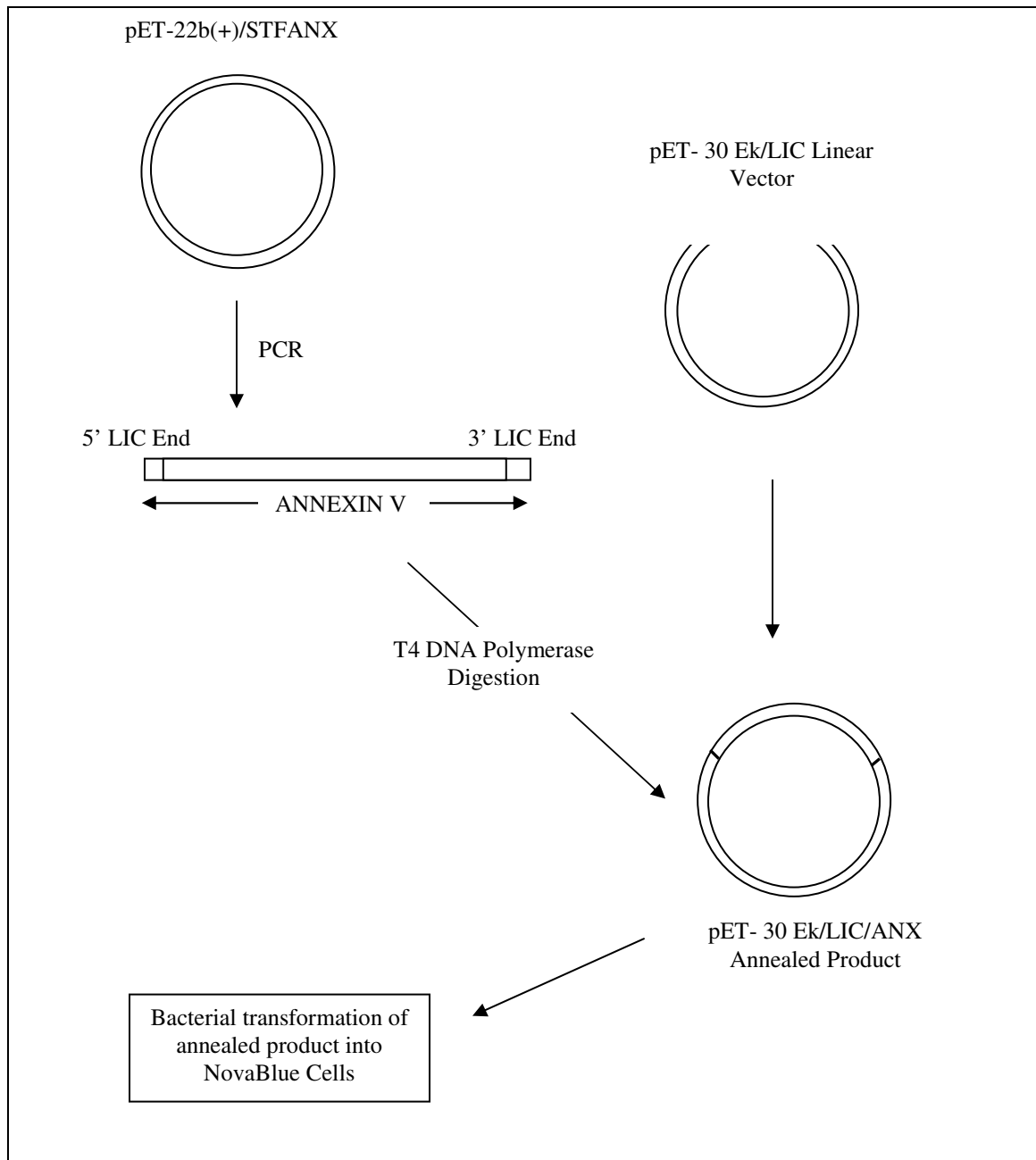


Figure 3.4. Construction of pET-30 Ek/LIC/ANX expression vector. First, the gene for annexin V was amplified by PCR from parental plasmid that inserts 5' and 3' LIC ends. Next, the gene was digested with T4 DNA polymerase to create sticky ends and annealed to linear pET-30 Ek/LIC vector. Finally, annealed product is transformed in NovaBlue cells.

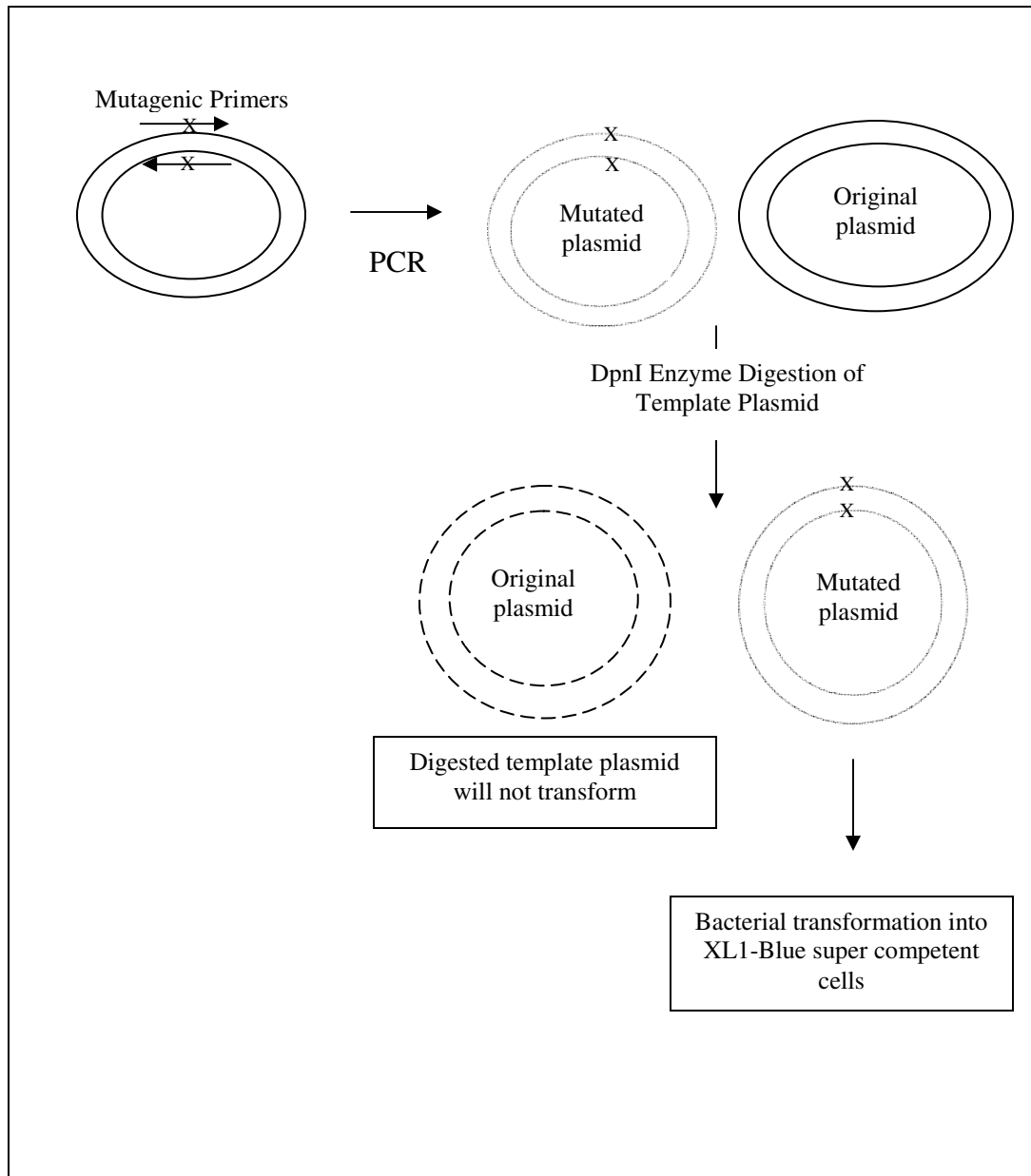


Figure 3.5. Site directed mutagenesis of pET-30 Ek/LIC/ATF-METH plasmid. First, PCR was performed using pET-30 Ek/LIC/ATF-METH as plasmid and mutagenic primers (Y114F, indicated by X). Next, original plasmid was digested by using DpnI enzyme, and finally the mutated plasmid is transformed in XL1-Blue super competent cells.

primers, mMETH 5' and mMETH 3' contained the desired mutation at 114th residue of L-methioninase (Y114F) and anneal to the complimentary sequence on opposite strands of the plasmid (Appendix A). All the criteria were followed in designing the primers as discussed in the primer design section. PCR was performed according to Stratagene protocol (Appendix B). Colonies with the mutation were identified by DNA sequencing, and plasmid from these colonies was purified and transformed into BL21(DE3) cells, which was used as protein expression host.

Sequencing Methods

The Oklahoma Medical Research Foundation (OMRF) DNA sequencing facility used ABI3730 capillary sequencers to sequence all the plasmids containing gene. All the sequences obtained from the facility were compared with the sequences from GenBank. This sequencer was able to read sequences up to 600 base pairs. Primers for the sequencing were designed to have at least 50 base pairs overlapping. The typical size of the fusion protein gene is around 1350 base pairs, so three primers were used to read entire sequence. The first primer was designed to have an overlap region with the vector, and the last primer was made sure to read the sequence on the 3' end of the vector. The primers sequences used are given in Appendix A.

Protein Expression

A culture of *E. coli* BL21(DE3) harboring pET- 30 Ek/LIC with the fusion gene of interest (ATF-methioninase, mutated ATF-methioninase, L-methioninase, methioninase-annexin V or annexin V) was grown in 50 ml of LB medium containing 35 µg/ml kanamycin overnight at 37 °C with shaking. This cell culture was added to 1 liter of fresh culture medium, and the culture was grown with shaking at 37 °C. This cell culture was grown to mid-log phase ($OD_{600} = 0.5$) and protein expression was induced by adding isopropyl β-D-thiogalactopyranoside (IPTG) to a final concentration of 0.4 mM. After addition of IPTG, the shaking of cell culture was continued at 30 °C for 5 h and harvested by centrifugation for 10 min at 1000 x g. For the expression of TGF-methioninase using plasmid pET-44 Ek/LIC, the same procedures were used, except ampicillin at 100 µg/ml was used instead of kanamycin for the cell culture and protein expression was induced using 1 mM IPTG for 3 h at 37 °C. The cell pellet was resuspended in 40 ml of sonication buffer containing 0.05 mM N- *p*-tosyl-L-phenylalanine chloromethyl ketone (TPCK), 1 mM phenylmethylsulfonyl fluoride (PMSF), 1% ethanol, 0.02 mM pyridoxal phosphate, 0.01% β-mercaptoethanol and 0.02 M sodium phosphate at pH 7.4. The sonication buffer used for cell pellet containing annexin V contains 0.05 mM TPCK, 1 mM PMSF, and 0.02 M sodium phosphate at pH 7.4. The cells were lysed by sonication at 4 °C for 30 sec at 4.5 watts per ml of lysate and then allowed to cool for 30 sec on ice. This cycle was repeated for four times for a total sonication time of 2.5 min. The lysate obtained was centrifuged at 12,000 x g for 30 min to remove the cell debris.

Protein Purification

All the fusion proteins expressed using a pET-30 Ek/LIC vector have an N-terminal His-tag (His₆) sequence with an integrated thrombin (Thr) cleavage site, enterokinase (Ek) cleavage site, and an engineered HRV 3C protease site next to the start of the fusion protein (His₆/Thr/Ek/3C/Fusion protein). The TGF-methioninase expressed using pET-44 Ek/LIC has an N-terminal His-tag sequence with an integrated NusA-tag, Ek cleavage site, and an engineered HRV 3C protease site next to the start of fusion protein (His₆/NusA/Ek/3C/TGF-methioninase). All the purification steps are performed at 4 °C. The entire purification procedure is outlined in **Figure 3.6**. Imidazole (40 mM) and NaCl (500 mM) were added to the lysate to reduce non-specific protein binding. This resulting mixture was fed to 5 ml HisTrap chromatography column with immobilized Ni²⁺, which was equilibrated with wash buffer containing 20 mM sodium phosphate, 40 mM imidazole, 500 mM NaCl, 0.02 mM pyridoxal phosphate (not added for annexin V expression) at pH 7.4. The column was washed with the wash buffer to remove unwanted proteins. His-tagged fusion protein was eluted using elution buffer containing 20 mM sodium phosphate, 500 mM imidazole, 500 mM NaCl, and 0.02 mM pyridoxal phosphate at pH 7.4. Eluted protein was dialyzed overnight against buffer containing 20 mM sodium phosphate, 0.02 mM pyridoxal phosphate at pH 7.4 to remove NaCl and imidazole from the protein solution and make suitable for N-terminal His-tag cleavage. Buffers used for purification of annexin V do not contain pyridoxal phosphate. The cleavage of N-terminal His-tag was achieved by using HRV 3C protease. HRV 3C protease (0.5 Units/mg of protein) and recommended 10X buffer (1.5 M NaCl, 0.5 M Tris-HCl, pH 7.5) were added to protein solution. This reaction was carried out for 8 h at

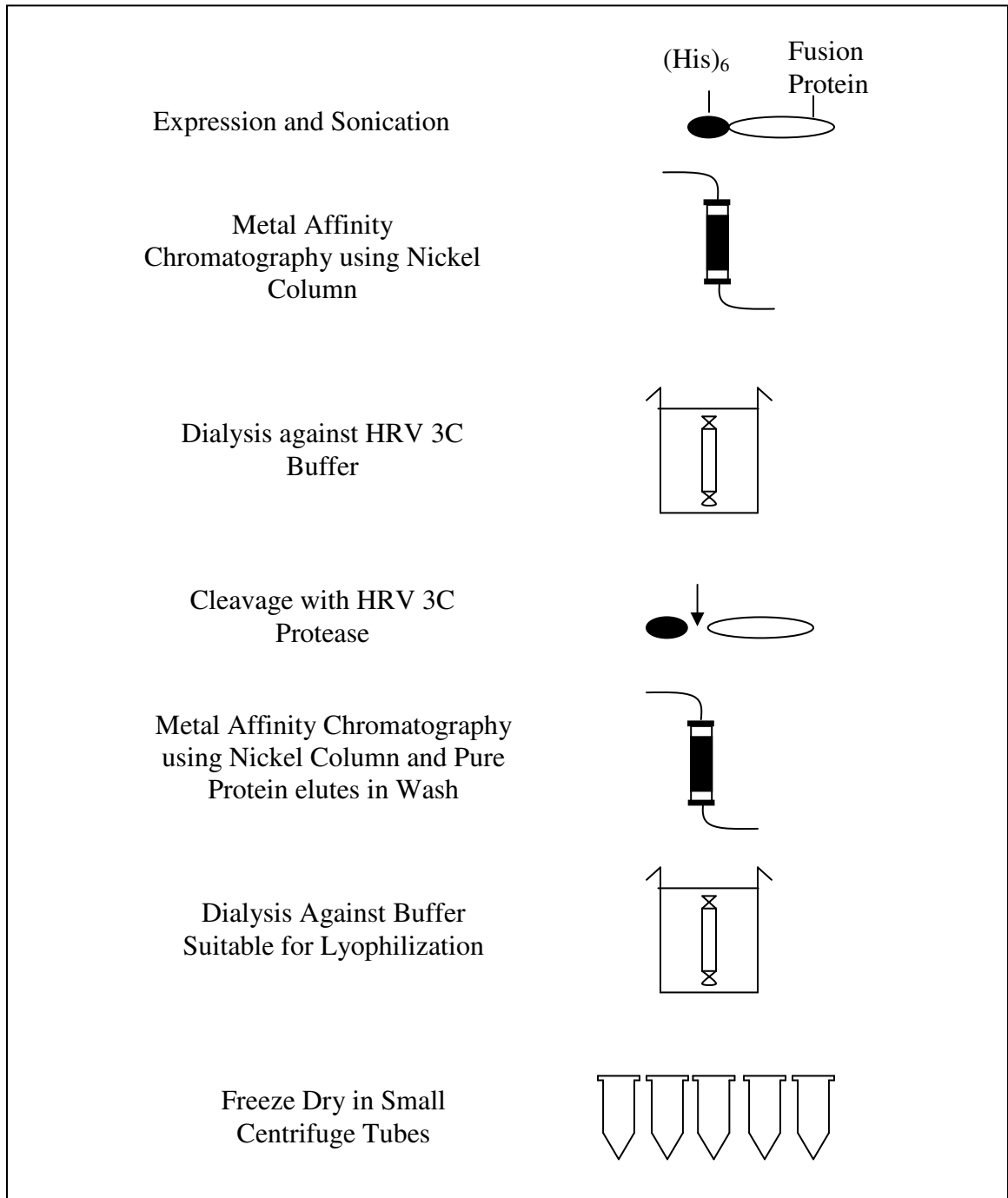


Figure 3.6. Scheme for the purification of fusion proteins using immobilized metal affinity chromatography.

4 °C. Imidazole (40 mM) and NaCl (500 mM) were added to the cleaved protein solution, which was fed again onto a 5 ml HisTrap column. Pure protein was eluted in a linear gradient of 0-0.5 M imidazole. Purified protein was dialyzed overnight against 20 mM sodium phosphate buffer at pH 7.4 containing 0.02 mM pyridoxal phosphate and 0.1 M NaCl.

Freeze Drying / Lyophilization.

Purified protein obtained after chromatography was concentrated to the desired concentration using Centriprep centrifugal filters. Concentrated protein solution was then transferred to small 1.5 mL centrifuge tubes. A small pinhole was introduced on the cap of each tube to let vapors escape. These tubes were flash frozen using liquid nitrogen and transferred in 20 mL lyophilization vials holding 10-15 centrifuge tubes. Lyophilization vials were then loaded onto the freeze dryer for lyophilization. Typically, lyophilization was carried out for 8 h.

Methioninase Activity Assay

The enzymatic activity of L-methioninase was determined by measuring the absorbance of azine derivatives formed by reacting 3-methyl-2-benzothiazolone hydrazone hydrochloride and α -ketobutyrate [98]. α -ketobutyrate was the product obtained by enzymatic elimination of L-methionine by L-methioninase (Appendix B).

SDS-PAGE, Western blotting, and Protein Assays

Cellular proteins and proteins after purification were separated on 12 % (w/v) SDS-PAGE and stained with Coomassie brilliant blue (see Appendix B). Protein concentration was measured by the Bradford assay (Bio-Rad, see Appendix B). The complete protocol for the Western blotting is given in Appendix B. Densitometry scanning of SDS-PAGE gels was carried out using Quantity One software (Bio-Rad).

Amino-terminal Sequencing

Protein sequencing was performed on an Applied Biosystems Procise model 492-protein sequencer equipped with an on-line PTH-amino acid analyzer and model 610A data system by the Molecular Biology Resource Facility at the University of Oklahoma Health Sciences Center. This protein sequencing was done only on the ATF-methioninase fusion protein, and results obtained from the facility were compared with the available protein sequence. This method was also used to determine the purity of the given sample.

Culture Wounding Assay

Cancer cells (5.0×10^5) were seeded into 60 mm culture dishes in 3 ml of RPMI medium. Three days after seeding, at approximately 80 % confluency, the cell cultures were wounded. The wound was created by pressing the edge of a razor blade, placed in a blade holder, into the confluent monolayer. The blade created a distinct mark on the culture dish. While holding the razor firmly, a rubber policeman was used to gently scrape away cells on one side of the razor blade creating a wounded area. The culture was then washed twice with PBS, and the wounded area carefully examined under the microscope to verify that the wound was completely cell free as previously described [95].

The wounded culture was treated with media containing either various concentrations of the fusion proteins or L-methioninase. In each experiment control cultures received RPMI media alone. At 24, 48 and 72 hours following treatment, cell migration and proliferation were determined by measuring both the maximum distance traveled by the cell front into the wounded area (migration) and number of cells in the wounded area (proliferation)/microscopic field. Measurements were taken from 10-12

individual microscopic fields in each experiment, and data was summarized from 2-3 experiments. Wounded cultures were examined at 100X magnification under an inverted phase-contrast microscope equipped with grid-containing eyepiece.

Mouse Xenograft Assay

In this study, MCF-7 human breast cancer cells (10^6) suspended in 0.2 ml Matrigel were injected into the flank of nude mice as previously described [95]. A pellet of estradiol (100 μ g) was placed adjacent to the gel implantation site 48 h prior to cell implantation. These cells are stably transfected with the β -galactosidase (β -gal) reporter gene so that tumor metastasis could be determined and quantified. The longest perpendicular diameters of tumors were measured twice weekly to document tumor growth. Tumor measurements were converted to tumor volume (V) using the formula: $V = W^2 \times Y/2$, where W and Y are the smaller and larger perpendicular diameters, respectively. The body weight of mice was also measured twice weekly. The development of tumor masses was monitored over a period of 30 days. The animals were then randomly placed into treatment groups containing 10 animals per group. Treatment groups received either the fusion protein (each treated with 25 μ l/day of 10^{-6} , 10^{-7} , or 10^{-8} M fusion protein or L-methioninase or vehicle in the control group by intra-tumoral injection on alternate days (see Appendix B). The animals were treated for period of 20 days. At the end of the treatment period, the animals were euthanized. Cancer cells in the tumor tissue were quantified by colorimetric measurement of the β -gal reporter in each sample.

Measurement Using the Colorimetric Substrate, Chlorophenol Red β -D-Galactopyranoside (CPRG)

Fresh tissue samples were collected from tumors, lung, and liver of nude mice. These samples were analyzed for number of cancer cells by measuring endogenous β -gal activity as previously described [95]. Samples were flash frozen using liquid nitrogen and ground. Then the samples were resuspended in lysis buffer (50 mM HEPES, 5 mM CHAPS, pH 7.5). The tissue samples were lysed by sonication at 4 °C for 30 sec at 4.5 watts per ml of lysate and then allowed to cool for 30 sec on ice. This cycle was repeated for four times for a total sonication time of 2.5 min. The lysate obtained was centrifuged at 12,000 x g for 30 min to remove the cell debris. The CPRG assay was performed on the tissue samples collected as outlined in the protocol provided with the kit (See Appendix B). A standard curve of absorbance versus cell number was generated by blank MCF-7 cells, which were transfected by the β -gal reporter gene.

Binding of Methioninase-Annexin V on Plastic-immobilized Phosphatidylserine

Phosphatidylserine (PS) was dissolved in chloroform at a concentration of 50 μ l/ml. This solution (100 μ l) added to wells of a 96-well polypropylene microtiter plates. This plate was allowed stay in a laminar flow hood until all the chloroform was evaporated. The plate was then blocked/washed by using wash/dilution buffer (phosphate buffered saline (PBS) solution containing 10% fetal bovine serum at pH 7.0 and 2 mM calcium chloride) for 2 h at room temperature in the laminar flow hood. Methioninase-annexin V fusion protein was added to wash buffer at an initial concentration of 6.7 nM. Serial 2-fold dilutions of this concentrated fusion protein were done using dilution buffer to give a final concentration of 6.7 pM. Methioninase-annexin V was added to wells in

the increasing concentration of methioninase-annexin V. For each concentration of methioninase-annexin V, the experiment was done in triplets. After adding 100 µl of methioninase-annexin V, the plates were incubated for 2 h. The plates were washed with wash buffer, and primary antibody (rabbit anti-methioninase) diluted in wash buffer (1:1000) was added and incubated for 12 h at 4 °C. The plates are again washed with wash buffer, and 100 µl of goat anti-rabbit IgG secondary antibody with HRP conjugated (1:1000 dilution in binding buffer) was added to the wells for 2 h at room temperature. The chromogenic substrate O-phenylenediamine (OPD, 200 µl) was used to detect the HRP by reading the plates at 450 nm. Further details of this procedure are given in Appendix B.

Binding of Methioninase-Annexin V on Externally Positioned PS on the Surface of Cells

MCF-7 breast cancer cells were grown using DMEM media containing 10% FBS until they reached 85 % confluence in T-75 flasks. Cancer cells (5×10^4) were transferred to 24 well plates and grown until they reached 85 % confluence. PS was exposed on the surface of cells by the addition of hydrogen peroxide (1 mM). Cells were treated with wash/binding buffer containing the DMEM media with 1 mM of H₂O₂ for 1 h at 37 °C. Cells were fixed with 0.25 % glutaraldehyde diluted in PBS buffer containing Ca²⁺ (2 mM). Excess aldehyde groups were quenched by incubation with 50 mM of NH₄Cl for 5 min. Methioninase-annexin V fusion protein was added to wash buffer at an initial concentration of 6.7 nM. Serial 2-fold dilutions of this concentrated fusion protein solution were done to give a final concentration of 6.7 pM. Methioninase-annexin V was added to wells in the increasing concentration of methioninase-annexin V. For each concentration of methioninase-annexin, the experiment was done in triplets. After adding

300 μ l of methioninase-annexin V, the plates were incubated for 2 h. The plates were washed with wash buffer, and primary antibody (rabbit anti-methioninase) diluted in wash buffer (1:1000) was added and incubated for 12 h at 4 °C. The plates are again washed with wash buffer, and 300 μ l of goat anti-rabbit IgG secondary antibody with HRP conjugated (1:1000 dilution in binding buffer) was added to the wells for 2 h at room temperature. After washing with PBS, the chromogenic substrate O-phenylenediamine (OPD, 300 μ l) was added. After 30 min 100 μ l of the supernatant was transferred to 96-well plates, and absorbance was measured at 450 nm. Further details of this procedure are given in Appendix B.

4. RESULTS AND DISCUSSION

Construction of Fusion Genes

Construction of the ATF-Methioninase Fusion Gene and the L-Methioninase Gene

Figure 4.1.A presents the results of the PCR reactions using pKK223-3/ATF-METH as template and primers for the ATF-methioninase fusion gene, and the L-methioninase gene, as visualized by agarose gel electrophoresis. Visualization of PCR fragments of correct lengths (1452 base pairs for the ATF-methioninase gene and 1284 base pairs for the L-methioninase gene) provided confirmation that the gene fragments were indeed the desired synthesis products. Only a fraction of the PCR product (5% of the total) was used to visualize by agarose gel electrophoresis, and the rest was purified using Qiaquick PCR purification protocol (Appendix B). Purified product was treated with T4 DNA polymerase, and the treated gene was annealed to linear pET-30 Ek/LIC vector. After transformation of the annealed product into *E. coli* NovaBlue Giga Singles, five colonies were picked and cultured. Plasmids were extracted using Qiaquick plasmid purification protocol (See Appendix B) from these cultures and sent for DNA sequencing. Four out of five colonies were shown to have the ATF-methioninase fusion gene inserted, and one of colonies showed self-ligation of the vector. This self-ligation of the vector is attributed to degradation of the linear vector during handling. For the L-methioninase gene as insert, all the five colonies picked showed the gene to be inserted. The consensus DNA sequence resulting from the sequencing of the pET-30 Ek/LIC/ATF-METH and pET-30 Ek/LIC/METH vectors is shown in Appendix A.

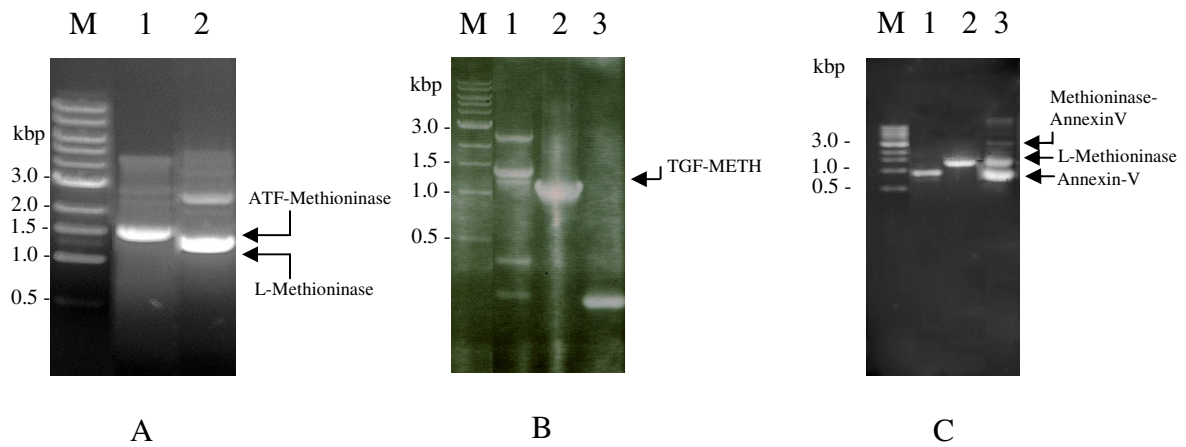


Figure 4.1. (A) Agarose gel image of PCR products. *Lane 1*, ATF-methioninase (1452 bp) fusion gene, and *Lane 2*, L-methioninase gene (1284 bp). (B) Agarose gel image of PCR products. *Lane 1*, different ligated products formed after ligation reaction of L-methioninase and TGF. TGF-METH is indicated by arrow. *Lane 2*, L-methioninase (1284 bp); *Lane 3*, TGF (214 bp), and (C) Agarose gel image of PCR products. *Lane 1*, Annexin V, *Lane 2*, L-methioninase; and *Lane 3*, different ligated products formed after ligation reaction of L-methioninase (1284 bp) and annexin V (1013 bp). *Lane M*, the 1 kb DNA ladder (0.5 kb, 1 kb, 1.5 kb, 2.0 kb, 3 kb, 4 kb).

Construction of TGF-Methioninase Fusion Gene

Figure 4.1.B presents the result of the PCR reaction using pKK223-3/ATF-METH as template for the L-methioninase gene (lane 2) and the result of the PCR reaction using pVC387/TGF as template for the TGF gene (lane 3), as visualized by agarose gel electrophoresis. Visualization of PCR fragments of correct lengths (1284 base pairs for the L-methioninase gene and 165 base pairs for the TGF gene) provided confirmation that the gene fragments were indeed the desired synthesis products. The L-methioninase and TGF genes are treated with BamHI restriction enzyme at 37 °C for 1 h. These two genes were ligated using T4 DNA ligase at room temperature for 3 h. Lane 1 of **Figure 4.1.B** presents the result for the ligation reaction, as visualized by agarose gel electrophoresis. Five bands are visualized corresponding to different ligated products: 1) L-methioninase gene ligated to itself (~2548 bp), 2) L-methioninase gene ligated to the TGF gene (a 1438 base pairs gene as shown in **Figure 4.1.B** by an arrow), 3) unligated L-methioninase gene (1284 bp), 4) TGF gene ligated to itself (~ 326 bp), and 5) 165 base pair unligated TGF gene. The band corresponding to the TGF-methoninase gene was excised from agarose gel and purified using the Qiaquick agarose gel purification protocol (see Appendix B). Purified product was treated with T4 DNA polymerase and annealed onto the linear pET-44 Ek/LIC vector. After transformation of annealed product into *E. coli* NovaBlue Giga Singles, five colonies were picked and cultured. Plasmids were extracted using the Qiaquick Plasmid purification protocol (see Appendix B) from these cultures and sequenced. The consensus DNA sequence resulting from the sequence of the pET-44 Ek/LIC/TGF-METH is shown in Appendix A.

Construction of the L-Methioninase-Annexin Gene

Figure 4.1.C presents the result of the PCR reaction using pKK223-3/ATF-METH as template for the L-methioninase gene (lane 2), and the result for the PCR reaction using pET-22b(+)/STF-ANX as template for the annexin V gene (lane 3), as visualized by agarose gel electrophoresis. Visualization of PCR fragments of correct lengths (1284 base pairs for the L-methioninase gene and 1013 base pairs for the annexin V gene) provided confirmation that the gene fragments were indeed the desired synthesis products. The L-methioninase and annexin V genes are treated with BamHI restriction enzyme at 37 °C for 1 h. These two genes were ligated using T4 DNA ligase at room temperature for 3 h. Lane 1 of **Figure 4.1.C** presents the result for the ligation reaction, as visualized by agarose gel electrophoresis. Five bands are visualized corresponding to different ligated products: 1) L-methioninase gene ligated to itself (~2548 bp), 2) L-methioninase gene ligated to annexin V gene (a 2297 base pairs gene as shown in **Figure 4.1.C** by an arrow), 3) unligated L-methioninase gene, 4) annexin V gene ligated to itself (~ 2026 bp), and 5) 1013 base pair unligated annexin V gene. The band corresponding to the L-methioninase–annexin V gene was excised from the agarose gel and purified using the Qiaquick agarose gel purification protocol (see Appendix B). The purified product was treated with T4 DNA polymerase and annealed to the linear pET-30 Ek/LIC vector. After transformation of annealed product into *E. coli* NovaBlue Giga Singles, five colonies were picked and cultured. Plasmids were extracted using Qiaquick plasmid purification protocol (See Appendix B) from these cultures and sent for DNA sequencing. The consensus DNA sequence resulting from the sequencing of the pET-30 Ek/LIC/L-METHANX is shown in Appendix A.

On a whole, the efficiency of LIC is much greater than for conventional cloning. Both the linearized vector and the PCR product containing the gene to be cloned are treated with T4 DNA polymerase in the presence of a single dNTP to generate complementary overhangs, which are unique for each end of the gene. Therefore, it is impossible for the vector to anneal to itself with no insert, which commonly occurs in conventional cloning. The 3'-endonuclease activity of the polymerase removes bases from the 3'-end of each duplex DNA until it encounters the nucleotide matching the single added dNTP. At that point, polymerase activity dominates, stopping the endonuclease activity and leaving a 5' single-stranded overhang.

Site Directed Mutagenesis of pET- 30 Ek/LIC/ATF-METH

PCR was performed on pET-30 Ek/LIC/ATF-METH, and after DpnI enzyme digestion of the PCR products, 1 µl of the PCR product was used for the transformation into *E. coli* XL1-Blue. Many colonies were picked and cultured. Plasmid was extracted from these colonies and sequenced. Two out of ten colonies picked showed the point mutation (Y114F). The entire gene was sequenced to check for any mutations caused by the PCR. Using this method for creating site directed mutations was easy, but the DpnI enzyme digestion of the template plasmid was critical.

Protein Expression and Purification

Plasmids containing the gene inserts were extracted using the Qiaquick purification protocol and then transformed into *E. coli* BL21 (DE3). Expression of ATF-METH fusion protein using 1 mM IPTG at 37 °C for 3 h, or using 0.4 mM IPTG at 37 °C for 3 h resulted in completely insoluble fusion protein based on SDS-PAGE gels.

Expression of fusion protein using 0.4 mM IPTG at 30 °C for 6 h resulted in soluble fusion protein. Expression for 6 h at 30 °C was used for all the proteins except for TGF-METH fusion protein. TGF-METH fusion protein was expressed using 1 mM IPTG for 3 h at 37 °C. This produced a soluble fusion protein with a NusA tag attached at the N-terminal of the TGF-METH.

Purification of all the fusion proteins was done by immobilized metal affinity chromatography using a Ni²⁺ column. L-methioninase, ATF-methioninase, mutated ATF-methioninase, annexin V, and methioninase-annexin V all had an integrated His₆ tag, thrombin cleavage site, enterokinase site and engineered HRV 3C protease site next to the start of fusion protein (His₆/Thr/Ek/3C/Fusion protein). The TGF-methioninase fusion protein had a NusA tag next to thrombin cleavage site (His₆/NusA/Thr/Ek/3C Fusion protein).

Figure 4.2 is the SDS-PAGE gel image showing the purification of ATF-methioninase fusion protein at different stages. The concentrations of 40 mM of imidazole and 500 mM of NaCl were chosen for the wash buffer and elution buffer, respectively, to reduce the non specific binding of the unwanted proteins. Use of this concentration of imidazole has resulted in some loss of fusion protein in wash, but the protein obtained in elution pool was pure. Following this IMAC purification, the pure fusion protein was dialyzed against HRV 3C enzyme buffer. The reason for engineering HRV 3C protease next to fusion protein is because of previous experience of using bovine enterokinase to cleave the His₆ tag from the fusion proteins. For fusion proteins with no HRV 3C site, use of enterokinase to cleave the His₆ tag resulted in incomplete cleavage. Cleaved protein bound to un-cleaved protein (since L-methioninase exists as

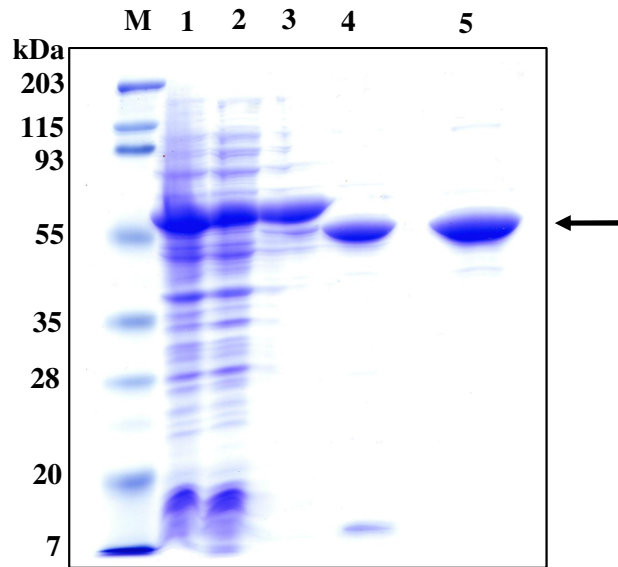


Figure 4.2. SDS-PAGE analysis with Coomassie blue staining of the expression and purification of the ATF-methioninase fusion protein (position indicated by the arrow). The fusion protein was expressed from plasmid pET-30/Ek/LIC/ATF-Meth in *E. coli* BL21(DE3) cells at 30 °C (*lane 1* whole cells, *lane 2* soluble lysate, *lane 3* eluted fraction from first metal affinity chromatography, *lane 4* eluted fraction after cleavage with HRV 3C protease, *lane 5* pooled fractions from second metal affinity chromatography, *M* marker proteins with molecular masses indicated on the left in kiloDaltons).

tetramer in native state), and this resulted in a low yield of purified product after purification. Use of HRV 3C protease resulted in complete cleavage of protein and did not give non-specific cleavage of fusion proteins. However, use of HRV 3C protease left an N-terminal Gly-Pro on the target protein. HRV 3C protease has a His₆ tag, and it was easily removed by IMAC. Use of thrombin was not a choice because it was positioned next to enterokinase site. Following HRV 3C protease cleavage of the fusion protein, it was fed onto a HisTrap column again, and usually the target protein was collected in the start of the elution gradient of 0-0.5 M imidazole. This could be due to the non-specific binding of the ATF-methioninase fusion protein to the column. A similar procedure was used to purify the L-methioninase, mutated ATF-methioninase, annexin V, and methioninase-annexin V fusion proteins. **Figure 4.3** is the SDS-PAGE gel image showing the purification of L-methioninase protein at different stages of purification. The SDS-PAGE gel image showing the purification of mutated ATF-methioninase is not shown, but it is similar to **Figure 4.2**.

Figure 4.4 is the SDS-PAGE gel image showing the purification of TGF-methioninase fusion protein at different stages of purification. The procedure used to purify TGF-methioninase is similar to that of ATF-methioninase. Lane 4 in the **Figure 4.4** corresponds to the pooled fractions from the second metal affinity chromatography, and lane 5 corresponds to eluted fraction from second metal affinity chromatography. Although there was nearly complete cleavage of NusA and TGF-methioninase by HRV 3C protease as shown in lane 3 of **Figure 4.4**, TGF-methioninase and the protein with the NusA tag eluted together for some of the fractions (see lane 5). Since L-methioninase is a homotetramer, incomplete cleavage can result in noncleaved protein binding up to three

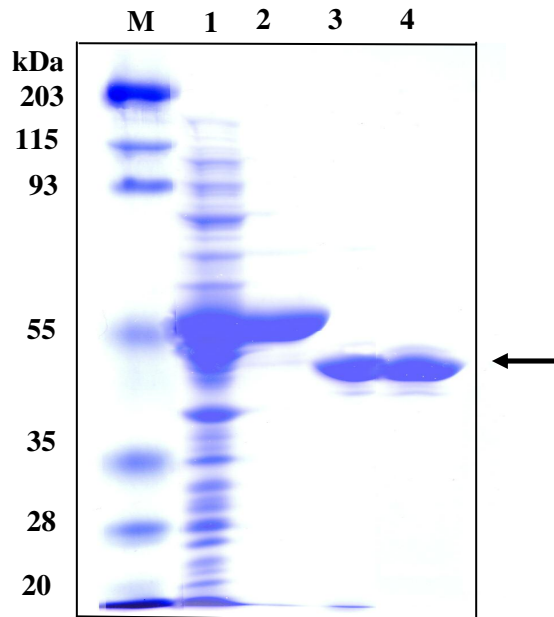


Figure 4.3. SDS-PAGE analysis with Coomassie blue staining of the expression and purification of the L-methioninase protein (position indicated by the arrow). The fusion protein was expressed from plasmid pET-30/Ek/LIC/METH in *E. coli* BL21(DE3) cells at 30 °C (*lane 1* soluble lysate, *lane 2* eluted fraction from first metal affinity chromatography, *lane 3* eluted fraction after cleavage with HRV 3C protease, *lane 4* pooled fractions from second metal affinity chromatography, *M* marker proteins with molecular masses indicated on the left in kiloDaltons).

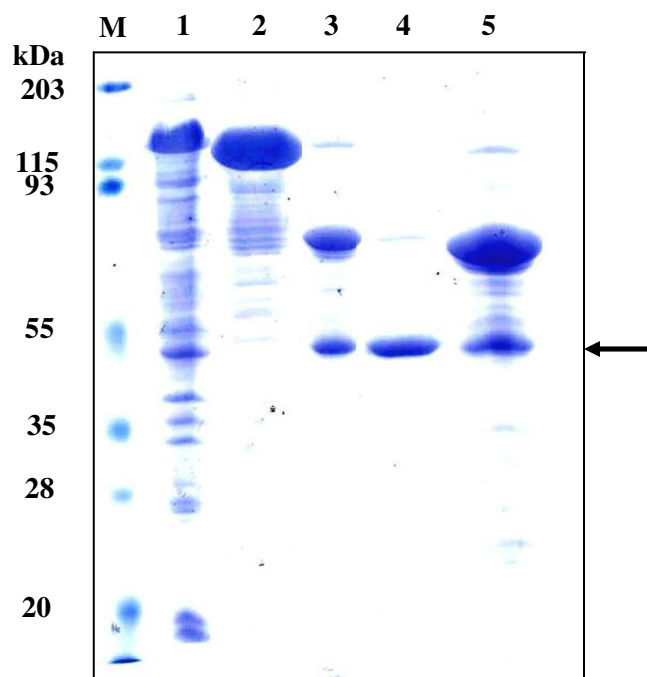


Figure 4.4. SDS-PAGE analysis with Coomassie blue staining of the expression and purification of the TGF-methioninase fusion protein (position indicated by the arrow). The fusion protein was expressed from plasmid pET-44/Ek/LIC/TGF-METH in *E. coli* BL21(DE3) cells at 30 °C (*lane 1* soluble lysate, *lane 2* eluted fraction from first metal affinity chromatography, *lane 3* eluted fraction after cleavage with HRV 3C protease, *lane 4* pooled fractions from second metal affinity chromatography, *lane 5* eluted fraction from second metal affinity chromatography, *M* marker proteins with molecular masses indicated on the left in kiloDaltons).

cleaved protein fragments to give a complex that will have a His₆ tag and will bind to the column more strongly than a complex that was completely cleaved. If, for example, the cleavage was 90% complete, half of the cleaved TGF-methioninase would elute with the His₆ tag because of the association of the L-methioninase monomers. This contributed to a lower yield for TGF-methioninase than for the other fusion proteins (**Table 4.1**).

Figure 4.5 is the SDS-PAGE gel image showing the purified protein products of annexin V, L-methioninase, and methioninase-annexin V. The yield and specific activity of the fusion proteins are shown in **Table 4.1**. There was a relatively high yield of purified proteins expressed using pET-30 Ek/LIC vector. The yield of TGF-methioninase, expressed using the pET-44 Ek/LIC vector, was 4-6 fold lower than for the proteins expressed by the pET-30 Ek/LIC vector. The specific activity of methioninase-annexin V was lower when compared to L-methioninase and ATF-methioninase as expected. This is due to fusion of the 36 kDa annexin V protein to L-methioninase when compared to the 5 kDa proteins ATF or TGF.

The purity of the ATF-methioninase fusion protein was estimated to be 94% using Quantity One densitometry software analysis of lane 5 of the SDS-PAGE gel in **Figure 4.2**. Amino acid sequencing of the purified ATF-methioninase fusion protein was performed on the first eight amino-terminal amino acids. The sequence was identical to the amino-terminus of the urokinase A chain (Gly-Pro-Ser-Asn-Glu-Leu-His-Gln) for 90 ± 5% of the protein, which is consistent with the purity estimation of the SDS-PAGE gel of the purified protein. The purity of the TGF-methioninase fusion protein was estimated to be 97 % using the densitometry software analysis of lane 4 of SDS-PAGE gel in **Figure 4.4**. Amino acid sequencing of the TGF-methioninase fusion protein was

Protein	Amino Acids	Theoretical Molecular Weight (kDa)	Runs	Yield (mg/liter of culture)	Specific Activity (Units/mg)
L-methioninase	399	42.75	2	65.3	14.6
ATF-methioninase	455	48.64	2	53.5	13.9
Mutated ATF-methioninase	455	48.64	1	55.4	0
Methioninase-annexin V	729	79.62	1	41.3	8.6
Annexin V	321	35.92	1	59.2	0
TGF-methioninase	457	48.87	1	11.3	12.5

Table 4.1. Average yield and specific activity of purified fusion proteins.

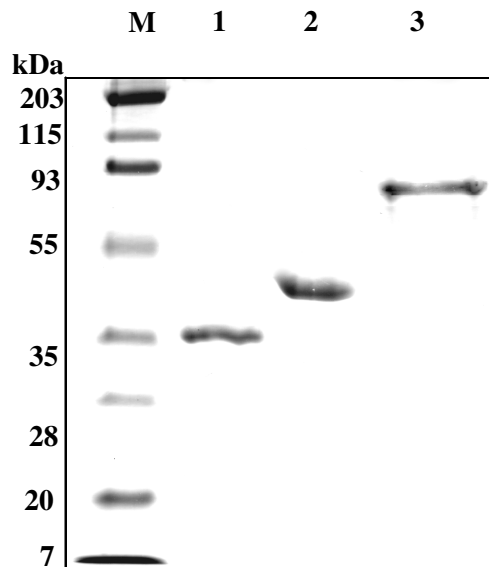


Figure 4.5. SDS-PAGE analysis with Coomassie blue staining of three of the purified proteins. *Lane 1* annexin V, *lane 2* L-methioninase, *lane 3* methioninase-annexin V, *M* marker proteins with molecular masses indicated on the left in kiloDaltons.

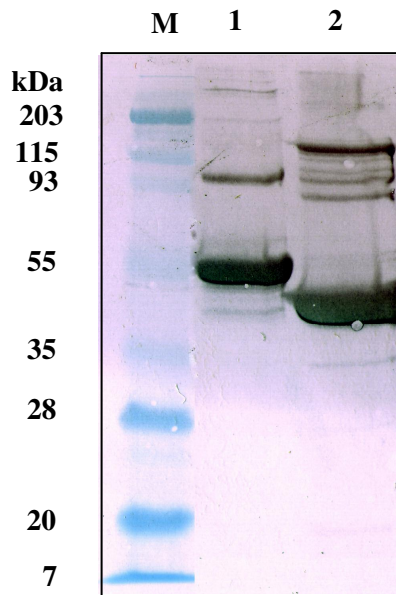


Figure 4.6. Western blot analysis of ATF-methioninase and L-methioninase proteins. *Lane 1*, ATF-methioninases; *lane 2*, L-methioninase.

performed on the amino-terminus. and the result obtained showed that 65% of sequence was identical to the amino terminal sequence of the TGF- α which is not consistent with the purity estimated by SDS-PAGE gel. The impurity sequence was not from the protein tag cleaved off or from TGF- α .

Dimer Formation of ATF-Methioninase and L-Methioninase

Western blot analysis shown by the **Figure 4.6** confirms that the ATF-methioninase and L-methioninase were not completely reduced to a monomeric state in an SDS-PAGE gel. An increase of the concentration of β -mercaptoethanol (BME) or the use of a stronger reducing agent, dithiothreitol (DTT), was not effective in reducing these proteins. After using newly purchased DTT and BME, the dimer formations were greatly reduced, but not completely eliminated.

Freezing and Freeze Drying

Figure 4.7 summarizes the effect of freezing on the ATF-methioninase fusion protein. Freezing of the fusion protein proved to be detrimental to the protein activity. This could be due to complex physical and chemical changes caused by freeze-thaw cycles. In an initial attempt, slow freezing of the protein was tried, by placing the sample in the -20 °C freezer, and it resulted in a loss of 67 % of the activity. This activity loss was reduced to 31 % by flash freezing in liquid nitrogen (-170 °C). One main possible reason for substantial loss of activity during slow freezing is that, as water crystallizes out, the remaining solutes are concentrated with the proteins, which might cause the phase separation of some solutes due to their low solubility limit; this concentration of solutes may not dissipate immediately during thawing, leading to the protein instability [99, 100]. Selective crystallization of disodium phosphate upon freezing has been reported earlier [101]. Also surface denaturation at the ice-water interface was also reported earlier [102]. However, during flash freezing of the fusion protein, relatively smaller crystals are formed, and therefore there was a relatively equal distribution of proteins and solutes in the frozen liquid. Although the loss of activity of fusion protein during flash freezing was reduced when compared to the loss of activity during slow freezing of fusion protein, there was a significant loss of activity (31 %) during this unit operation. This loss was probably due to the increase in surface area by formation of smaller ice crystals, eventually increasing the protein-ice interaction and causing the denaturation of fusion protein. Addition of salt (NaCl 100 mM) resulted in 94% of the activity being retained after flash freezing and 87% of activity retained after flash freezing followed by freeze drying. This higher yield of activity is believed to be caused by a reduction in the

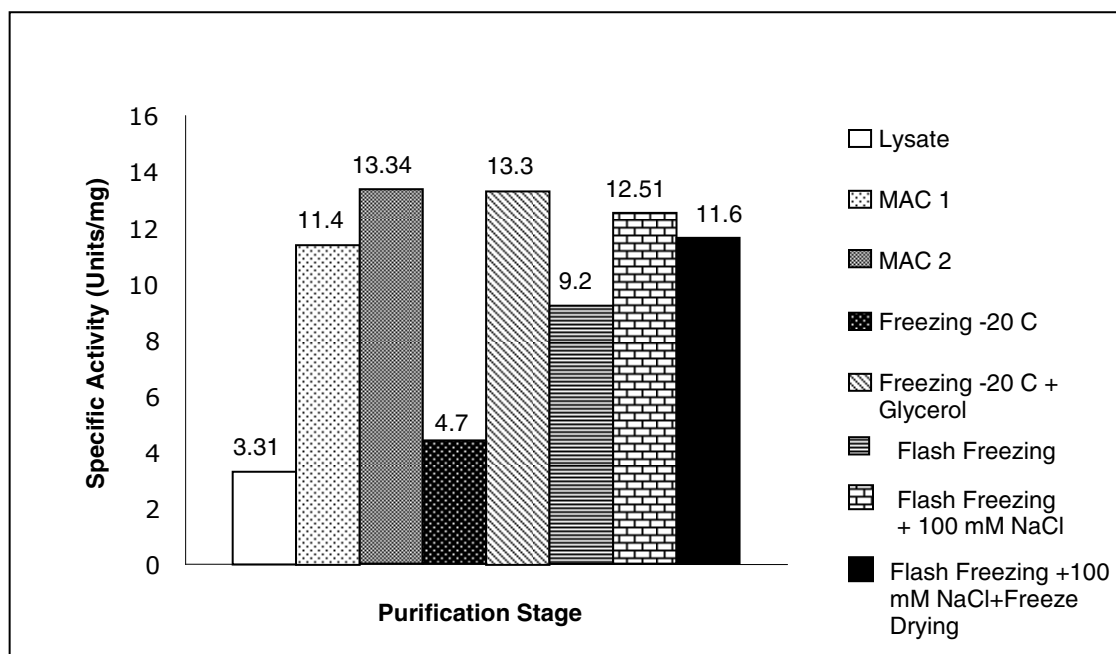


Figure 4.7. Effect of different unit operations on specific activity of ATF-methioninase. MAC 1: First Metal Affinity Chromatography, MAC 2: Second Metal Affinity Chromatography. Each bar corresponds to the specific activity of the fusion at different purification stage and also freezing.

interaction between protein and ice crystals [100]. Similar effects of freezing were observed on all the fusion proteins containing L-methioninase.

Inhibitory effects of ATF-methioninase on Cancer Cells *In Vitro*

In control experiments for the culture wounding assay, MCF-7 cancer cells were treated with buffer 1 (20 mM sodium phosphate, 0.02 mM pyridoxal phosphate, 1mM ethylene diamine tetra-acetic acid (EDTA), 1 % ethanol, and 1 mM PMSF, NaCl), and also with the buffer 2 (20 mM sodium phosphate, 0.02 mM pyridoxal phosphate and 0.02 % BME). These two buffers were used to dissolve the proteins before administration. It was observed that this buffer 2 produced a significant, but very small cytotoxicity to the MCF-7 cancer cells when compared to buffer 1 (**Figure 4.8**). Based on this result, the proteins were dissolved in buffer 1 before the administration to the cells or mouse xenografts.

The cell migration and proliferation indices of MCF-7 breast cancer cells were significantly reduced in methionine-free media containing homocysteine, verifying that these cells are methionine-dependent [93]. In the culture wounding experiments, ATF-methioninase over the concentration range of 10^{-8} M to 10^{-6} M produced a dose-related inhibition of cell migration and proliferation for MCF-7 breast cancer cells on days 2 and 3 ($p < 0.05$, **Figure 4.9**). Mutated ATF-methioninase did not inhibit cell migration or proliferation over the same concentration range. L-methioninase produced a smaller but significant ($p < 0.05$) reduction in migration and proliferation on days 2 and 3 [95].

The effects of ATF-methioninase on SK-LU-1 lung cancer cells were examined over a concentration range of 10^{-8} to 10^{-6} M as shown in **Figure 4.10**. In these experiments, the fusion protein consistently produced a dose-related inhibition of both the

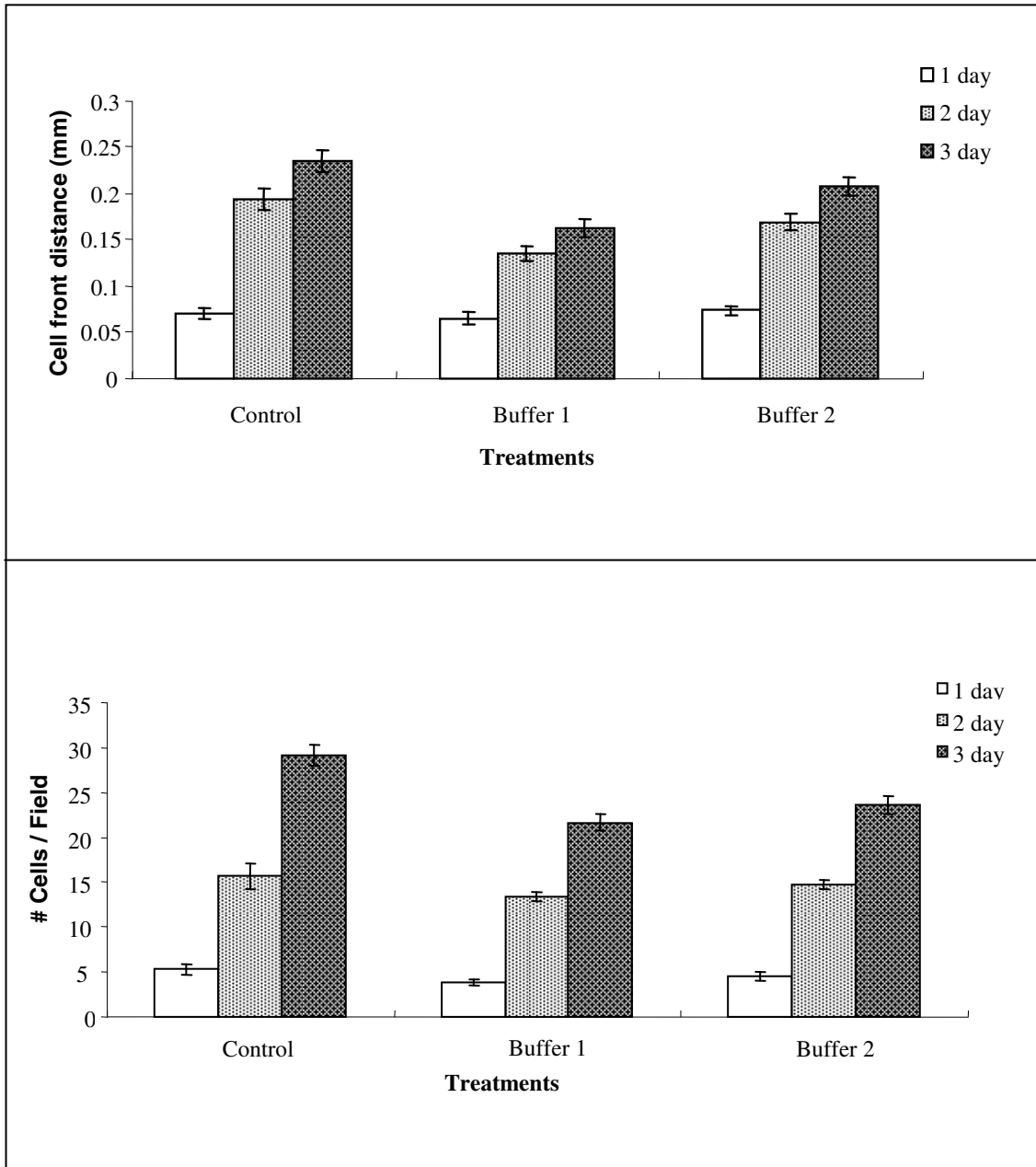


Figure 4.8. Effect of buffers on MCF-7 breast cancer cell migration and proliferation. *Control*, cells treated with RPMI media alone; *Buffer 1*, cells treated with RPMI media and buffer containing 20 mM sodium phosphate, 0.02 mM pyridoxal phosphate 1 mM EDTA, 1 mM PMSF, and 1 % ethanol; *Buffer 2*, Cells treated with RPMI media and buffer containing 20 mM sodium phosphate, 0.02 mM pyridoxal phosphate and 0.02 % BME.

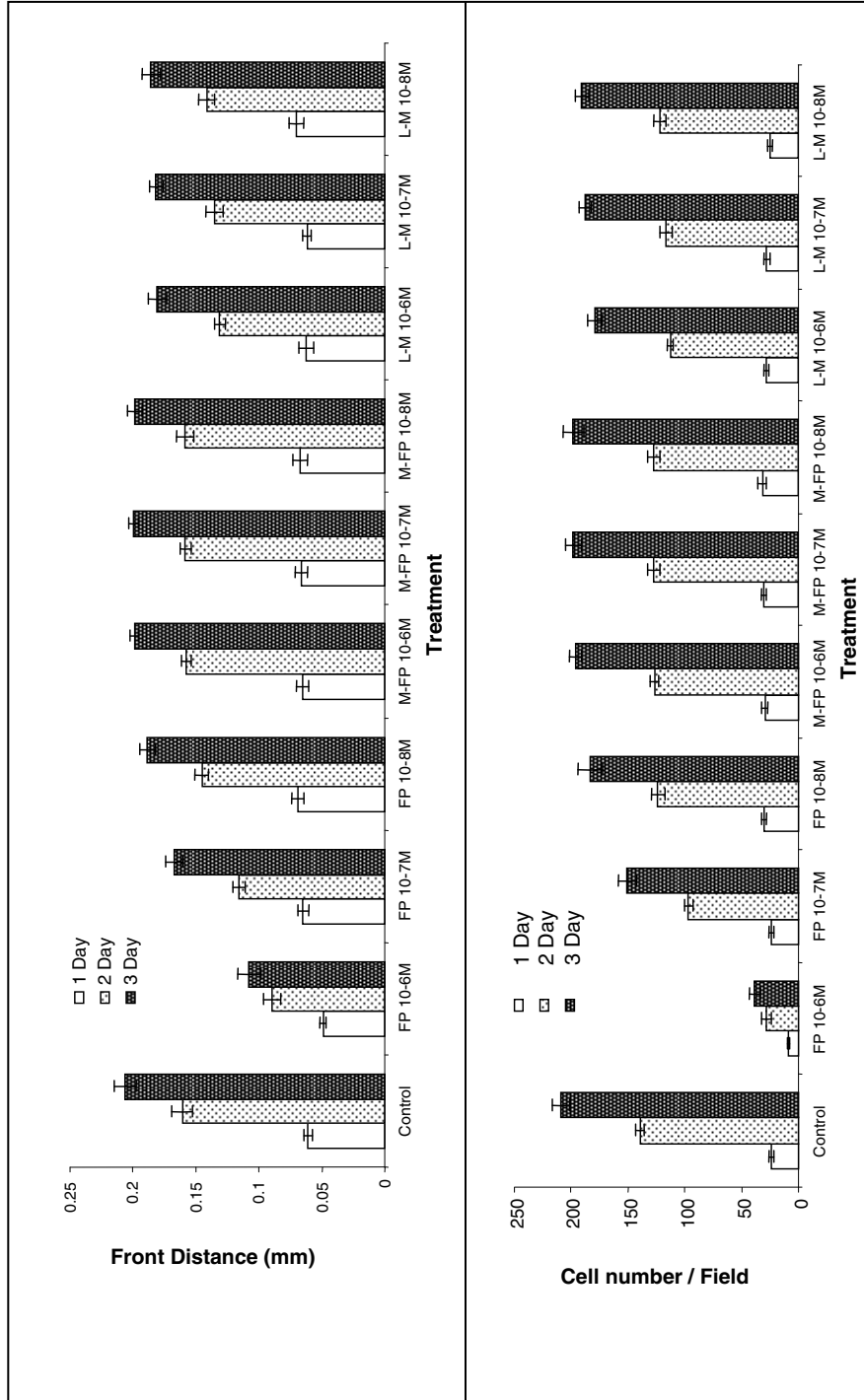


Figure 4.9. Dose-response effect of fusion protein on MCF-7 breast cancer cell migration and proliferation. ATF-methioninase (FP); mutated ATF-methioninase (M-FP); L-methioninase (L-M) were administered immediately following culture wounding. Each bar in the top panel represents the maximum distance traveled by cells in the wounded area (mean \pm SEM from 10 to 12 microscope fields). Each bar in the bottom panel represents number of viable cells in the wounded area (mean \pm SEM from 10 to 12 microscope fields).

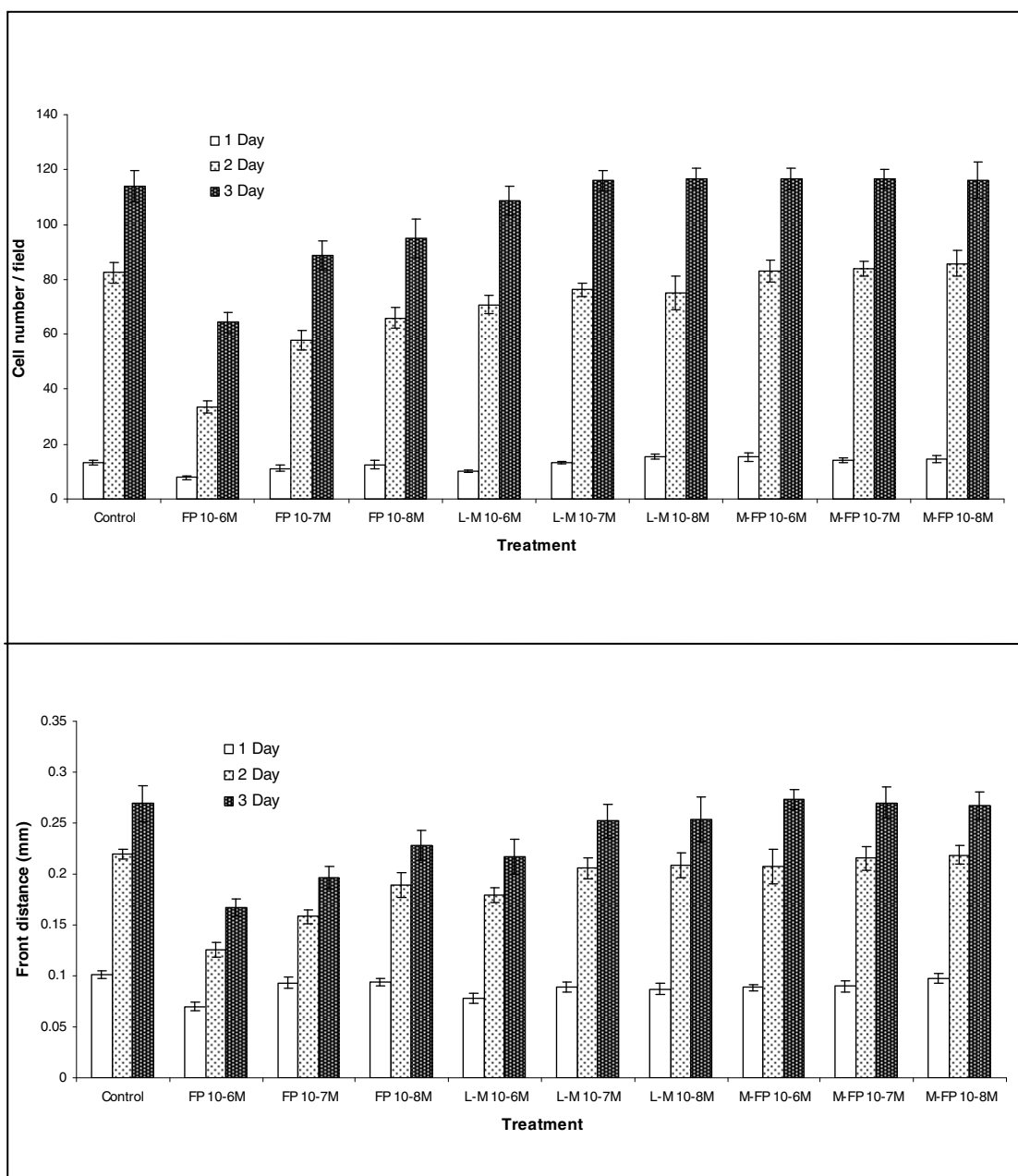


Figure 4.10. Dose-response effect of fusion protein on SK-LU-1 lung cancer cells on proliferation and migration. ATF-methioninase (FP); mutated ATF-methioninase (M-FP); L-methioninase (L-M) were administered immediately following culture wounding. Each bar in the top panel represents the number of cells that migrated into the wounded area (mean \pm SEM from 10 to 12 microscope fields). Each bar in the bottom panel represents number of viable cells in the wounded area (mean \pm SEM from 10 to 12 microscope fields).

proliferation and migration of the lung cancer cells on days 2 and 3 following fusion protein treatment at all concentrations ($p < 0.05$) [96]. The fusion protein with a mutated L-methioninase produced little or no inhibition of cell proliferation or migration over the same concentration range. Treatment of SK-LU-1 cancer cells with L-methioninase alone produced a significant inhibition ($p < 0.05$) of cell migration on days 2 and 3 following treatment only at the highest concentration of 10^{-6} M, and proliferation was significantly inhibited ($p < 0.05$) on day 2 only at 10^{-6} M but was not inhibited on day 3 at any of the concentrations. Thus, L-methioninase induced inhibition was much smaller than that produced by the fusion protein.

The effects of ATF-methioninase fusion protein on PC-3 prostate cancer cells were examined over a concentration range of 10^{-6} to 10^{-8} M as shown in **Figure 4.11**. In these experiments, the fusion protein consistently produced a dose-related inhibition of both the proliferation and migration of the cancer cells on days 2 and 3 following fusion protein treatment at all concentrations ($p < 0.05$) [96]. The fusion protein with a mutated L-methioninase again produced little or no cell proliferation or migration over the same concentration range. Treatment of the PC-3 cancer cells with L-methioninase alone consistently produced a significant reduction in proliferation and migration on all three days only at the highest concentration of 10^{-6} M ($p < 0.05$). The L-methioninase-induced inhibition was significantly less than that produced by the fusion protein on day 3 at all concentrations tested ($p < 0.05$).

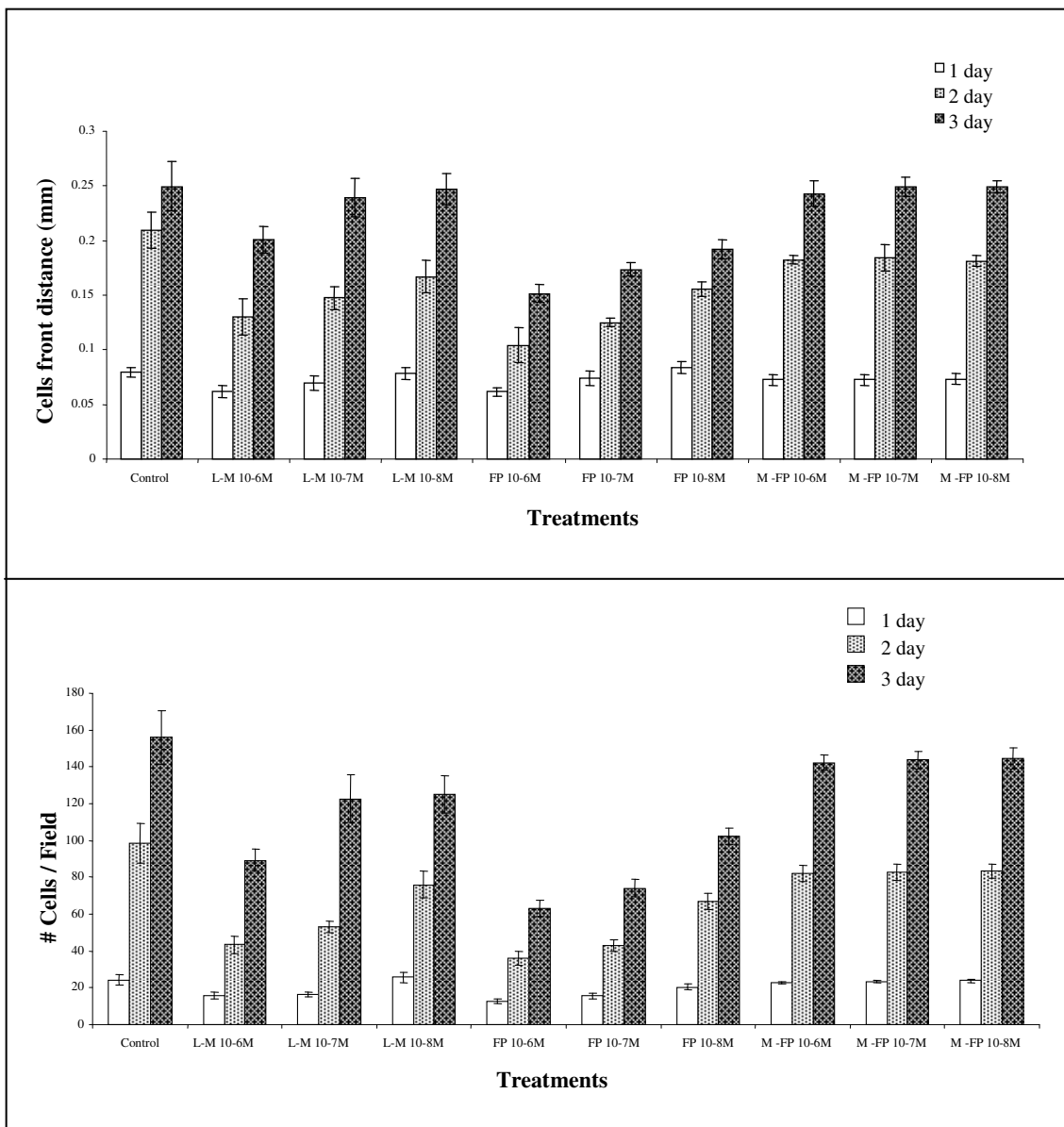


Figure 4.11. Dose-response effect of fusion protein on PC-3 prostate cancer cells on proliferation and migration. ATF-methioninase (FP); mutated ATF-methioninase (M-FP); L-methioninase (L-M) were administered immediately following culture wounding. Each bar in the top panel represents the number of cells that migrated into the wounded area (mean \pm SEM from 10 to 12 microscope fields). Each bar in the bottom pannel represents number of viable cells in the wounded area (mean \pm SEM from 10 to 12 microscope fields).

Specific peptide-based inhibitors of the uPAR were developed where the peptide blocks the uPAR interactions and reduce the progression of the human breast cancer [103, 104]. For example, maspin, a serine protease was found to inhibit tumor growth *in vivo* [105]. Another example, the antagonists of uPA binding to uPAR has been developed based on the binding region of the growth factor domain of uPA. These peptides were successfully used to inhibit the binding of uPA to uPAR [106, 107]. Fusion protein uPA/IgG was found to be useful antagonist to uPAR which inhibited the metastasis of PC3 prostate cancer cells, human melanoma, colon cancer, and head and neck cancer cells [63, 108]. Although in this fusion protein uPA containing 135 amino acids was used, this was believed to have stronger binding affinity to uPAR.

As expected synergistic inhibitive effect of ATF-methioninase as antagonist to the uPAR receptor and methioninase activity was not found in either of these experiments. This can be seen by the lack of inhibition with the mutated ATF-methioninase which implied that cytotoxicity is only caused by L-methioninase which is targeted to the cell surface. Inactivation of urokinase receptor on cancer cell surface by mutated ATF-methioninase at a concentration of 10^{-6} M (**Figure 4.8**, **Figure 4.9**, and **Figure 4.10**) had no effect on cancer cell proliferation and migration which suggested that the concentrations of mutated ATF-methioninase used were not sufficient to saturate the urokinase receptors on the cancer cell surface to prevent the signaling cascade caused by binding of ATF. Use of mutated ATF-methioninase as an antagonist to urokinase was not studied in this project.

The inhibitive effect on cell proliferation produced by ATF-methioninase for the concentration of 10^{-6} M is higher for MCF-7 breast cancer cells than for PC-3 prostate

cancer cells or SK-LU-1 lung cancer cells. Cancer cells have varying degrees of methionine dependence, and it is therefore, likely that the MCF-7 cancer cells have a greater degree of methionine dependence than the SK-LU-1 or PC-3 cancer cells.

Daily Administration of ATF-Methioninase

In this experiment, culture plates received a fresh batch of ATF-methioninase fusion proteins after every 24 h for 3 days. Each day the media was removed and refilled with the media containing the fusion protein at the desired concentration. There was no significant difference in inhibition of cell proliferation and migration after 3 days for the plates which received fusion proteins daily compared to single administration of fusion protein as shown in **Figure 4.12**.

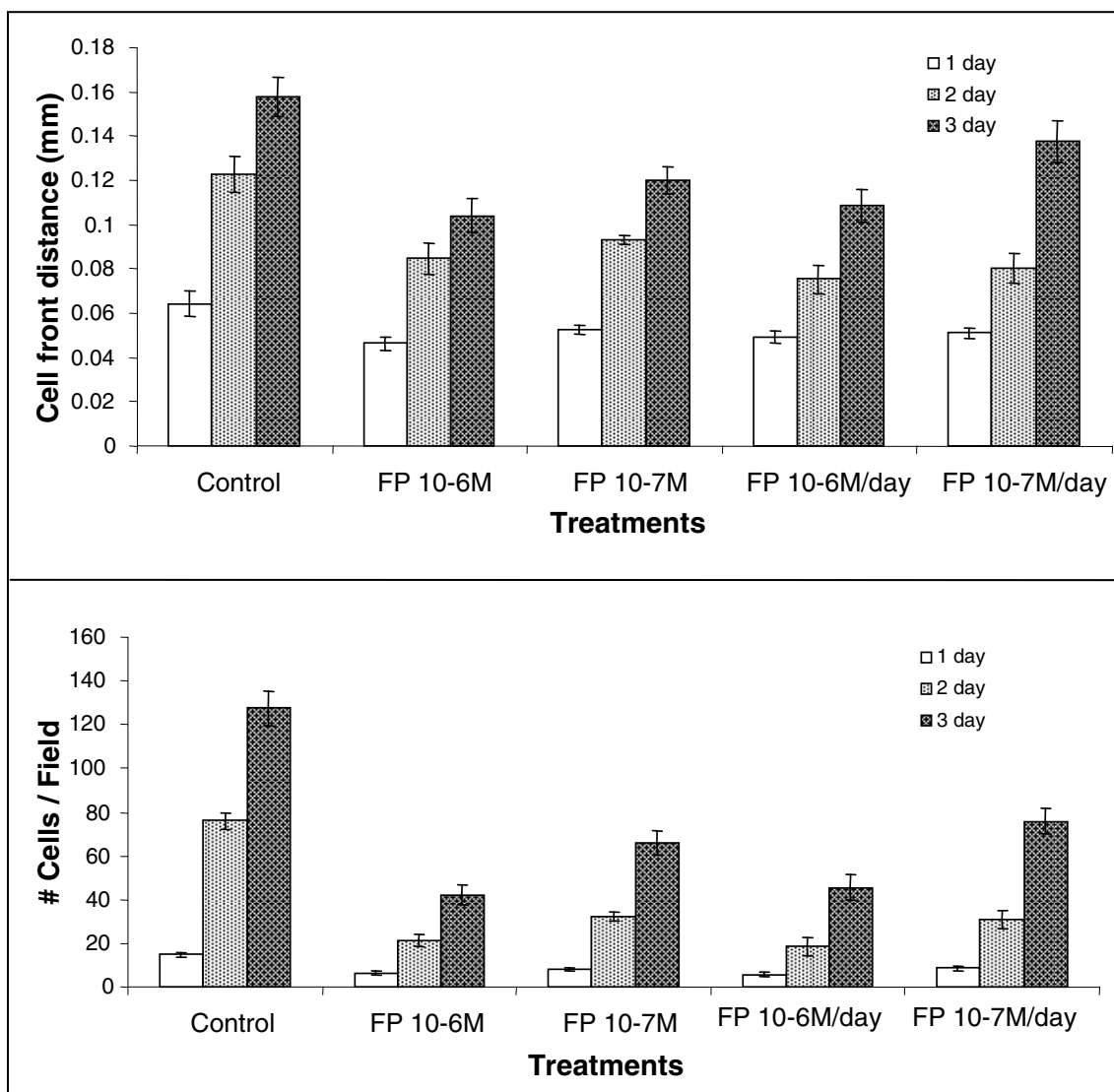


Figure 4.12. Effect of daily administration of ATF-methioninase fusion protein (FP) to the MCF-7 cancer cells.

Effect of TGF-methioninase on MCF-7 Cancer Cells

TGF-methioninase over concentration range of 10^{-8} M to 10^{-6} M in general did not show any response in inhibition of cell migration and proliferation of MCF-7 breast cancer cells over a period of 3 days (**Figure 4.13**). The exceptions where there was a slight statistically significant ($p < 0.05$) inhibition were at 10^{-6} M on days 2 and 3 for proliferation and day 3 for migration [97]. One main reason for this non-inhibitory effect is due to the internalization of ligand after binding to the TGF receptor. Upon binding of TGF-methioninase, the TGF receptor at the cell surface gets phosphorylated and propagates the signal to the cell nucleus for cell proliferation. After ligand binding, the TGF receptor is internalized and partially degraded in lysosomes. The inhibition caused by TGF-methioninase at concentration of 10^{-6} M could be due to the excess exogenous present in the media. Based on these results, the approach of targeting L-methioninase to overexpressed TGF receptors was not pursued further.

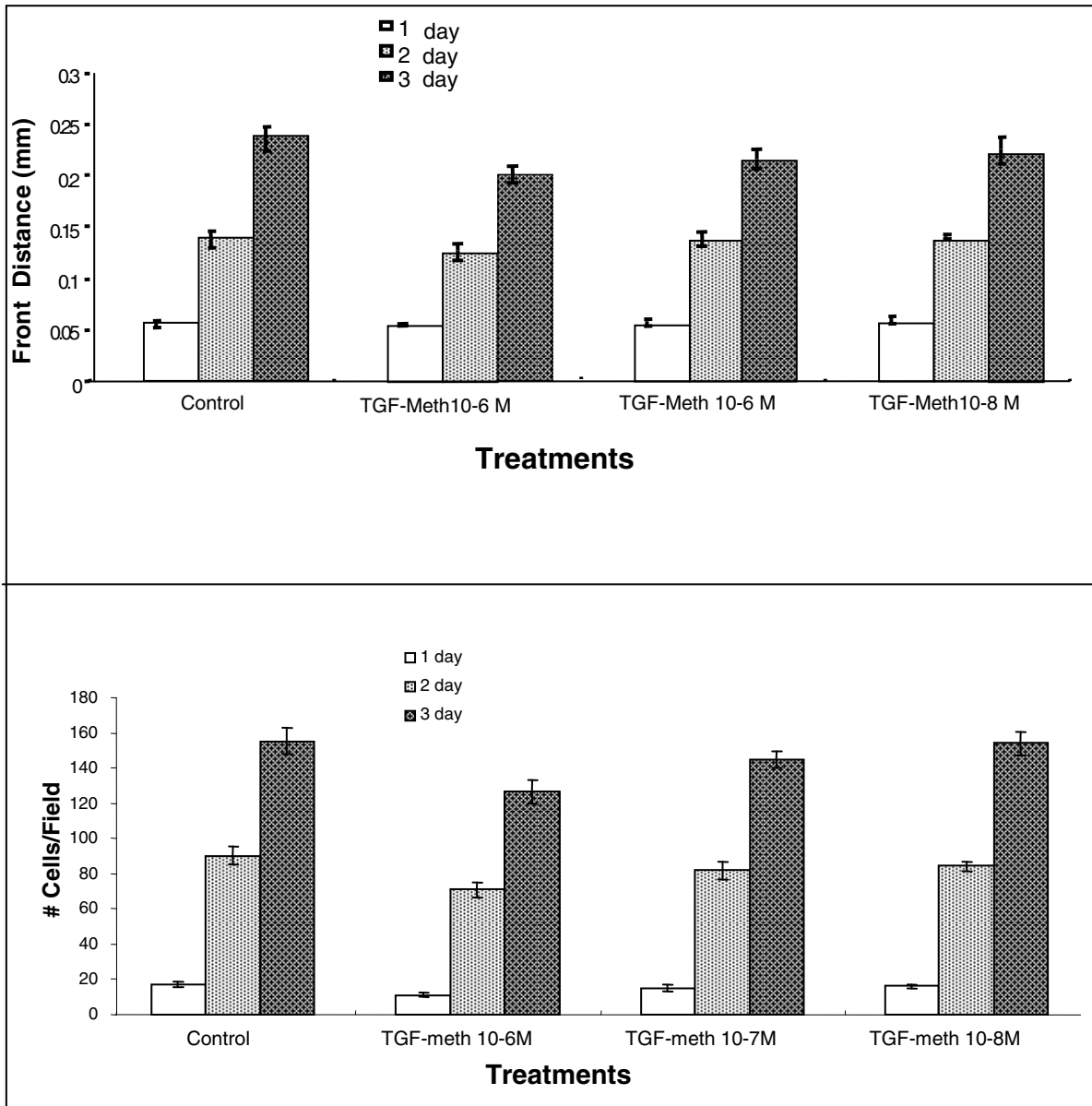


Figure 4.13. Effect of TGF-methioninase fusion protein on MCF-7 breast cancer cell migration and proliferation. Each bar in the top panel represents the maximum distance traveled by cells in the wounded area (mean \pm SEM from 10 to 12 microscope fields). Each bar in the bottom panel represents number of viable cells in the wounded area (mean \pm SEM from 10 to 12 microscope fields).

Specific Binding of ATF-methioninase to MCF-7 Cells

Previously, it was found that ATF-methioninase binds specifically to the urokinase receptor on MCF-7 breast cancer cells, which was demonstrated by measuring the displacement of ATF-methioninase with the increasing concentrations of urokinase [93]. In this present study, the specific binding of ATF-methioninase fusion protein to cancer cells was also measured by immunocytochemical localization [95]. The binding of the fusion protein to MCF-7 cells was demonstrated using a specific L-methioninase antibody for immunocytochemistry. As shown in **Figure 4.14**, the treatment of cells with ATF-methioninase fusion protein (FP), or mutated FP resulted in a positive immunolocalization at the cell membrane, indicated by the red brown staining of the antibody specific to L-methioninase. Immunolocalization was not observed with cells treated with ATF-methioninase fusion protein and urokinase, indicating a specific displacement of fusion protein by urokinase. Further, immunolocalization was not observed for cells treated with L-methioninase alone. ATF-methioninase fusion protein did not get internalized because the ATF does not have a catalytic domain, which is essential for the internalization [62]. This allows ATF-methioninase fusion protein to remain bound on the cell surface.

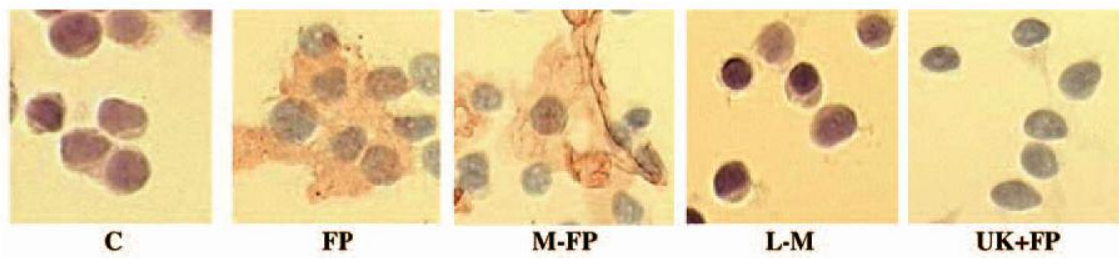


Figure 4.14. Photomicrographs (40X) of MCF-7 cells treated for 18 hours with either: vehicle control (C); ATF-methioninase fusion protein (FP); mutated ATF-methioninase (M-FP); L-methioninase (L-M); or fusion protein + urokinase (UK+FP). All treatments were for 18 hours at a concentration of 10^{-6} M. The red/brown color represents positive staining of the L-methioninase-specific primary antibody.

Mouse Xenograft Assay

The influence of ATF-methioninase on the growth of MCF-7 breast cancer cells in nude mouse xenografts was studied for a period of 20 days. The tumor volume and the nude mouse weight were measured during the period of ATF-methioninase administration. The top panel of **Figure 4.15** indicates that there was no significant change in the weight of the nude mice over the period of administration, indicating that the mice were healthy over the period of administration and ATF-methioninase had no adverse effects on the mice. The bottom panel of **Figure 4.15** indicates that there was a significant decrease in tumor volume for the mice treated with ATF-methioninase compared to the mice treated with L-methioninase. This decrease in volume gives an indication of the cancer cell growth inhibition by ATF-methioninase. After the mice were euthanized, the cell number/mg of tissue was quantified by measuring β -gal activity in tissue homogenates. **Figure 4.16** shows the results for the β -gal activity in tumor tissue after 20-day ATF-methioninase treatment. The ATF-methioninase produced more than a four-fold reduction in cancer cell number/mg tumor tissue as compared to the vehicle-treated control group, and more than a two-fold reduction in cell number/mg compared to the group that received L-methioninase. This latter finding validates the hypothesis that L-methioninase targeted to the cancer cell surface will be more effective in inhibiting cell growth than free L-methioninase [95].

The effect of ATF-methioninase as shown in β -gal activity measurement (**Figure 4.16**) was more when compared to the change in the tumor volumes (**Figure 4.15**). This difference is due to the fact that the tumor contains a large fraction of connective tissue, which occupies a significant volume even after the tumor cells die.

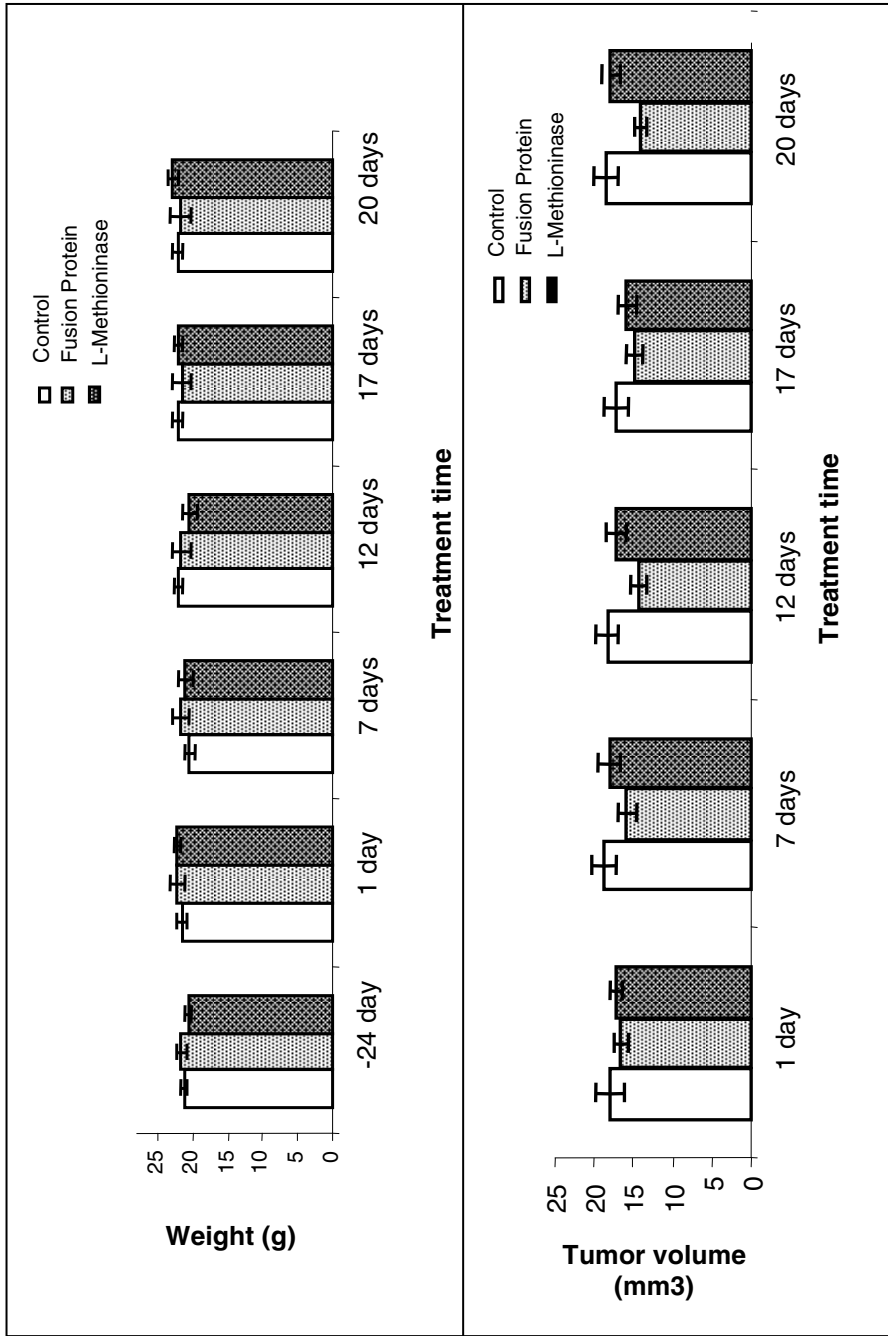


Figure 4.15. (Top Panel) Effect of proteins on weight of nude mice. Each bar represents the weight of nude mice during the course of administration of the proteins (mean \pm SEM). **(Bottom Panel)** Effect of proteins on tumor volume in nude mice (mean \pm SEM). Ten animals were included in each group.

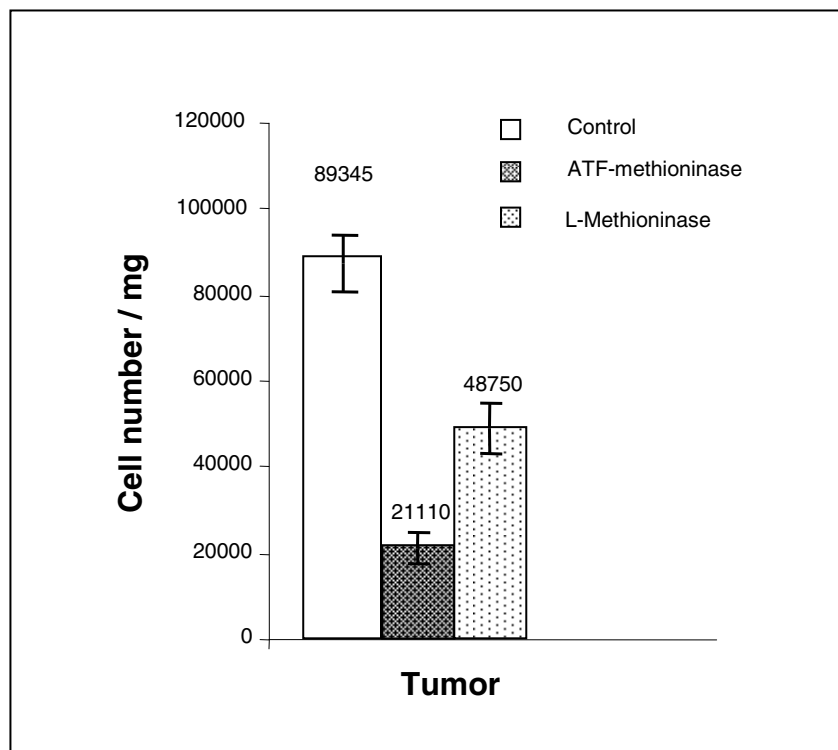


Figure 4.16. Effect of a 20-day with ATF-methioninase or L-methioninase treatment on the growth of MCF-7 tumors and in nude mouse xenografts. The cell number/mg of tissue was quantified by measuring the β -gal activity in tissue homogenates (mean \pm SEM). Ten animals were included in each group. The treatment was administered by intra-tumoral injection.

The main reason to deliver the ATF-methioninase to mouse xenografts intratumorally was to reduce the loss of the fusion protein. Although this approach of delivering drugs is rarely used in a clinical setting, it has many advantages over systemic delivery in experimental studies like this one. This method makes it possible to deliver the exact and known concentrations of the drug to the primary sites of the tumor. Due to this, the amount of drug used will be minimum and much more effective. In a recent study, intratumoral infusion placed stereotactically in a malignant glioma was used to deliver a fusion protein consisting of IL-4 linked to *Pseudomonas aeruginosa* exotoxin A [109]. This resulted in a long term survival of a patient for three years after fusion protein infusion with a durable tumor response. In another clinical application, eleven patients suffering from metastatic breast and colorectal cancers and from malignant melanomas were treated by intratumoral injection of a single chain antibody toxin fusion protein, with complete regression of tumor nodules in 40 % of the patients and partial reduction in tumor size in 20 % of the patients [110].

One drawback to the use of L-methioninase for more than few weeks in human cancer therapy is the immunogenicity of bacterially derived L-methioninase. One way to reduce the immunogenicity is to conjugate it to polyethylene glycol (PEG). L-methioninase has been conjugated to PEG, resulting in a significant increase in serum half life in rats and 36 fold increase in serum half life in primates and elimination of anaphylactic reactions. [37, 38].

Binding of Methioninase-Annexin V to Plastic-immobilized Phosphatidylserine

Methioninase-annexin specifically recognizes PS and binds strongly to plates coated with PS in the presence of 10% bovine serum albumin. The results in **Figure 4.17** show that the binding of methioninase-annexin V to PS immobilized on plastic plates increased as its concentration increased. The control result for L-methioninase was very low (A_{450} less than 10 % of that for methioninase-annexin V). One further control that should be performed in the future is in which all the conditions are the same except no PS is added. It is expected that neither methioninase-annexin V nor L-methioninase will show any appreciable binding with no PS present.

Binding of Methioninase-Annexin V on Externally Positioned PS on the Surface of MCF-7 Breast Cancer Cells

The binding of methioninase-annexin V to cell surfaces was examined using MCF-7 breast cancer cells with hydrogen peroxide added in the medium to induce exposure of PS on the cell surface. The results in **Figure 4.18** indicate that the binding of methioninase-annexin V to PS on the surface of MCF-7 breast cancer cells increased as its concentration is increased, especially at concentrations above 0.3 nM. The binding of the L-methioninase control was negligible. These results indicate specific binding of methioninase-annexin V to PS on the surface of MCF-7 breast cancer cells.

All the experiments were done in the presence of Ca^{2+} because it has been shown previously that binding of annexin V to PS is Ca^{2+} dependent and binding of annexin V in its absence was found to bind most avidly to phosphatidylcholine. Annexin V binds to other anionic phospholipids in the order of

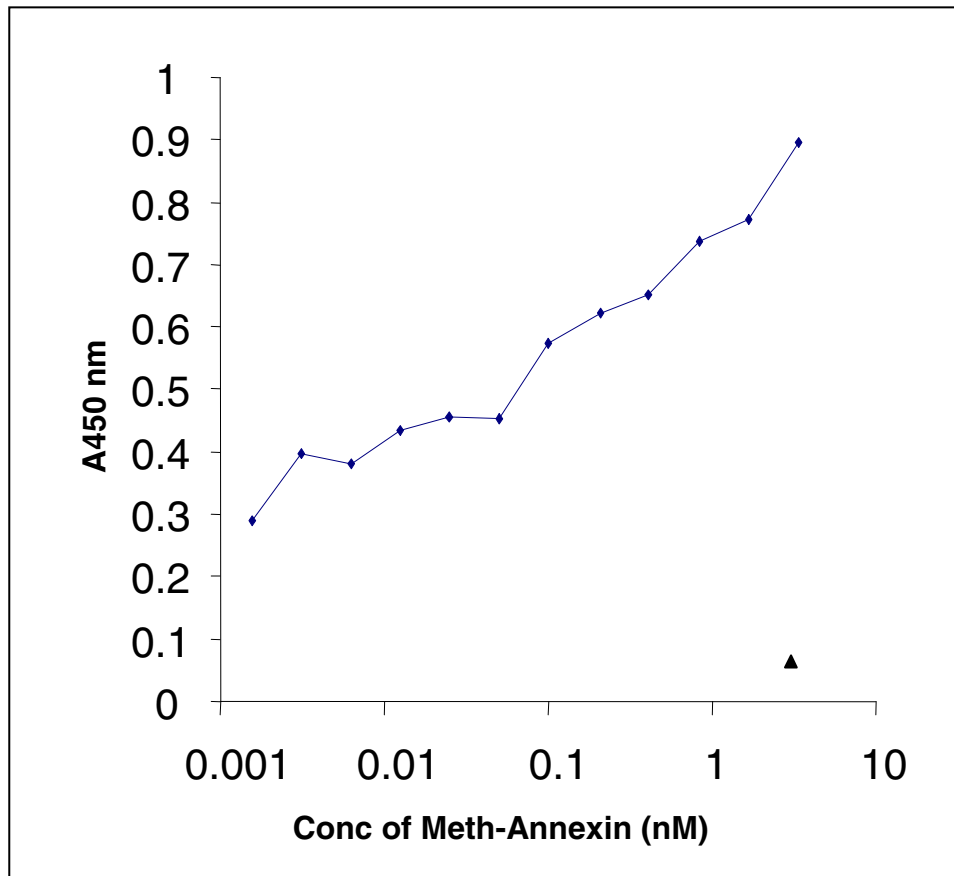


Figure 4.17. Binding of methioninase-annexin V to phosphatidylserine adsorbed to plastic. Blank for assay: +1^o Ab, +2^o Ab. Control for assay (▲): L-methioninase, +1^o Ab, +2^o Ab. (each A₄₅₀ measured in triplicate).

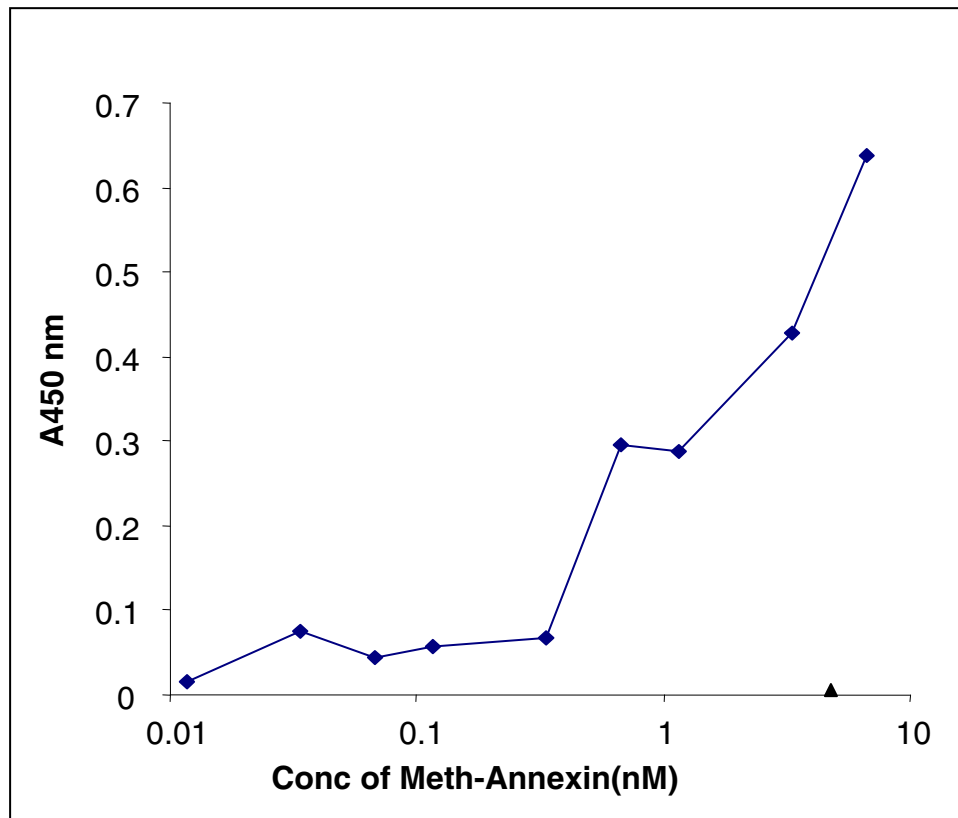


Figure 4.18. Binding of methioninase-annexin V to phosphatidylserine exposed on MCF-7 breast cancer cells. Blank for assay: +1° Ab, +2° Ab. Control for assay (▲): L-methioninase, +1° Ab, +2° Ab. (each A₄₅₀ measured in triplicate).

phosphatidylethanolamine, PS, cardiolipin, phosphatic acid, phosphatidylinositol, and phosphatidylglycerol. It is known PS is exposed on apoptotic cells, aging cells and activated platelets, and methioninase-annexin V is expected to bind to these cells. However, methioninase is not toxic to these cells, so binding to these cells is of less concern. Another advantage using annexin V as targeting molecule other than its abundant exposure on tumor vessel endothelial cells ($> 10^6$ molecules per cell) is that ease of application of methioninase-annexin V intraperitoneally in the mouse xenograft models. Diffusional limitations of the drugs to core of tumor sites is eliminated by using methioninase-annexin V because binding of methioninase-annexin at tumor vasculature may be effective as complete diffused drug in the tumor site.

5. CONCLUSIONS

The major objective of this work was to examine three fusion proteins (ATF-methioninase, TGF-methioninase, and methioninase-annexin V) for targeting the human cancer cells selectively and inhibiting the migration and proliferation of the cells. A secondary objective was to evaluate the ability of the methioninase-annexin fusion protein to bind selectively to plastic-immobilized PS and to PS exposed on the surface of cancer cells.

The three fusion proteins were expressed as soluble proteins and purified to homogeneity from the pET-30 Ek/LIC and pET-44 Ek/LIC vector expression systems. Use of the pET-44 Ek/LIC vector introduced a NusA protein tag to TGF-methioninase. All of the fusion proteins expressed had an N-terminal His₆ tag to facilitate purification by immobilized metal affinity chromatography. An HRV 3C protease site was incorporated after the enterokinase site, and HRV 3C protease was found effective in cleavage of the His₆ tag. Flash freezing in liquid nitrogen in buffer with 100 mM NaCl followed by lyophilization was found to be the most effective way to store the samples for longer period of times. This process resulted in proteins with purities above 90% consistently.

Based on the results of the culture wounding assays using MCF-7 breast cancer cells, SK-LU-1 lung cancer cells, and PC-3 prostate cancer cells, ATF-methioninase was significantly more effective than free L-methioninase *in vitro* in inhibiting cell proliferation and migration. In the culture wounding tests, it was found that cytotoxicity to cancer cells was caused by methioninase activity alone. Treatment with TGF-methioninase in general did not show any inhibition of the proliferation and migration of

MCF-7 cells. ATF-methioninase with the L-methioninase mutated to give no activity gave negligible inhibition of cancer cell proliferation and migration. ATF-methioninase bound specifically to MCF-7 breast cancer cells and did not internalize upon binding to the uPAR. Treatment of s.c. implanted MCF-7 breast cancer cells mouse xenografts with ATF-methioninase gave significantly more tumor regression when compared to mouse xenografts treated with L-methioninase alone.

The methioninase-annexin V fusion protein bound specifically to PS immobilized on plastic plates as well as on the surface of MCF-7 cancer cells in which PS was induced to be on the surface by the addition of hydrogen peroxide.

Based on the results obtained in this research, future research methods should include full length ATF (135 amino acids) in fusion with L-methioninase, 2) pegylation of ATF-methioninase to reduce the immunogenicity, 3) testing the ATF-methioninase with other cancer cell types like colon, melanoma, and ovarian, 4) testing the binding of methioninase-annexin V fusion protein to human endothelial cells grown *in vitro* on which PS has been induced to be exposed on the surface, 5) finally, testing the effect of methioninase-annexin V fusion protein injected i.p. in mice on the growth of tumor xenografts.

BIBLIOGRAPHY

1. Cheng, K.C. and M.O. Diaz, *Genomic instability and cancer: cause and effect*. Cancer Cells, 1991. **3**(5): p. 188-92.
2. Rusciano, D. and M.M. Burger, *Why do cancer cells metastasize into particular organs?* Bioessays, 1992. **14**(3): p. 185-94.
3. Blagosklonny, M.V. and A.B. Pardee, *Exploiting cancer cell cycling for selective protection of normal cells*. Cancer Res, 2001. **61**(11): p. 4301-5.
4. Fominaya, J. and W. Wels, *Target cell-specific DNA transfer mediated by a chimeric multidomain protein. Novel non-viral gene delivery system*. J Biol Chem, 1996. **271**(18): p. 10560-8.
5. Glover, C.P., A.S. Bienemann, D.J. Heywood, A.S. Cosgrave, and J.B. Uney, *Adenoviral-mediated, high-level, cell-specific transgene expression: a SYN1-WPRE cassette mediates increased transgene expression with no loss of neuron specificity*. Mol Ther, 2002. **5**(5 Pt 1): p. 509-16.
6. Glover, D.J., H.J. Lipps, and D.A. Jans, *Towards safe, non-viral therapeutic gene expression in humans*. Nat Rev Genet, 2005. **6**(4): p. 299-310.
7. Verma, I.M. and M.D. Weitzman, *Gene therapy: twenty-first century medicine*. Annu Rev Biochem, 2005. **74**: p. 711-38.
8. Leach, R.A. and M.T. Tuck, *Methionine depletion induces transcription of the mRNA (N6-adenosine)methyltransferase*. Int J Biochem Cell Biol, 2001. **33**(11): p. 1116-28.
9. Mato, J.M., L. Alvarez, P. Ortiz, and M.A. Pajares, *S-adenosylmethionine synthesis: molecular mechanisms and clinical implications*. Pharmacol Ther, 1997. **73**(3): p. 265-80.
10. Chiang, P.K., R.K. Gordon, J. Tal, G.C. Zeng, B.P. Doctor, K. Pardhasaradhi, and P.P. McCann, *S-Adenosylmethionine and methylation*. Faseb J, 1996. **10**(4): p. 471-80.
11. Thomas, T. and T.J. Thomas, *Polyamines in cell growth and cell death: molecular mechanisms and therapeutic applications*. Cell Mol Life Sci, 2001. **58**(2): p. 244-58.
12. Anderson, M.E., *Glutathione: an overview of biosynthesis and modulation*. Chem Biol Interact, 1998. **111-112**: p. 1-14.
13. Halpern, B.C., B.R. Clark, D.N. Hardy, R.M. Halpern, and R.A. Smith, *The effect of replacement of methionine by homocystine on survival of malignant and*

- normal adult mammalian cells in culture*. Proc Natl Acad Sci U S A, 1974. **71**(4): p. 1133-6.
14. Hoffman, D.R., J.A. Haning, and W.E. Cornatzer, *Effects of a methyl-deficient diet on rat liver phosphatidylcholine biosynthesis*. Can J Biochem, 1981. **59**(7): p. 543-50.
 15. Hoffman, R.M., *Altered methionine metabolism and transmethylation in cancer*. Anticancer Res, 1985. **5**(1): p. 1-30.
 16. Hoffman, R.M., *Methioninase: a therapeutic for diseases related to altered methionine metabolism and transmethylation: cancer, heart disease, obesity, aging, and Parkinson's disease*. Hum Cell, 1997. **10**(1): p. 69-80.
 17. Mecham, J.O., D. Rowitch, C.D. Wallace, P.H. Stern, and R.M. Hoffman, *The metabolic defect of methionine dependence occurs frequently in human tumor cell lines*. Biochem Biophys Res Commun, 1983. **117**(2): p. 429-34.
 18. Tan, Y., X. Sun, M. Xu, Z. An, X. Tan, Q. Han, D.A. Miljkovic, M. Yang, and R.M. Hoffman, *Polyethylene glycol conjugation of recombinant methioninase for cancer therapy*. Protein Expr Purif, 1998. **12**(1): p. 45-52.
 19. Tan, Y., J. Zavala, Sr., M. Xu, J. Zavala, Jr., and R.M. Hoffman, *Serum methionine depletion without side effects by methioninase in metastatic breast cancer patients*. Anticancer Res, 1996. **16**(6C): p. 3937-42.
 20. Judde, J.G., M. Ellis, and P. Frost, *Biochemical analysis of the role of transmethylation in the methionine dependence of tumor cells*. Cancer Res, 1989. **49**(17): p. 4859-65.
 21. Kokkinakis, D.M., *Methionine-stress: a pleiotropic approach in enhancing the efficacy of chemotherapy*. Cancer Lett, 2006. **233**(2): p. 195-207.
 22. Kokkinakis, D.M., R.M. Hoffman, E.P. Frenkel, J.B. Wick, Q. Han, M. Xu, Y. Tan, and S.C. Schold, *Synergy between methionine stress and chemotherapy in the treatment of brain tumor xenografts in athymic mice*. Cancer Res, 2001. **61**(10): p. 4017-23.
 23. Cellarier, E., X. Durando, M.P. Vasson, M.C. Farges, A. Demiden, J.C. Maurizis, J.C. Madelmont, and P. Chollet, *Methionine dependency and cancer treatment*. Cancer Treat Rev, 2003. **29**(6): p. 489-99.
 24. Kenyon, S.H., T. Ast, A. Nicolaou, and W.A. Gibbons, *Polyamines can regulate vitamin B12 dependent methionine synthase activity*. Biochem Soc Trans, 1995. **23**(3): p. 444S.

25. Kenyon, S.H., C.J. Waterfield, J.A. Timbrell, and A. Nicolaou, *Methionine synthase activity and sulphur amino acid levels in the rat liver tumour cells HTC and Phi-1*. *Biochem Pharmacol*, 2002. **63**(3): p. 381-91.
26. Kreis, W. and C. Hession, *Isolation and purification of L-methionine-alpha-deamino-gamma-mercaptomethane-lyase (L-methioninase) from Clostridium sporogenes*. *Cancer Res*, 1973. **33**(8): p. 1862-5.
27. Nakayama, T., N. Esaki, K. Sugie, T.T. Beresov, H. Tanaka, and K. Soda, *Purification of bacterial L-methionine gamma-lyase*. *Anal Biochem*, 1984. **138**(2): p. 421-4.
28. Hori, H., K. Takabayashi, L. Orvis, D.A. Carson, and T. Nobori, *Gene cloning and characterization of Pseudomonas putida L-methionine-alpha-deamino-gamma-mercaptomethane-lyase*. *Cancer Res*, 1996. **56**(9): p. 2116-22.
29. Inoue, H., K. Inagaki, M. Sugimoto, N. Esaki, K. Soda, and H. Tanaka, *Structural analysis of the L-methionine gamma-lyase gene from Pseudomonas putida*. *J Biochem (Tokyo)*, 1995. **117**(5): p. 1120-5.
30. Motoshima, H., K. Inagaki, T. Kumasaka, M. Furuichi, H. Inoue, T. Tamura, N. Esaki, K. Soda, N. Tanaka, M. Yamamoto, and H. Tanaka, *Crystal structure of the pyridoxal 5'-phosphate dependent L-methionine gamma-lyase from Pseudomonas putida*. *J Biochem (Tokyo)*, 2000. **128**(3): p. 349-54.
31. Inoue, H., K. Inagaki, N. Adachi, T. Tamura, N. Esaki, K. Soda, and H. Tanaka, *Role of tyrosine 114 of L-methionine gamma-lyase from Pseudomonas putida*. *Biosci Biotechnol Biochem*, 2000. **64**(11): p. 2336-43.
32. Tan, Y., X. Sun, M. Xu, X. Tan, A. Sasson, B. Rashidi, Q. Han, X. Tan, X. Wang, Z. An, F.X. Sun, and R.M. Hoffman, *Efficacy of recombinant methioninase in combination with cisplatin on human colon tumors in nude mice*. *Clin Cancer Res*, 1999. **5**(8): p. 2157-63.
33. Yoshioka, T., T. Wada, N. Uchida, H. Maki, H. Yoshida, N. Ide, H. Kasai, K. Hojo, K. Shono, R. Maekawa, S. Yagi, R.M. Hoffman, and K. Sugita, *Anticancer efficacy in vivo and in vitro, synergy with 5-fluorouracil, and safety of recombinant methioninase*. *Cancer Res*, 1998. **58**(12): p. 2583-7.
34. Kokkinakis, D.M., S.C. Schold, Jr., H. Hori, and T. Nobori, *Effect of long-term depletion of plasma methionine on the growth and survival of human brain tumor xenografts in athymic mice*. *Nutr Cancer*, 1997. **29**(3): p. 195-204.
35. Kokkinakis, D.M., J.B. Wick, and Q.X. Zhou, *Metabolic response of normal and malignant tissue to acute and chronic methionine stress in athymic mice bearing human glial tumor xenografts*. *Chem Res Toxicol*, 2002. **15**(11): p. 1472-9.

36. Miki, K., W. Al-Refaie, M. Xu, P. Jiang, Y. Tan, M. Bouvet, M. Zhao, A. Gupta, T. Chishima, H. Shimada, M. Makuuchi, A.R. Moossa, and R.M. Hoffman, *Methioninase gene therapy of human cancer cells is synergistic with recombinant methioninase treatment*. *Cancer Res*, 2000. **60**(10): p. 2696-702.
37. Yang, Z., J. Wang, Q. Lu, J. Xu, Y. Kobayashi, T. Takakura, A. Takimoto, T. Yoshioka, C. Lian, C. Chen, D. Zhang, Y. Zhang, S. Li, X. Sun, Y. Tan, S. Yagi, E.P. Frenkel, and R.M. Hoffman, *PEGylation Confers Greatly Extended Half-Life and Attenuated Immunogenicity to Recombinant Methioninase in Primates*. *Cancer Res*, 2004. **64**(18): p. 6673-6678.
38. Yang, Z., J. Wang, T. Yoshioka, B. Li, Q. Lu, S. Li, X. Sun, Y. Tan, S. Yagi, E.P. Frenkel, and R.M. Hoffman, *Pharmacokinetics, methionine depletion, and antigenicity of recombinant methioninase in primates*. *Clin Cancer Res*, 2004. **10**(6): p. 2131-8.
39. Sun, X., Z. Yang, S. Li, Y. Tan, N. Zhang, X. Wang, S. Yagi, T. Yoshioka, A. Takimoto, K. Mitsushima, A. Suginaka, E.P. Frenkel, and R.M. Hoffman, *In vivo efficacy of recombinant methioninase is enhanced by the combination of polyethylene glycol conjugation and pyridoxal 5'-phosphate supplementation*. *Cancer Res*, 2003. **63**(23): p. 8377-83.
40. Meeker, T., J. Lowder, M.L. Cleary, S. Stewart, R. Warnke, J. Sklar, and R. Levy, *Emergence of idiotype variants during treatment of B-cell lymphoma with anti-idiotypic antibodies*. *N Engl J Med*, 1985. **312**(26): p. 1658-65.
41. Miller, R.A., D.G. Maloney, R. Warnke, and R. Levy, *Treatment of B-cell lymphoma with monoclonal anti-idiotypic antibody*. *N Engl J Med*, 1982. **306**(9): p. 517-22.
42. Trail, P.A. and A.B. Bianchi, *Monoclonal antibody drug conjugates in the treatment of cancer*. *Curr Opin Immunol*, 1999. **11**(5): p. 584-8.
43. Firestone, R.A., *Low-density lipoprotein as a vehicle for targeting antitumor compounds to cancer cells*. *Bioconjug Chem*, 1994. **5**(2): p. 105-13.
44. Kahan, Z., A. Nagy, A.V. Schally, G. Halmos, J.M. Arencibia, and K. Groot, *Administration of a targeted cytotoxic analog of luteinizing hormone-releasing hormone inhibits growth of estrogen-independent MDA-MB-231 human breast cancers in nude mice*. *Breast Cancer Res Treat*, 2000. **59**(3): p. 255-62.
45. Poznansky, M.J., R. Singh, B. Singh, and G. Fantus, *Insulin: carrier potential for enzyme and drug therapy*. *Science*, 1984. **223**(4642): p. 1304-6.
46. Denekamp, J., *The current status of targeting tumour vasculature as a means of cancer therapy: an overview*. *Int J Radiat Biol*, 1991. **60**(1-2): p. 401-8.

47. Denekamp, J., *Inadequate vasculature in solid tumours: consequences for cancer research strategies*. BJR Suppl, 1992. **24**: p. 111-7.
48. Denekamp, J., *Limited role of vasculature-mediated injury in tumor response to radiotherapy*. J Natl Cancer Inst, 1993. **85**(12): p. 935-7.
49. Mazar, A.P., J. Henkin, and R.H. Goldfarb, *The urokinase plasminogen activator system in cancer: implications for tumor angiogenesis and metastasis*. Angiogenesis, 1999. **3**(1): p. 15-32.
50. Bianchi, E., R.L. Cohen, A.T. Thor, R.F. Todd, 3rd, I.F. Mizukami, D.A. Lawrence, B.M. Ljung, M.A. Shuman, and H.S. Smith, *The urokinase receptor is expressed in invasive breast cancer but not in normal breast tissue*. Cancer Res, 1994. **54**(4): p. 861-6.
51. Pyke, C., N. Graem, E. Ralfkiaer, E. Ronne, G. Hoyer-Hansen, N. Brunner, and K. Dano, *Receptor for urokinase is present in tumor-associated macrophages in ductal breast carcinoma*. Cancer Res, 1993. **53**(8): p. 1911-5.
52. Pyke, C., P. Kristensen, E. Ralfkiaer, J. Grondahl-Hansen, J. Eriksen, F. Blasi, and K. Dano, *Urokinase-type plasminogen activator is expressed in stromal cells and its receptor in cancer cells at invasive foci in human colon adenocarcinomas*. Am J Pathol, 1991. **138**(5): p. 1059-67.
53. Suzuki, S., Y. Hayashi, Y. Wang, T. Nakamura, Y. Morita, K. Kawasaki, K. Ohta, N. Aoyama, S.R. Kim, H. Itoh, Y. Kuroda, and W.F. Doe, *Urokinase type plasminogen activator receptor expression in colorectal neoplasms*. Gut, 1998. **43**(6): p. 798-805.
54. Wagner, S.N., M.J. Atkinson, S. Thanner, C. Wagner, M. Schmitt, O. Wilhelm, M. Rotter, and H. Hofler, *Modulation of urokinase and urokinase receptor gene expression in human renal cell carcinoma*. Am J Pathol, 1995. **147**(1): p. 183-92.
55. Morita, Y., Y. Hayashi, Y. Wang, T. Kanamaru, S. Suzuki, K. Kawasaki, K. Ohta, M. Yamamoto, Y. Saitoh, H. Itoh, and W.F. Doe, *Expression of urokinase-type plasminogen activator receptor in hepatocellular carcinoma*. Hepatology, 1997. **25**(4): p. 856-61.
56. Pedersen, H., N. Brunner, D. Francis, K. Osterlind, E. Ronne, H.H. Hansen, K. Dano, and J. Grondahl-Hansen, *Prognostic impact of urokinase, urokinase receptor, and type 1 plasminogen activator inhibitor in squamous and large cell lung cancer tissue*. Cancer Res, 1994. **54**(17): p. 4671-5.
57. Casslen, B., B. Gustavsson, and B. Astedt, *Cell membrane receptors for urokinase plasminogen activator are increased in malignant ovarian tumours*. Eur J Cancer, 1991. **27**(11): p. 1445-8.

58. Nozaki, S., Y. Endo, S. Kawashiri, K. Nakagawa, E. Yamamoto, Y. Yonemura, and T. Sasaki, *Immunohistochemical localization of a urokinase-type plasminogen activator system in squamous cell carcinoma of the oral cavity: association with mode of invasion and lymph node metastasis*. *Oral Oncol*, 1998. **34**(1): p. 58-62.
59. Nozaki, S., Y. Endo, H. Nakahara, K. Yoshizawa, T. Ohara, and E. Yamamoto, *Targeting urokinase-type plasminogen activator and its receptor for cancer therapy*. *Anticancer Drugs*, 2006. **17**(10): p. 1109-17.
60. Appella, E., E.A. Robinson, S.J. Ullrich, M.P. Stoppelli, A. Corti, G. Cassani, and F. Blasi, *The receptor-binding sequence of urokinase. A biological function for the growth-factor module of proteases*. *J Biol Chem*, 1987. **262**(10): p. 4437-40.
61. Rabbani, S.A., A.P. Mazar, S.M. Bernier, M. Haq, I. Bolivar, J. Henkin, and D. Goltzman, *Structural requirements for the growth factor activity of the amino-terminal domain of urokinase*. *J Biol Chem*, 1992. **267**(20): p. 14151-6.
62. Cubellis, M.V., T.C. Wun, and F. Blasi, *Receptor-mediated internalization and degradation of urokinase is caused by its specific inhibitor PAI-1*. *Embo J*, 1990. **9**(4): p. 1079-85.
63. Crowley, C.W., R.L. Cohen, B.K. Lucas, G. Liu, M.A. Shuman, and A.D. Levinson, *Prevention of metastasis by inhibition of the urokinase receptor*. *Proc Natl Acad Sci U S A*, 1993. **90**(11): p. 5021-5.
64. Liang, O.D., T. Chavakis, S.M. Kanse, and K.T. Preissner, *Ligand binding regions in the receptor for urokinase-type plasminogen activator*. *J Biol Chem*, 2001. **276**(31): p. 28946-53.
65. Dano, K., P.A. Andreasen, J. Grondahl-Hansen, P. Kristensen, L.S. Nielsen, and L. Skriver, *Plasminogen activators, tissue degradation, and cancer*. *Adv Cancer Res*, 1985. **44**: p. 139-266.
66. Pardee, A.B., *G1 events and regulation of cell proliferation*. *Science*, 1989. **246**(4930): p. 603-8.
67. Schmidt, M.H., F.B. Furnari, W.K. Cavenee, and O. Bogler, *Epidermal growth factor receptor signaling intensity determines intracellular protein interactions, ubiquitination, and internalization*. *Proc Natl Acad Sci U S A*, 2003. **100**(11): p. 6505-10.
68. Sorkina, T., A. Bild, F. Tebar, and A. Sorkin, *Clathrin, adaptors and eps15 in endosomes containing activated epidermal growth factor receptors*. *J Cell Sci*, 1999. **112** (Pt 3): p. 317-27.
69. Wilde, A., E.C. Beattie, L. Lem, D.A. Riethof, S.H. Liu, W.C. Mobley, P. Soriano, and F.M. Brodsky, *EGF receptor signaling stimulates SRC kinase*

- phosphorylation of clathrin, influencing clathrin redistribution and EGF uptake.* Cell, 1999. **96**(5): p. 677-87.
70. Di Fiore, P.P., J.H. Pierce, T.P. Fleming, R. Hazan, A. Ullrich, C.R. King, J. Schlessinger, and S.A. Aaronson, *Overexpression of the human EGF receptor confers an EGF-dependent transformed phenotype to NIH 3T3 cells.* Cell, 1987. **51**(6): p. 1063-70.
 71. Herlyn, M., R. Kath, N. Williams, I. Valyi-Nagy, and U. Rodeck, *Growth-regulatory factors for normal, premalignant, and malignant human cells in vitro.* Adv Cancer Res, 1990. **54**: p. 213-34.
 72. Hendler, F.J. and B.W. Ozanne, *Human squamous cell lung cancers express increased epidermal growth factor receptors.* J Clin Invest, 1984. **74**(2): p. 647-51.
 73. Gullick, W.J., J.J. Marsden, N. Whittle, B. Ward, L. Bobrow, and M.D. Waterfield, *Expression of epidermal growth factor receptors on human cervical, ovarian, and vulval carcinomas.* Cancer Res, 1986. **46**(1): p. 285-92.
 74. Yamamoto, T., N. Kamata, H. Kawano, S. Shimizu, T. Kuroki, K. Toyoshima, K. Rikimaru, N. Nomura, R. Ishizaki, I. Pastan, and et al., *High incidence of amplification of the epidermal growth factor receptor gene in human squamous carcinoma cell lines.* Cancer Res, 1986. **46**(1): p. 414-6.
 75. Imai, Y., C.K. Leung, H.G. Friesen, and R.P. Shiu, *Epidermal growth factor receptors and effect of epidermal growth factor on growth of human breast cancer cells in long-term tissue culture.* Cancer Res, 1982. **42**(11): p. 4394-8.
 76. Neal, D.E., C. Marsh, M.K. Bennett, P.D. Abel, R.R. Hall, J.R. Sainsbury, and A.L. Harris, *Epidermal-growth-factor receptors in human bladder cancer: comparison of invasive and superficial tumours.* Lancet, 1985. **1**(8425): p. 366-8.
 77. Gullick, W.J., *Prevalence of aberrant expression of the epidermal growth factor receptor in human cancers.* Br Med Bull, 1991. **47**(1): p. 87-98.
 78. Phillips, P.C., C. Levow, M. Catterall, O.M. Colvin, I. Pastan, and H. Brem, *Transforming growth factor-alpha-Pseudomonas exotoxin fusion protein (TGF-alpha-PE38) treatment of subcutaneous and intracranial human glioma and medulloblastoma xenografts in athymic mice.* Cancer Res, 1994. **54**(4): p. 1008-15.
 79. Waksal, H.W., *Role of an anti-epidermal growth factor receptor in treating cancer.* Cancer Metastasis Rev, 1999. **18**(4): p. 427-36.
 80. Williamson, P. and R.A. Schlegel, *Back and forth: the regulation and function of transbilayer phospholipid movement in eukaryotic cells.* Mol Membr Biol, 1994. **11**(4): p. 199-216.

81. Zwaal, R.F. and A.J. Schroit, *Pathophysiologic implications of membrane phospholipid asymmetry in blood cells*. Blood, 1997. **89**(4): p. 1121-32.
82. Rao, L.V., *Mechanisms of activity of lupus anticoagulants*. Curr Opin Hematol, 1997. **4**(5): p. 344-50.
83. Utsugi, T., A.J. Schroit, J. Connor, C.D. Bucana, and I.J. Fidler, *Elevated expression of phosphatidylserine in the outer membrane leaflet of human tumor cells and recognition by activated human blood monocytes*. Cancer Res, 1991. **51**(11): p. 3062-6.
84. Blankenberg, F.G., P.D. Katsikis, J.F. Tait, R.E. Davis, L. Naumovski, K. Ohtsuki, S. Kopiwoda, M.J. Abrams, M. Darkes, R.C. Robbins, H.T. Maecker, and H.W. Strauss, *In vivo detection and imaging of phosphatidylserine expression during programmed cell death*. Proc Natl Acad Sci U S A, 1998. **95**(11): p. 6349-54.
85. Herrmann, A. and P.F. Devaux, *Alteration of the aminophospholipid translocase activity during in vivo and artificial aging of human erythrocytes*. Biochim Biophys Acta, 1990. **1027**(1): p. 41-6.
86. Sessions, A. and A.F. Horwitz, *Myoblast aminophospholipid asymmetry differs from that of fibroblasts*. FEBS Lett, 1981. **134**(1): p. 75-8.
87. Rote, N.S., A.K. Ng, D.A. Dostal-Johnson, S.L. Nicholson, and R. Siekman, *Immunologic detection of phosphatidylserine externalization during thrombin-induced platelet activation*. Clin Immunol Immunopathol, 1993. **66**(3): p. 193-200.
88. Demo, S.D., E. Masuda, A.B. Rossi, B.T. Thronset, A.L. Gerard, E.H. Chan, R.J. Armstrong, B.P. Fox, J.B. Lorens, D.G. Payan, R.H. Scheller, and J.M. Fisher, *Quantitative measurement of mast cell degranulation using a novel flow cytometric annexin-V binding assay*. Cytometry, 1999. **36**(4): p. 340-8.
89. Ran, S., A. Downes, and P.E. Thorpe, *Increased exposure of anionic phospholipids on the surface of tumor blood vessels*. Cancer Res, 2002. **62**(21): p. 6132-40.
90. Ran, S. and P.E. Thorpe, *Phosphatidylserine is a marker of tumor vasculature and a potential target for cancer imaging and therapy*. Int J Radiat Oncol Biol Phys, 2002. **54**(5): p. 1479-84.
91. Huber, R., J. Romisch, and E.P. Paques, *The crystal and molecular structure of human annexin V, an anticoagulant protein that binds to calcium and membranes*. Embo J, 1990. **9**(12): p. 3867-74.
92. Argos, P., *An investigation of oligopeptides linking domains in protein tertiary structures and possible candidates for general gene fusion*. J Mol Biol, 1990. **211**(4): p. 943-58.

93. Peron, K., T.N. Jones, S.A. Gauthier, T.N. Nguyen, X.P. Zang, M. Barriere, D. Preveraud, C.E. Soliman, R.G. Harrison, and J.T. Pento, *Targeting of a novel fusion protein containing methioninase to the urokinase receptor to inhibit breast cancer cell migration and proliferation*. *Cancer Chemother Pharmacol*, 2003. **52**(4): p. 270-6.
94. Stephens, R.W., A.M. Bokman, H.T. Myohanen, T. Reisberg, H. Tapiovaara, N. Pedersen, J. Grondahl-Hansen, M. Llinas, and A. Vaheiri, *Heparin binding to the urokinase kringle domain*. *Biochemistry*, 1992. **31**(33): p. 7572-9.
95. Zang, X.P., N.R. Palwai, M.R. Lerner, D.J. Brackett, J.T. Pento, and R.G. Harrison, *Targeting a methioninase-containing fusion protein to breast cancer urokinase receptors inhibits growth and migration*. *Anticancer Res*, 2006. **26**(3A): p. 1745-51.
96. Naveen R. Palwai, Xiao-Ping Zang, R.G. Harrison, and J.T. Pento, *Influence of L-methioninase targeted to the urokinase receptor on the proliferation and motility of lung and prostate cancer cells*. *Anticancer Res*, 2007. **27**(5).
97. Zang, X.-P., N. Palwai, P. , J. T.,, and R.G. and Harrison, *Internalizing versus and non-internalizing receptor for targeting L-methioninase to cancer cells*. . *American Journal of Pharmacology and Toxicology*, 2006. **1**(3): p. 60-64.
98. Esaki, N. and K. Soda, *L-methionine gamma-lyase from Pseudomonas putida and Aeromonas*. *Methods Enzymol*, 1987. **143**: p. 459-65.
99. Van Den Berg, L., *The effect of addition of sodium and potassium chloride to the reciprocal system: KH₂PO₄-Na₂HPO₄-H₂O on pH and composition during freezing*. *Arch Biochem Biophys*, 1959. **84**: p. 305-15.
100. Van Den Berg, L. and D. Rose, *Effect of freezing on the pH and composition of sodium and potassium phosphate solutions; the reciprocal system KH₂PO₄-Na₂-HPO₄-H₂O*. *Arch Biochem Biophys*, 1959. **81**(2): p. 319-29.
101. Randolph, T.W., *Phase separation of excipients during lyophilization: effects on protein stability*. *J Pharm Sci*, 1997. **86**(11): p. 1198-203.
102. Andrade, J.D.H., Vladimir; Feng, L.; Tingey, K. , *Proteins at interfaces: Principles, problems, and potential*. *Bioprocess Technology* 1996. **23**: p. 19-55.
103. Wei, Y., M. Lukashev, D.I. Simon, S.C. Bodary, S. Rosenberg, M.V. Doyle, and H.A. Chapman, *Regulation of integrin function by the urokinase receptor*. *Science*, 1996. **273**(5281): p. 1551-5.
104. van der Pluijm, G., B. Sijmons, H. Vloedgraven, C. van der Bent, J.W. Drijfhout, J. Verheijen, P. Quax, M. Karperien, S. Papapoulos, and C. Lowik, *Urokinase-receptor/integrin complexes are functionally involved in adhesion and progression of human breast cancer in vivo*. *Am J Pathol*, 2001. **159**(3): p. 971-82.

105. Zou, Z., A. Anisowicz, M.J. Hendrix, A. Thor, M. Neveu, S. Sheng, K. Rafidi, E. Seftor, and R. Sager, *Maspin, a serpin with tumor-suppressing activity in human mammary epithelial cells*. Science, 1994. **263**(5146): p. 526-9.
106. Burgle, M., M. Koppitz, C. Riemer, H. Kessler, B. Konig, U.H. Weidle, J. Kellermann, F. Lottspeich, H. Graeff, M. Schmitt, L. Goretzki, U. Reuning, O. Wilhelm, and V. Magdolen, *Inhibition of the interaction of urokinase-type plasminogen activator (uPA) with its receptor (uPAR) by synthetic peptides*. Biol Chem, 1997. **378**(3-4): p. 231-7.
107. Goodson, R.J., M.V. Doyle, S.E. Kaufman, and S. Rosenberg, *High-affinity urokinase receptor antagonists identified with bacteriophage peptide display*. Proc Natl Acad Sci U S A, 1994. **91**(15): p. 7129-33.
108. Ignar, D.M., J.L. Andrews, S.M. Witherspoon, J.D. Leray, W.C. Clay, K. Kilpatrick, J. Onori, T. Kost, and D.L. Emerson, *Inhibition of establishment of primary and micrometastatic tumors by a urokinase plasminogen activator receptor antagonist*. Clin Exp Metastasis, 1998. **16**(1): p. 9-20.
109. Rainov, N.G. and V. Heidecke, *Long term survival in a patient with recurrent malignant glioma treated with intratumoral infusion of an IL4-targeted toxin (NBI-3001)*. J Neurooncol, 2004. **66**(1-2): p. 197-201.
110. Azemar, M., S. Djahansouzi, E. Jager, C. Solbach, M. Schmidt, A.B. Maurer, K. Mross, C. Unger, G. von Minckwitz, P. Dall, B. Groner, and W.S. Wels, *Regression of cutaneous tumor lesions in patients intratumorally injected with a recombinant single-chain antibody-toxin targeted to ErbB2/HER2*. Breast Cancer Res Treat, 2003. **82**(3): p. 155-64.

APPENDIX A

Primers for PCR of Carrier and Target Genes

The general design and use of these primers is described in the Methods section. The particular enzyme sequence (or other relevant sequence) within each primer is also indicated.

1) Primers for L-methioninase with BamHI site at 5' end

Meth 5' Primer

5' – CgC / ggA / TCC / CgC / gAC / TCC / CAT / AAC / AAC / ACC – 3'

Meth 3' Primer

5' – gAg / gAg / AAg / CCC / ggT / TAT / CAT / gCA / CAC / gCC / TCC / AAT / gCC / AAC / TCg – 3'

2) Primers for TGF with 5' LIC end

TGF 5' Primer

5' – gAC / gAC / gAC / AAg / ATg / ggA / gTg / gTg / TCC / CAT / TTT / AAT / gAC / TgC / CC – 3'

TGF 3' Primer

5' – gC / ggA / TCC / AgA / ACC / gCT / gCC / AgC / CAg / gAg gTC / CgC / ATg / CTC / ACA / gCg – 3'

TGF 3C 5' Primer

5' – gAC / gAC / gAC / AAg / ATg / CTT / gAA / gTC / CTC / TTT / CAg / ggA / gTg / gTg / TCC / CAT / TTT / AAT / gAC / TgC / CC – 3'

3) Primers to mutate ATF-methioninase

mutMeth 5' Primer

5' – gCg / CAC / CTT / gTT / Tgg / CTg / CAC / CTT / Tg – 3'

mutMeth 3' Primer

5' – CAA / Agg / TgC / AgC / CAA / ACA / Agg / TgC / gC – 3'

4) 5' Primer for urokinase

Uro 5' Primer

5' – gAC / gAC / gAC / AAg / ATg / AgC / AAT / gAA / CTT / CAT / CAA / gTT / CC – 3'

5) 5' Primer for urokinase with 3C site

Uro 3C 5' Primer

5' - gAC / gAC / gAC / AAg / ATg / CTT / gAA / gTC / CTC / TTT / CAg / ggA / CCC / AgC / AAT / gAA / CTT / CAT / CAA / gTT / CC - 3'

Meth 3C 5' Primer

5' - gAC / gAC / gAC / AAg / ATg / CTT / gAA / gTC / CTC / TTT / CAg / ggA / CCC / CgC / gAC / TCC / CAT / AAC / AAC / ACC - 3'

Methhexalysine 3' Primer

5' - gAg / gAg / AAg / CCC / ggT / TAT / TTC / TTT / TTC / TTC / TTT / TTT / CCA / gAA / CCg / CTg / CCT / gCA / CAC / gCC / TCC / AAT / gCC / AAC / TCg - 3'

AnnexinMeth 5' Primer

5' - Cg / ATT / CgC / ggA / TCC / gCA / CAg / gTT / CTC / AgA / ggC - 3'

Annexin 3' Primer

5' - gAg / gAg / AAg / CCC / ggT / TAg / TCA / TCT / TCT / CCA / CAg / AgC - 3'

Methxin 3' Primer

5' - gC / CgC / ATT / ggA / TCC / AgA / ACC / gCT / gCC / TgC / ACA / CgC / CTC / CAA / TgC / CAA / CTC / g - 3'

Annexin 5' Primer

5' - gAC / gAC / gAC / AAg / ATg / CTT / gAA / gTC / CTC / TTT / CAg / gCA / CAg / gTT / CTC / AgA / ggC - 3'

Sequencing Results for the ATF/Methioninase Fusion Gene.

ATF ->

agcaatgaacttcatcaagttccatcgaactgtgactgtctaaatggaggaacatgtgtg
S N E L H Q V P S N C D C L N G G T C V
tccaacaagtacttctccaacattcactggtgcaactgcccaaagaaattcggagggcag
S N K Y F S N I H W C N C P K K F G G Q

BamHI Methioninase ->

cactgtgaaatagataagtcaaaaacc**ggcagcgggttctggatccc**gcgactcccataac
H C E I D K S K T **G S G S G S** R D S H N
aacaccgggtttttccacacggggccattcaccacgggtacgacccgctttcccacgggtggt
N T G F S T R A I H H G Y D P L S H G G
gccttgggtgccaccgggtgtaccagaccgacatgccttcccgactgtcgaatacggc
A L V P P V Y Q T A T Y A F P T V E Y G
gctgctgtgcttcgcccgggaggaggcggggcacttctacagccgcatctccaaccccacc
A A C F A G E E A G H F Y S R I S N P T
ctggccttgctcgcagcaacgcacatggcctcgttggaggggtgagggcgggattggcgctg
L A L L E Q R M A S L E G G E A G L A L
gcgtcggggatgggagccattacttcgaccctctggaccctgctgcggcctgggtgatgag
A S G M G A I T S T L W T L L R P G D E
ctgatcgtggggcgacacttgtatggctgcacctttgcttccctgcacatggcattggc
L I V G R T L Y G C T F A F L H H G I G
gagttcggggtaagatccaccatgtcgcacttaacgatgccaaggccctgaaagcggcg
E F G V K I H H V D L N D A K A L A G C
atcaacagcaaaacgcggatgatcacttcgaaacaccggccaacccaacatgcaactg
I N S K T R M I Y F E T P A N P N M Q L
gtggatatagcggcgggtcgtcgcagggcagtcgccccgggagtgatgtgcttgggtgggtcgac
V D I A A V V E A V R G S D V L V V V D
aacacctactgcacgccctacctgcagcggccactggaactggggggcagacctgggtgggtg
N T Y C T P Y L Q R P L E L G A D L V V
cattcggcaaccaagtacctcagtgccatggcgacatcactgcgggcctgggtgggtgggg
H S A T K Y L S G H G D I T A G L V V G
cgcaaggccttgggtcgcaccgattcggctggaagggtgaaagacatgaccggggcagcc
R K A L V D R I R L E G L K D M T G A A
ttgtcaccgcatgacgctgcgttgttgatgcgcggcatcaagaccctggcgctgcgcatg
L S P H D A A L L M R G I K T L A L R M
gaccggcattgcgccaacgccctggaggtcgcgcagttcctggccggggcagccccagggtg
D R H C A N A L E V A Q F L A G Q P Q V
gagctgatccactacccgggcttgccttgccttggccagtacgaactggcacagcggcag
E L I H Y P G L P S F A Q Y E L A Q R Q
atgcgtttgcccgggcgggatgattgcctttgagctcaaggcgggtatcgaggccggggcg
M R L P G G M I A F E L K G G I E A G R
ggcttcatgaatgccctgcagctttttgcccgtgcggtgagcctgggggatgccgagtcg
G F M N A L Q L F A R A V S L G D A E S
ctggcacagcaccggcgagcatgacgcaactccagttacacgccacaagagcggggcgcat
L A Q H P A S M T H S S Y T P Q E R A H
cacgggatatcagaggggctgggtgaggttgcagtggggctggaggatgtggaggacctg
H G I S E G L V R L S V G L E D V E D L
ctggcagatcagagttggcgttggaggcgtgtgcatga
L A D I E L A L E A C A -

GenBank sequences used for comparison

ATF: NM_002658

Methioninase: PSEMEGL

Sequencing Results for the TGF/Methioninase Fusion Gene.

TGF →

ggagtggtgtcccattttaatgactgccagattcccacactcagttctgcttccatgga
G V V S H F N D C P D S H T Q F C F H G
acatgcagggttttgggtgcaggaggacaagccggcatgtgtctgccattctgggtacgtt
T C R F L V Q E D K P A C V C H S G Y V

Methioninase →

ggtgcgcgctgtgagcatgcccggacctcctggctggcagcggttctggatcccgcgactcc
G A R C E H A D L L A G S G S G S R D S
cataacaacaccgggttttccacacgggccattcaccacggctacgaccgccttcccac
H N N T G F S T R A I H H G Y D P L S H
ggtgggtgccttgggtgccaccgggtgtaccagaccgcgacctatgccttcccgactgtcgaa
G G A L V P P V Y Q T A T Y A F P T V E
tacggcgctgcgtgcttcgccggggaggaggcggggcacttctacagccgcatctccaac
Y G A A C F A G E E A G H F Y S R I S N
cccaccctggccttgcctcgagcaacgcagatggcctcgttggagggtggtgaggcgggattg
P T L A L L E Q R M A S L E G G E A G L
gcgctggcgctcggggatgggagccattacttgcaccctctggaccctgctgcccctgggt
A L A S G M G A I T S T L W T L L R P G
gatgagctgatcgtggggcgacaccttgatggctgcacctttgcgttccctgcacatggc
D E L I V G R T L Y G C T F A F L H H G
attggcgagttcgggggtcaagatccacatgtcgaccttaacgatgccaaggccctgaaa
I G E F G V K I H H V D L N D A K A L K
gcgccgatcaacagcaaaacgcggatgatctacttgcgaaacaccggccaaccccaacatg
A A I N S K T R M I Y F E T P A N P N M
caactggtggatagcggcggtcgtcgaggcagtgccggggaggatgatgtgcttgtgggtg
Q L V D I A A V V E A V R G S D V L V V
gtcgacaacacctactgcacgccctacctgcagcggccactggaactggggggcagacctg
V D N T Y C T P Y L Q R P L E L G A D L
gtgggtgcattcggcaaccaagtacctcagtgggccatggcgcacatcactgcccgcctgggtg
V V H S A T K Y L S G H G D I T A G L V
gtggggcgcaaggcttttggctgaccgcattcggctggaagggtgaaagacatgaccggg
V G R K A L V D R I R L E G L K D M T G
gcagccttgtcaccgcatgacgctgcgttgttgatgcgcggcatcaagacctggcgctg
A A L S P H D A A L L M R G I K T L A L
cgcatggaccggcattgcgccaacgcacctggagggtcgcgcagttcctggccggggcagccc
R M D R H C A N A L E V A Q F L A G Q P
caggtggagctgatccactaccgggcttgcgctcgtttgccagtacgaactggcacag
Q V E L I H Y P G L P S F A Q Y E L A Q
cggcagatgcgttttgcggggcgggatgattgcctttgagctcaagggcgggtatcgaggcc
R Q M R L P G G M I A F E L K G G I E A
gggcgcggttcatgaatgccctgcagctttttgcccgctgcgggtgagcctgggggatgcc
G R G F M N A L Q L F A R A V S L G D A
gagtcgctggcacagcaccggcgagcagcagcactccagttacacgccacaagagcgg
E S L A Q H P A S M T H S S Y T P Q E R
gcgcatcacgggatatcagaggggctgggtgaggttgtcagtggggctggaggatgtggag
A H H G I S E G L V R L S V G L E D V E
gacctgctggcagatatacagattggcgttggaggcgtgtgca
D L L A D I E L A L E A C A

GenBank sequences used for comparison

Methioninase: PSEMEGL

Sequencing Results for the Methioninase Gene.

Methioninase ->

```
cgcgactcccataacaacaccgggtttttccacacggggccattcaccacgggctacgaccgg
R D S H N N T G F S T R A I H H G Y D P
ctttccacgggtgggtgccttgggtgccaccgggtgtaccagaccgacgacctatgccttcccg
L S H G G A L V P P V Y Q T A T Y A F P
actgtcgaatacggcgctgctgcttgcggggaggaggcggggcacttctacagccgc
T V E Y G A A C F A G E E A G H F Y S R
atctccaacccccaccctggccttgcctcgagcaacgcacatggcctcgttggagggtggtag
I S N P T L A L L E Q R M A S L E G G E
gcgggattggcgctggcgctggggatgggagccattacttcgaccctctggaccctgctg
A G L A L A S G M G A I T S T L W T L L
cggcctgggtgatgagctgatcggtggggcgaccttgcctgacacctttgcgttccctg
R P G D E L I V G R T L Y G C T F A F L
caccatggcattggcgagttcggggcaagatccacatgctcgaccttaacgatgccaag
H H G I G E F G V K I H H V D L N D A K
gcctgaaagcggcgatcaacagcaaaacgcgggatgatctacttcgaaacaccggccaac
A L K A A I N S K T R M I Y F E T P A N
cccaacatgcaactgggtggatagcggcggtcgtcgaggcagtgcgggggagtgatgtg
P N M Q L V D I A A V V E A V R G S D V
cttgtgggtggcgacaacacctactgcacgcctacctgcagcggccactggaactgggg
L V V V D N T Y C T P Y L Q R P L E L G
gcagacctgggtgcatcggcaaccaagtacctcagtgccatggcgacatcactgcg
A D L V V H S A T K Y L S G H G D I T A
ggcctgggtggggcgcaaggccttgggtgcaccgcattcggctggaagggtgaaagac
G L V V G R K A L V D R I R L E G L K D
atgaccggggcagccttgtcaccgcatgacgctgctggttggatgctggcgatcaagacc
M T G A A L S P H D A A L L M R G I K T
ctggcgctgctgcatggaccggcattgcgccaacgcctggagggtcgcgcagttcctggcc
L A L R M D R H C A N A L E V A Q F L A
gggcagccccagggtggagctgatccactaccgggcttgcctgctgttggccagtacgaa
G Q P Q V E L I H Y P G L P S F A Q Y E
ctggcacagcggcgagatgctgttgcggggcgggatgattgcctttgagctcaagggcggt
L A Q R Q M R L P G G M I A F E L K G G
atcgaggccgggcgcggttcatgaatgccttgcagctttttgcccgtgcggtgagcctg
I E A G R G F M N A L Q L F A R A V S L
ggggatgccgagtcgctggcacagcaccggcgagcatgacgcactccagttacagcca
G D A E S L A Q H P A S M T H S S Y T P
caagagcggggcgcatcacgggatatcagaggggctgggtgaggttgtcagtggggctggag
Q E R A H H G I S E G L V R L S V G L E
gatgtggaggacctgctggcagatatcgagttggcggtggaggcggtgcatga
D V E D L L A D I E L A L E A C A -
```

GenBank sequences used for comparison

Methioninase: PSEMEGL

Sequencing Results for the Methioninase-annexin V Fusion Gene.

Methioninase ->

cgcgactcccataacaacaccgggtttttccacacggggccattcaccacggctacgaccgg
R D S H N N T G F S T R A I H H G Y D P
ctttccacgggtgggtgccttgggtgccaccgggtgtaccagaccgacacctatgccttccccg
L S H G G A L V P P V Y Q T A T Y A F P
actgtcgaatacggcgctgctgcttccgcccgggaggaggcggggcacttctacagccgc
T V E Y G A A C F A G E E A G H F Y S R
atctccaacccccaccctggccttgcctgagcaacgcacatggcctcgttggagggtggtag
I S N P T L A L L E Q R M A S L E G G E
gccccgattggcgctggcgctggggatgggagccattacttccgaccctctggaccctgctg
A G L A L A S G M G A I T S T L W T L L
cggcctgggtgatgagctgatcgtggggcgcaccttggatggctgcacctttgcttccctg
R P G D E L I V G R T L Y G C T F A F L
caccatggcattggcgagttcggggcaagatccaccatgtcgcacctaacgatgccaag
H H G I G E F G V K I H H V D L N D A K
gcccgtgaaagcggcgatcaacagcaaaacgcggatgatctacttccgaaacaccggccaac
A L K A A I N S K T R M I Y F E T P A N
cccaacatgcaactgggtggatagcggcggtcgtcgcaggcagtgccgggggagtgatgtg
P N M Q L V D I A A V V E A V R G S D V
cttgggtgggtcgacaacacctactgcacgccctacctgcagcggccactggaactgggg
L V V V D N T Y C T P Y L Q R P L E L G
gcagactgggtgggtgcattcgggaaccaagtacctcagtgggccatggcgacatcactgcg
A D L V V V H S A A T K Y L S G H G D I T A
ggcctgggtgggtggggcgcaaggccttgggtcgcaccgcattcggctggaagggtgaaagac
G L V V G R K A L V D R I R L E G L K D
atgaccggggcagccttgtcaccgcacatgacgctgctgcttggatgcgcggcatcaagacc
M T G A A L S P H D A A L L M R G I K T
ctggcgctgcgcatggaccggcatttgcgccaacgccctggagggtcgcgcagttcctggcc
L A L R M D R H C A N A L E V A Q F L A
gggcagccccagggtggagctgatccactaccgggcttggcctgcttggccagtacgaa
G Q P Q V E L I H Y P G L P S F A Q Y E
ctggcacagcggcagatgctgcttggccggggcgggatgattgccttggagctcaagggcggt
L A Q R Q M R L P G G M I A F E L K G G
atcgaggccggggcgggcttcatgaatgccctgcagctttttgcccgtgcggtgagcctg
I E A G R G F M N A L Q L F A R A V S L
ggggatgcccagtgctgctggcacagcaccggcgagcatgacgcactccagttacagcca
G D A E S L A Q H P A S M T H S S Y T P
caagagcggggcgcacacgggatatcagaggggctgggtgaggttgtcagtggggctggag
Q E R A H H G I S E G L V R L S V G L E
gatgtggaggacctgctggcagatatcgagttggcgttggaggcgtgtgcaggcagcgggt
D V E D L L A D I E L A L E A C A G S G

Annexin->

tctggatccgcacaggttctcagaggcactgtgactgactgccctggatttggatgagcgg
S G S A Q V L R G T V T D C P G F D E R
gctgatgcagaaactcttcggaaggctatgaaaggccttggggcacagatgaggagagcatc
A D A E T L R K A M K G L G T D E E S I
ctgactctgttgacatcccgaagtaatgctcagcggccaggaaatctctgcagcttttaag
L T L L T S R S N A Q R Q E I S A A F K
actctgtttggcagggatcttctggatgacctgaaatcagaactaactggaaaatttgaa
T L F G R D L L D D L K S E L T G K F E

...CONTD

aaattaattgtggctctgatgaaaccctctcggctttatgatgcttatgaaactgaaacat
K L I V A L M K P S R L Y D A Y E L K H
gccttgaagggagctggaacaaatgaaaaagtactgacagaaattattgcttcaaggaca
A L K G A G T N E K V L T E I I A S R T
cctgaagaactgagagccatcaaacaagtttatgaagaagaatattggctcaagcctggaa
P E E L R A I K Q V Y E E E Y G S S L E
gatgacgtgggtgggggacacttcagggtactaccagecggatggttgggtggttctccttcan
D D V V G D T S G Y Y Q R M L V V L L X
gctaacagagaccctgatgctggaatcgatgaagctcnagttgaacaagatgctcangct
A N R D P D A G I D E A X V E Q D A X A
ttatttcaggctggagaacttaaattgggggacagatgaagaaaagtttatcaccatcttt
L F Q A G E L K W G T D E E K F I T I F
ggaacacgaagtgtgtctcatttgagaaaggtgtttgacaagtacatgactatatcagga
G T R S V S H L R K V F D K Y M T I S G
tttcaaattgaggaaaccattgaccgagacttctggcaatttagagcaaatatcagga
F Q I E E T I D R E T S G N L E Q I S G
tttcaaattgaggaaaccattgaccgagacttctggcaatttagagcaatattatgct
F Q I E E T I D R E T S G N L E Q Y Y A
atgaagggagctgggacagatgatcataccctcatcagagtcatggtttccaggagtgag
M K G A G T D D H T L I R V M V S R S E
attgatctgtttaacatcaggaaggagtttaggaagaattttgccacctctctttattcc
I D L F N I R K E F R K N F A T S L Y S
atgattaagggagatacatctggggactataagaaagctcttctgctgctctgtggagaa
M I K G D T S G D Y K K A L L L L C G E
gatgac
D D

GenBank sequences used for comparison

Methioninase: PSEMEGL

APPENDIX B

QIAquick PCR Purification Kit Protocol

Fragments ranging from 100 bp to 10 kb are purified from primers, nucleotides, polymerases, and salts using QIAquick spin columns in a microcentrifuge.

Notes:

- Add ethanol (96–100%) to Buffer PE before use (see bottle label for volume).
 - All centrifuge steps are at 13,000 rpm (~17,900 x *g*) in a conventional tabletop microcentrifuge.
1. Add 5 volumes of Buffer PB to 1 volume of the PCR sample and mix. It is not necessary to remove mineral oil or kerosene. For example, add 500 µl of Buffer PB to 100 µl PCR sample (not including oil).
 2. Place a QIAquick spin column in a provided 2 ml collection tube.
 3. To bind DNA, apply the sample to the QIAquick column and centrifuge for 30–60 s.
 4. Discard flow-through. Place the QIAquick column back into the same tube. Collection tubes are re-used to reduce plastic waste.
 5. To wash, add 0.75 ml Buffer PE to the QIAquick column and centrifuge for 30–60 s.
 6. Discard flow-through and place the QIAquick column back in the same tube. Centrifuge the column for an additional 1 min.

IMPORTANT: Residual ethanol from Buffer PE will not be completely removed unless the flow-through is discarded before this additional centrifugation.

7. Place QIAquick column in a clean 1.5 ml microcentrifuge tube.
8. To elute DNA, add 50 μ l Buffer EB (10 mM Tris·Cl, pH 8.5) or H₂O to the center of the QIAquick membrane and centrifuge the column for 1 min.

QIAquick Gel Extraction Kit Protocol

This protocol is designed to extract and purify DNA of 70 bp to 10 kb from standard or low-melt agarose gels in TAE or TBE buffer. Up to 400 mg agarose can be processed per spin column. For DNA cleanup from enzymatic reactions using this protocol, add 3 volumes of BufferQG and 1 volume of isopropanol to the reaction, mix, and proceed with step 6 of the protocol.

- The yellow color of Buffer QG indicates a pH ≤ 7.5 .
 - Add ethanol (96–100%) to Buffer PE before use (see bottle label for volume).
 - Isopropanol (100%) and a heating block or water bath at 50°C are required.
 - All centrifugation steps are carried out at 13,000 rpm ($\sim 17,900 \times g$) in a conventional table-top microcentrifuge.
 - 3 M sodium acetate, pH 5.0, may be necessary.
1. Excise the DNA fragment from the agarose gel with a clean, sharp scalpel. Minimize the size of the gel slice by removing extra agarose.
 2. Weigh the gel slice in a colorless tube. Add 3 volumes of Buffer QG to 1 volume of gel (100 mg \sim 100 μ l). For example, add 300 μ l of Buffer QG to each 100 mg of gel. For $>2\%$ agarose gels, add 6 volumes of Buffer QG. The maximum amount of gel slice per QIAquick column is 400 mg; for gel slices >400 mg use more than one QIAquick column.

3. Incubate at 50°C for 10 min (or until the gel slice has completely dissolved). To help dissolve gel, mix by vortexing the tube every 2–3 min during the incubation.
IMPORTANT: Solubilize agarose completely. For >2% gels, increase incubation time.
4. After the gel slice has dissolved completely, check that the color of the mixture is yellow (similar to Buffer QG without dissolved agarose). If the color of the mixture is orange or violet, add 10 µl of 3 M sodium acetate, pH 5.0, and mix. The color of the mixture will turn to yellow. The adsorption of DNA to the QIAquick membrane is efficient only at pH ≤7.5. Buffer QG contains a pH indicator which is yellow at pH ≤7.5 and orange or violet at higher pH, allowing easy determination of the optimal pH for DNA binding.
5. Add 1 gel volume of isopropanol to the sample and mix. For example, if the agarose gel slice is 100 mg, add 100 µl isopropanol. This step increases the yield of DNA fragments <500 bp and >4 kb. For DNA fragments between 500 bp and 4 kb, addition of isopropanol has no effect on yield. Do not centrifuge the sample at this stage.
5. Place a QIAquick spin column in a provided 2 ml collection tube.
To bind DNA, apply the sample to the QIAquick column, and centrifuge for 1 min. The maximum volume of the column reservoir is 800 µl. For sample volumes of more than 800 µl, simply load and spin again.
6. Discard flow-through and place QIAquick column back in the same collection tube. Collection tubes are re-used to reduce plastic waste.
7. (Optional): Add 0.5 ml of Buffer QG to QIAquick column and centrifuge for 1 min. This step will remove all traces of agarose. It is only required when the DNA

will subsequently be used for direct sequencing, in vitro transcription or microinjection.

8. To wash, add 0.75 ml of Buffer PE to QIAquick column and centrifuge for 1 min.

Note: If the DNA will be used for salt sensitive applications, such as blunt-end ligation and direct sequencing, let the column stand 2–5 min after addition of Buffer PE, before centrifuging.

9. Discard the flow-through and centrifuge the QIAquick column for an additional 1 min at 13,000 rpm (~17,900 x g).

IMPORTANT: Residual ethanol from Buffer PE will not be completely removed unless the flow-through is discarded before this additional centrifugation.

10. Place QIAquick column into a clean 1.5 ml microcentrifuge tube.

11. To elute DNA, add 50 µl of Buffer EB (10 mM Tris·Cl, pH 8.5) or H₂O to the center of the QIAquick membrane and centrifuge the column for 1 min.

Agarose Gel Electrophoresis

The following protocol is for making a 1% (w/v) agarose gel using SeaKem[®] LE agarose (Cambrex) using a BRL Life Technologies Horizon 58 electrophoretic cell with a total gel volume of 35 ml.

1. Assemble the electrophoretic cell.
2. Weigh out 0.35 g of agarose in a beaker. Add 35 ml of 1X TAE buffer (40 mM Tris-acetate, 1 mM EDTA). Microwave on high for 90 sec. Let the solution cool to 55°C and add 35 µl of 0.5 mg/ml ethidium bromide stock (mix the solution

well to evenly distribute the ethidium bromide). Pour the gel into the cell and wait 20-30 min for solidification.

3. Add 5 ml of 50X TAE buffer and 250 μ l of 0.5 mg/ml ethidium bromide to 245 ml of dH₂O. Once the gel has solidified pour the TAE/EtBr solution over the gel until it covers the gel by about 1mm. The gel is now ready to be loaded.
4. To each DNA sample to be loaded, add 5 μ l of gel loading buffer (GLB). The composition of GLB is 0.25% (w/v) bromophenol blue and 30% (v/v) glycerol in water. The maximum volume of DNA sample is 20 μ l for each well of the 8 comb gel which has a total volume of 25 μ l.
5. For the marker lane add 2 μ l of 1 kb ladder to 3 μ l water and 1 μ l GLB mixture.

Site Directed Mutagenesis by Stratagene

This is the protocol followed to create the mutation on ATF-methioninase gene.

1. Mutant Strand Synthesis Reaction (Thermal Cycling)

Prepare the control reaction as indicated below:

Volume	Component
5 μ l	10 \times reaction buffer
2 μ l (10 ng)	pWhitescript 4.5-kb control plasmid (5 ng/ μ l)
1.25 μ l (125 ng)	Oligonucleotide control primer #1
1.25 μ l (125 ng)	Oligonucleotide control primer #2
1 μ l	dNTP mix
39.5 μ l	Double-distilled water (ddH ₂ O)
1 μ l	PfuTurbo DNA polymerase (2.5 U/ μ l)

Prepare the sample reaction(s) as indicated below:

Volume	Component
5 μ l	10 \times reaction buffer
X μ l (5–50 ng)	dsDNA template
X μ l (125 ng)	Oligonucleotide control primer #1
X μ l (125 ng)	Oligonucleotide control primer #2
1 μ l	dNTP mix
Y μ l	Double-distilled water (ddH ₂ O)
1 μ l	PfuTurbo DNA polymerase (2.5 U/ μ l)

Cycling Parameters

Segment	Cycles	Temperature	Time
1	1	95 °C	30 s
2	12	95 °C	30 s
		55 °C	1 min
		68 °C	7 min
3	∞	4 °C	∞ min

2. Dpn I enzyme digestion

- Add 1 μ l of the Dpn I restriction enzyme (10 U/ μ l) directly to each amplification reaction below the mineral oil overlay using a small, pointed pipet tip.
- Gently and thoroughly mix each reaction mixture by pipetting the solution up and down several times. Spin down the reaction mixtures in a microcentrifuge for 1 min and immediately incubate each reaction at 37°C for 1 h to digest the parental (i.e., the nonmutated) supercoiled dsDNA.

Transformation of XL1-Blue Supercompetent Cells

- Gently thaw the XL1-Blue supercompetent cells on ice. For each control and sample reaction to be transformed, aliquot 50 µl of the supercompetent cells to a prechilled 14-ml BD Falcon polypropylene round-bottom tube.
- Transfer 1 µl of the Dpn I-treated DNA from each control and sample reaction to separate aliquots of the supercompetent cells.
- Heat pulse the transformation reactions for 45 seconds at 42°C and then place the reactions on ice for 2 min.
- Add 0.5 ml of NZY+ broth preheated to 42°C and incubate the transformation reactions at 37°C for 1 h with shaking at 225–250 rpm.
- Plate the appropriate volume of each transformation reaction, on agar plates containing the appropriate antibiotic for the plasmid vector.
- Incubate the transformation plates at 37°C for >16 h.

Transformation protocol (For NovaBlue and BL21 (DE3) cells)

1. Thaw the required number of tubes of cells on ice and mix gently to ensure that the cells are evenly suspended.
2. Place the required number of 1.5-ml polypropylene microcentrifuge tubes on ice to pre-chill. Pipet 20 µl aliquots of cells into the pre-chilled tubes.
3. Add 1 µl of the DNA solution directly to the cells. Stir gently to mix.
4. Place the tubes on ice for 5 min.
5. Heat the tubes for exactly 30 s in a 42°C water bath; do not shake.
6. Place on ice for 2 min.
7. Add 80 µl of room temperature SOC Medium to each tube.

8. Incubate at 37°C while shaking at 250 rpm for 60 min prior to plating on selective medium.

Ligation Independent Cloning (LIC) Protocol

PCR of gene

1. Amplify the desired insert sequence using appropriately designed PCR primers.
2. The PCR product must be purified to completely remove the dNTPs, to inactivate the enzyme used for PCR, and to remove interfering DNA. This is done by using the Qiagen PCR purification protocol.

T4 DNA Polymerase treatment of target insert

1. Assemble the following components in a sterile 1.5-ml microcentrifuge tube kept on ice:

- x μ l 0.2 pmol purified PCR product.
- 2 μ l 10X T4 DNA polymerase buffer
- 2 μ l 25 mM dATP
- 1 μ l 100 mM DTT
- y μ l nuclease-free water (add to make 20 μ l total volume)
- 0.4 μ l 2.5 U/ μ l T4 DNA Polymerase (LIC-qualified; 0.5 unit per 0.1 pmol PCR product)
- 20 μ l total volume (Final concentration of insert is 0.01 pmol/ μ l.)

2. Start reaction by adding enzyme; stir with pipet tip to mix and incubate at 22°C for 30 min.
3. Inactivate enzyme by incubating at 75°C for 20 min.
4. This prepared insert can be annealed to any of the Ek/LIC vectors. Store prepared Ek/LIC insert.

Annealing the Vector and Ek/LIC Insert

1. For each insert, assemble the following components in a sterile 1.5-ml microcentrifuge tube:

- 1 μ l Ek/LIC vector
- 2 μ l T4 DNA polymerase treated Ek/LIC insert (0.02 pmol)

Incubate at 22°C for 5 min, then add:

- 1 μ l 25 mM EDTA

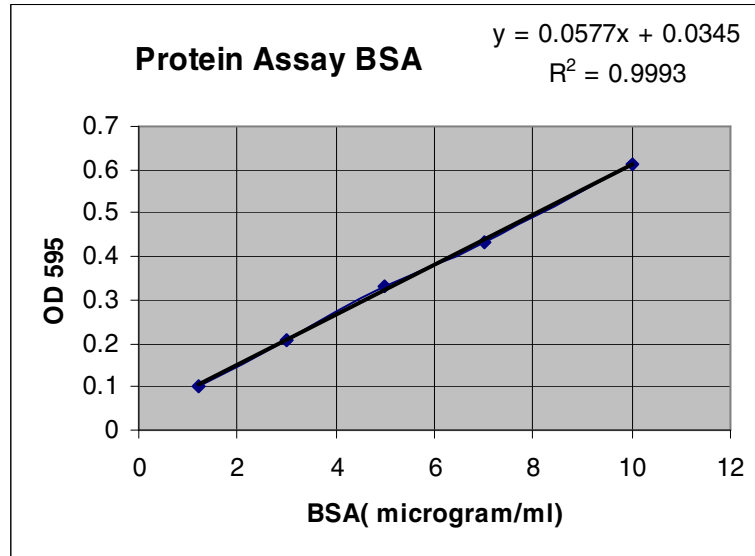
2. Mix by stirring with the pipet tip and incubate at 22°C for 5 min.
3. Transform the annealed product into NovaBlue Cells using the protocol described in Appendix B.

Bio-Rad's Protein Assay

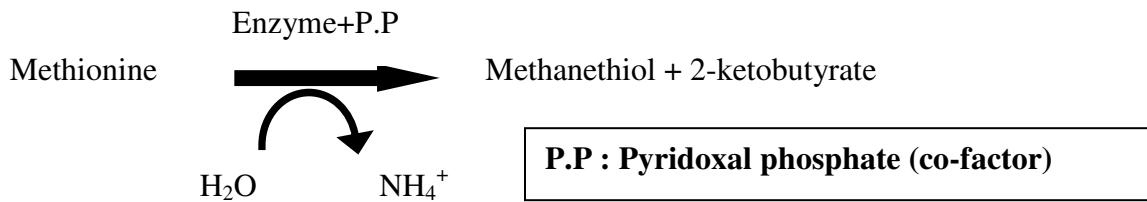
1. Mix
 - a. 5 to 200 μ l of enzyme sample
 - b. 200 μ l of concentrated Biorad reagent
 - c. x μ l of water to make a volume to 1 ml
2. Incubate at room temperature for 10 min.
3. Measure the absorbance at 595 nm.

4. Incubate at room temperature for 10 min.
5. Use the standard below to calculate the protein concentration.

Standard curve generated use bovine serum albumin (BSA)



Activity Assay (Methioninase Enzyme)



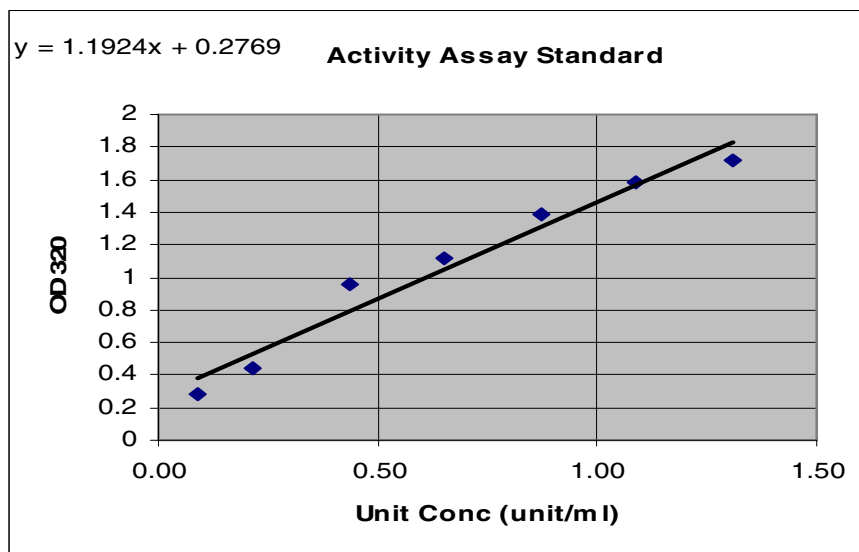
Mix:

- 100 μL of potassium phosphate buffer 0.5 M at ph 8
- 125 μL of L-methionine 0.1 M
- 50 μL of pyridoxal phosphate 0.1 mM
- 225 μL of enzyme sample (for the blank, replace by purification buffer)

1. Incubate the mixture at 37°C for 10 min.
2. Add 62.5 µL of 50 % (w/v) trichloroacetic acid to terminate the reaction.
3. Centrifuge at maximum speed for 2 min.
4. Mix :
 - 250 µL of the supernatant
 - 500 µL of sodium acetate buffer 1 M at pH 5
 - 200 µL of MTBH 0.1% (MTBH: 3-Methyl-2-benzo-thiazolinone hydrazone hydrochloride hydrate.)
5. Incubate at 50°C for 30 min.

Cool the solution at room temperature. Measure the absorbance at 320 nm against the blank. Use the standard below to calculate the methioninase unit concentration in the sample.

Standard curve is generated using α -Ketobutyrate and MTBH



Definition of unit: One unit of enzyme is defined as the amount that catalyzes the formation of 1 μmol of α -ketobutyrate per minute. Specific activity is expressed as units per milligram protein.

SDS-PAGE Analysis of Proteins

Components	Stacking gel 4%	Separating gel 12%
dH ₂ O	3.63 ml	3.34 ml
1.5 M Tris-HCL pH 8.8	-	2.5 ml
1 M Tris-HCL pH 6.8	625 μl	-
10 % (w/v) SDS	50 μl	100 μl
Acrylamide (29%) Bis (1%)	667 μl	4 ml
Ammonium persulfate 10%	25 μl	50 μl
TEMED	5 μl	10 μl
Total	5 ml	10 ml

1. Reagents required for the casting of mini-SDS-PAGE gels
2. Assemble the glass plates on the gel casting stand and fill with water to ensure that they are sealed.
3. Mix the components of separating gel, adding the TEMED last. Mix well and immediately fill the glass plates, leaving a 1.5 cm gap at the top (for the stacking gel).
4. Immediately add 1 ml of isopropanol on top of the gel to prevent oxygen from inhibiting the polymerization. Wait 20 min for solidification.
5. Pour off the isopropanol and rinse with dH₂O to remove any residual isopropanol. Mix the components for the 4% staking gel and pour on top of the separating gel. Insert the well-comb and wait 20 min for solidification.
6. Preheat a water bath to 100°C.

7. Prepare the SDS-PAGE loading buffer by diluting β -mercaptoethanol 20 X (1:20) with the SDS-blue buffer.
8. For a 4 ml culture with an approximate OD_{600} of 0.8, add 600 μ l of SLB to the cold, centrifuged pellet. Suspend pellet in the SLB by vortexing.
9. Immediately heat the sample to 100°C for 2 min.
10. Allow the samples to cool down for at least one min before loading the gel. Assemble the solidified gels in the buffer chamber. Fill the chamber with running buffer.
11. Load 10 μ l of each protein sample into the wells. Run the gel at a constant voltage of 165 V for about 1 hour, or until the dye reaches the bottom of the gel.
12. Cut off the stacking gel and discard it.
13. Stain the separating gel with a staining solution containing 45 % (w/v) dH₂O, 45% (w/v) methanol, 10 % (v/v) acetic acid, and 0.25 % (w/v) Coomassie Brilliant Blue R250. Stain for 1 hour with gentle shaking. If shaking is not possible, an overnight incubation will be sufficient.
14. Pour the stain back into its container (it can be re-used several times) and rinse the tray with water. To remove the extra stain on the gel, use a destain solution (same as the staining solution, but without the Coomassie Blue). Protein bands will be visible immediately on a light table.

Western Blot

1. Soak the PVDF membrane first in methanol. Thoroughly wet the membrane with water. Make the sandwich with sponge, 3 sheets of whatman, gel, PVDF membrane, whatman paper, sponge in order with BLACK down. gel on black side and membrane on clear side.

2. Face BLACK to BLACK and RED to RED and run the transfer for 2 h 30 min at 80 V (make sure it shows, approx. 1.5 amps for 2 transfers and 0.7-.75 amp for 1 gel)
3. Remove sandwich in order, note the protein side.
4. Use ponceau if needed, just about that the blots get properly rinsed.
5. Rinse off the ponceau, by washing it with 1XTBS, adding a single drop of NaOH.
6. Block in 5 % milk 1XTBS-t for 1 hr.
7. Wash 3 × with 1 × TBS-t;
8. 1st wash for 15 min.
9. 2nd wash and 3rd wash 5 min each, Rinse off thoroughly.
10. Add 1^o primary Ab,

Take proper care to avoid any bubbles between the blot and the inner side of the hybetube.

11. Remove 1^o Ab
12. Wash 3 × with 1 × TBS-t
13. 1st wash for 15 min.
14. 2nd wash and 3rd wash 5 min each, Rinse off thoroughly.
15. Add 2^o Ab,

Take proper care to avoid any bubbles between the blot and the inner side of the hybetube.

Protocol for Fusion Protein Injection in Nude Mice

1. Take the cart containing balance, dessicator container (with lid), gloves, isofuran, alcohol swabs, and forceps to animal room.

2. Turn on the light and blower of the hood and make sure that rooms are locked
3. Clean the surface of the hood with alcohol.
4. Take the balance and the green container into the hood.
5. Prepare the fusion protein sample injections into appropriate number of injections.
6. Keep the injections ready for use.
7. Take the green container onto the balance.
8. Take the cotton swabs and one drop of isofuran and drop the cotton swab into the green container.
9. Take the mouse and drop into the dessicator container then wait until it becomes unconscious. Measure the weight of the mouse.
10. Measure the size of the tumor (LxBxH) by vernier scale and take note of mouse tag number.

Mice tag no	L	B	H	Weight

11. Clean the mouse skin with alcohol swab.
12. Inject the fusion protein into middle of the tumor slowly and mark the tail of the mouse with the marker.
13. Repeat this for all the mice.
14. Clean the surface of the hood and clean all the containers with an alcohol swab.

CPRG Assay From Stratagene

1. Pipet 20 μ l of cell lysate into the wells of a 96-well microtiter dish. Prepare a blank (for zeroing the microtiter dish reader) by adding 20 μ l of lysis buffer to a well. Prepare the control for endogenous β -galactosidase activity by adding 20 μ l of lysate from the mocktransfected cells to a well.

2. Prepare 25× CPRG substrate by adding 1 ml of buffer A to a vial of CPRG substrate. Mix the two components by inversion. Dilute the 25× CPRG substrate to 1× CPRG substrate by adding 1 part of 25× CPRG substrate to 24 parts of buffer A.
3. Add 130 µl of 1× CPRG substrate to each well for a final volume of 150 µl. Record the time of CPRG substrate addition. Cover the dish with a microplate lid.
4. Incubate the reactions for 30 minutes or longer (up to 72 hours) in a 37°C incubator until the sample turns dark red. The incubation period will vary.
5. Terminate the reactions by adding 80 µl of stop solution to each well. Record the incubation period, which is the time expired between the addition of CPRG substrate and the addition of the stop solution.
6. *Note Because the CPRG substrate begins to oxidize after stop solution is added, perform step 6 within 2 hours.*
7. Scan the microtiter dish in a microtiter dish reader at a wavelength of 570–595 nm. Use the blank to zero the microtiter dish reader. Alternatively, measure the optical density (OD_{570–595}) of the blank and subtract it from the OD_{570–595} value of each well of cell lysate.
8. Determine the protein concentration and the specific activity of the sample

Binding of Methioninase-Annexin V on Externally Positioned PS on the Surface of Cells

1. Grow MCF-7 breast cancer cells using DMEM media containing 10% FBS until they reached 85 % confluence in T-75 flasks.
2. Count the cells using haemocytometer.

3. Transfer cancer cells (5×10^4) to 24 well plates and grow until 85 % confluence is reached.
4. PS was exposed on the surface of cells by the addition of hydrogen peroxide (1 mM). Treat cells with 100 μ l wash/binding buffer containing the DMEM media containing 1 mM of H_2O_2 for 1 h at 37 °C.
5. Fix the cells by adding 100 μ l PBS buffer containing 0.25 % glutaraldehyde and Ca^{2+} (2 mM).
6. Quench excess aldehyde groups incubating with 50 mM of NH_4Cl (100 μ l) for 5 min.
7. Prepare methioninase-annexin V fusion protein in wash buffer with an initial concentration of 6.7 nM.
8. Do serial 2-fold dilutions of this concentrated fusion protein solution until final concentration of 6.7 pM.
9. Add methioninase-annexin V (300 μ l) to wells in the increasing concentration of methioninase-annexin V.
10. For each concentration of methioninase-annexin, the experiment is done in triplets.
11. Incubate for 2 h.
12. Wash plates with wash buffer (300 μ l).
13. Add 300 μ l of primary antibody (rabbit anti-methioninase) diluted in wash buffer (1:1000) and incubate for 12 h at 4 °C.
14. Wash plates with wash buffer (300 μ l).
15. Add 300 μ l of goat anti-rabbit IgG secondary antibody with HRP conjugated (1:1000 dilution in binding buffer) to the wells and incubate for 2 h at room

temperature.

16. Wash the plates with PBS (300 μ l).
17. Add the chromogenic substrate O-phenylenediamine (OPD, 300 μ l).
18. Wait for 30 min and transfer 100 μ l of the supernatant to 96-well plates.
19. Measure absorbance at 450 nm.

Binding of Methioninase-Annexin V on Plastic-immobilized Phosphatidylserine

1. Phospholipids were received in chloroform and diluted further in chloroform to a concentration of 50 μ g/ml.
2. Add 100 μ l of above solution to wells of 96-well plates.
3. After evaporation of solvent in air (used laminar flow hood), block the plates for 2 h with 10 % fetal bovine serum diluted in PBS containing 2 mM Ca²⁺ (binding buffer).
4. Methioninase-Annexin V was diluted in binding buffer at an initial concentration of 6.7 nM.
5. Do serial 2-fold dilutions of this concentrated fusion protein solution until final concentration of 6.7 pM.
6. Add methioninase-annexin V (100 μ l) to wells in the increasing concentration of methioninase-annexin V.
7. The plates were incubated at room temperature for 2 h.
8. Wash plates with wash buffer (100 μ l).
9. Add 100 μ l Rabbit Anti L-Methioninase 1^o antibody to these wells (1:1000 dilution in binding buffer) for 12 h at 4 °C.

10. Wash plates with wash buffer (100 μ l).
11. Add 100 μ l of goat antirabbit IgG conjugated to HRP (1:1000 dilution in binding buffer) 2⁰ antibody to the wells for 2 h at room temperature.
12. Wash plates with wash buffer (100 μ l).
13. Add 200 μ l of O-phenylenediamine (OPD) solution (chromogenic substrate) to the wells.
14. Wait for 30 min.
15. Measure the absorbance at 450 nm.

Notes:

- OPD was added at concentration of 0.4 mg/ml in phosphate citrate buffer with sodium perborate capsule (Product number P4922).
- Reagents were added after four washings of plates with the binding buffer.